

University of Southern Queensland

School of Engineering

**Laboratory Simulation of Agricultural Soil Density Reduction  
and Pore Increase by Lifting and Raising Field Soil Elevation**

A dissertation submitted by

Hayden Doherty

in fulfillment of the requirements of

**ENP4111 Professional Engineer Research Project**

towards the degree of

**Bachelor of Engineering (Honours) (Agricultural)**

Submitted: November, 2024

**This page intentionally left blank**

# **University of Southern Queensland**

## **School of Engineering**

### **ENP4111 Research Project**

(This is a 2-unit research project in Bachelor of Engineering Honours Program)

#### **Limitations of Use**

The Council of the University of Southern Queensland, its Academic Affairs, and the staff of the University of Southern Queensland, do not accept any responsibility for the truth, accuracy or completeness of material contained within or associated with this dissertation.

Persons using all or any part of this material do so at their own risk, and not at the risk of the Council of the University of Southern Queensland, its Faculty of Health, Engineering and Science or the staff of the University of Southern Queensland.

This dissertation reports an educational exercise and has no purpose or validity beyond this exercise. The sole purpose of this dissertation project is to contribute to the overall education within the student's chosen degree program. This document, the associated hardware, software, drawings, and other material set out in the associated appendices should not be used for any other purpose: if they are so used, it is entirely at the risk of the user.

## **CERTIFICATION**

I certify that the ideas, designs and experimental work, results, analyses and conclusions set out in this dissertation are entirely my own effort, except where otherwise indicated and acknowledged.

I further certify that the work is original and has not been previously submitted for assessment in any other course or institution, except where specifically stated.

**Student Name:** Hayden Doherty

**Student Number:** [REDACTED]

## **ABSTRACT**

Water, retained or stored in the soil between rainfalls, is vital for all plants to ensure adequate and ongoing supply of water provided to the demand of their roots. Soil water retention curves, a curve of soil moisture as a function of matric potential or root suction, are constructed to characterise the amount of pressure and energy required to hold water within the voids of a soil at different moisture contents. The retention curve is influenced by a wide variety of soil factors, including shrinkage, swelling, density, compaction, porosity and tillage, which all have an impact on the energy required to hold water within the void structure of the soil. This curve has the potential to determine a range of agricultural soil properties such as field, water retention and plant available water capacities. However, little success has been achieved when trying to develop such curves in the field.

This study will look to create soil water retention curves in a laboratory setting based on such soil parameters as void ratio, moisture content and density, using results of soil consolidation tests. The methodology comprises of two stages, experimental and analytical. Experimentally, soil mechanic tests were performed on two types of soil to determine soil particle size distribution, classification, specific gravity, permeability, compaction and consolidation. Analytically, these experimental results were used to determine the soil water retention function mainly based on the hypothesis that the soil void-ratio as a function of consolidation pressure can be correlated to the soil volumetric moisture content as a function of the soil matric pressure potential or suction. The early results achieved in this study are promising rendering further research and development in this field.

## **ACKNOWLEDGEMENTS**

I would like to acknowledge all who have contributed to the completion of this research project. The following I would like to mention;

- Dr Habib Alehossein for not only the guidance and support provided as my USQ supervisor, but also the primary source of the concept for my project.
- Soil CRC for providing a range of soil samples and their support throughout the project, which was a significant part of the project.
- My family for the encouragement and support throughout not only my research project but also my entire studies, helping myself to progress in my studies but also as a person.

I am incredibly thankful for the input and support of these people.

HAYDEN DOHERTY

# TABLE OF CONTENTS

|  |          |
|--|----------|
| CERTIFICATION  | iv       |
| ABSTRACT   | v        |
| ACKNOWLEDGEMENTS   | vi       |
| TABLE OF CONTENTS  | vii      |
| LIST OF TABLES   | xi       |
| LIST OF FIGURES  | xii      |
| NOMENCLATURE   | xvii     |
| GLOSSARY   | xix      |
| <b>Chapter 1 INTRODUCTION</b>                              | <b>1</b> |
| 1.1 Background   | 1        |
| 1.2 Project Aims and Objectives                            | 2        |
| 1.3 Project Significance                                   | 3        |
| 1.4 Overview of Dissertation                               | 4        |
| <b>Chapter 2 LITERATURE REVIEW</b>                         | <b>5</b> |
| 2.1 Tillage Operations                                     | 5        |
| 2.1.1 Advantages and Disadvantages of Conventional Tillage | 5        |
| 2.1.2 Different Types of Tillage                           | 7        |
| 2.1.3 Past Research into Tilled Agricultural Soils         | 9        |
| 2.2 Soil Properties  | 9        |
| 2.3 Soil Consolidation                                     | 12       |
| 2.4 Soil Water Retention                                   | 14       |

|   |           |
|---|-----------|
| 2.5 Soil Water Retention Curve  | 14        |
| 2.5.1 Overview of Soil Water Retention Curve                                | 14        |
| 2.5.2 Experimental Determination of Soil Water Retention Curve              | 16        |
| 2.5.3 Inferential Determination of Soil Water Retention Curve               | 18        |
| <b>Chapter 3 EXPERIMENTAL METHODOLOGY</b>                                   | <b>20</b> |
| 3.1 Soil Sample collection  | 20        |
| 3.1.1 Soil Sample Site Locations  | 20        |
| 3.1.2 Soil Sample Collection Method   | 22        |
| 3.2 initial Soil Experiments  | 23        |
| 3.3 Main Experiments  | 24        |
| 3.3.1 Overview of Soil Experiments  | 24        |
| 3.3.2 Sieve Analysis and Soil Classification                                | 24        |
| 3.3.3 Atterberg and Shrinkage Limits  | 25        |
| 3.3.4 Specific Gravity Test   | 27        |
| 3.3.5 Standard Compaction Test  | 28        |
| 3.3.6 Vertical Permeability Test  | 29        |
| 3.3.7 Saturated One-Dimensional Consolidation Test                          | 32        |
| 3.4 Theory of Rien van Genuchten Function of Soil Water Retention Behaviour | 34        |
| <b>Chapter 4 RESULTS</b>  | <b>37</b> |
| 4.1 Experimental results  | 37        |
| 4.1.1 Initial Soil Experiment Results                                       | 37        |
| 4.1.2 Sieve Analysis and Particle Size Distribution Curves                  | 38        |
| 4.1.3 Atterberg and Shrinkage Limits  | 39        |
| 4.1.4 Specific Gravity Test   | 40        |
| 4.1.5 Standard Compaction Test  | 41        |



|  |           |
|--|-----------|
| 4.1.6 Vertical Permeability Test   | 42        |
| 4.1.7 Soil Consolidation Test  | 43        |
| 4.2 Soil Classification  | 48        |
| 4.3 Initial Soil Water retention curves  | 49        |
| 4.4 Revised Soil Water retention curves  | 55        |
| 4.5 Curve Fitting for Soil Water Retention Curves                                | 61        |
| <b>Chapter 5 DISCUSSIONS</b>   | <b>65</b> |
| 5.1 Experimental Results   | 65        |
| 5.2 Initial Soil Water Retention Curves  | 70        |
| 5.3 Revised Soil water Retention Curves  | 71        |
| 5.4 Comparison Between Revised Soil Water Retention Curves and Existing Research | 72        |
| <b>Chapter 6 CONCLUSIONS</b>   | <b>77</b> |
| 6.1 Summary of Findings  | 77        |
| 6.2 Project Outcomes   | 78        |
| 6.3 Further Research   | 80        |
| <b>Chapter 7 REFERENCES</b>  | <b>81</b> |
| <b>Appendix A: Project Specification</b>   | <b>85</b> |
| <b>Appendix B: Risk Assessment</b>   | <b>87</b> |
| <b>Appendix C: Resources and Timeline</b>  | <b>89</b> |
| <b>Appendix D: Soil Sample Images</b>  | <b>91</b> |
| <b>Appendix E: Laboratorial Equipment</b>  | <b>93</b> |

|  |            |
|--|------------|
| <b>Appendix F: Experimental Analysis</b>                                 | <b>102</b> |
| F.1: Sieve Analysis and Particle Size Distribution                       | 102        |
| F.2: Atterberg Limits  | 108        |
| F.3: Specific Gravity  | 109        |
| F.4: Standard Compaction Tests   | 110        |
| F.5: Vertical Permeability Test  | 115        |
| F.6 Soil Consolidation Deformation Data                                  | 117        |
| <b>Appendix G: Curve Fitting for initial Soil Water Retention Curves</b> | <b>122</b> |
| <b>Appendix H: Curve Fitting for Revised Soil Water Retention Curves</b> | <b>127</b> |

## LIST OF TABLES

|   |     |
|---|-----|
| Table 1: Mass required for apparatus 1 (50 mm lever arm).                                       | 33  |
| Table 2: Mass required for apparatus 2 (75 mm lever arm).                                       | 33  |
| Table 3: Depth, mass and moisture content for Greymare locations.                               | 37  |
| Table 4: Depth, mass and moisture content for Armatree locations.                               | 37  |
| Table 5: Particle size distribution for all locations and depths.                               | 38  |
| Table 6: Plastic, liquid and shrinkage limit for all locations and depths.                      | 39  |
| Table 7: Specific gravity results for all locations and depths.                                 | 40  |
| Table 8: Optimum moisture content and dry density when compacting for all locations and depths. | 41  |
| Table 9: Unsaturated and saturated permeability results for all locations and depths.           | 42  |
| Table 10: USCS soil groups, descriptors and symbols.  | 48  |
| Table 11: Timeline for the project.   | 90  |
| Table 12: Uniformity coefficient and coefficient of gradation for all soil types.               | 107 |

## LIST OF FIGURES

|  |    |
|--|----|
| Figure 1: Typical soil water retention curve (Fredlund and Xing, 1994).          | 15 |
| Figure 2: Armatree site sample locations.  | 21 |
| Figure 3 : Greymare site sample locations.                                       | 22 |
| Figure 4: Simple diagram of vertical permeability equipment used during project. | 30 |
| Figure 5: Void ratio for Greymare Mid North 0-10.                                | 43 |
| Figure 6: Void ratio for Greymare Mid North 20-30.                               | 44 |
| Figure 7: Void ratio for Greymare SW corner 0-10.                                | 44 |
| Figure 8: Void ratio for Greymare SW corner 20-30.                               | 45 |
| Figure 9: Void ratio for Armatree Mid East 0-10.                                 | 45 |
| Figure 10: Void ratio for Armatree Mid East 20-30.                               | 46 |
| Figure 11: Void ratio for Armatree NW corner 0-10.                               | 46 |
| Figure 12: Void ratio for Armatree NW corner 20-30.                              | 47 |
| Figure 13: Void ratio for Armatree SW corner 0-10.                               | 47 |
| Figure 14: Void ratio for Armatree SW corner 20-30.                              | 48 |
| Figure 15: Initial SWRC for Mid North 20-30 Greymare.                            | 50 |
| Figure 16: Initial SWRC for Mid North 20-30 Greymare.                            | 50 |
| Figure 17: Initial SWRC for Southwest corner 0-10 Greymare.                      | 51 |
| Figure 18: Initial SWRC for Southwest corner 20-30 Greymare.                     | 51 |
| Figure 19: Initial SWRC for Mid-East 0-10 Armatree.                              | 52 |
| Figure 20: Initial SWRC for Mid-East 20-30 Armatree.                             | 52 |
| Figure 21: Initial SWRC for Northwest corner 0-10 Armatree.                      | 53 |
| Figure 22: Initial SWRC for Northwest corner 20-30 Armatree.                     | 53 |
| Figure 23: Initial SWRC for Southwest corner 0-10 Armatree.                      | 54 |
| Figure 24: Initial SWRC for Southwest corner 20-30 Armatree.                     | 54 |
| Figure 25: Revised SWRC for Mid North 0-10 Greymare.                             | 56 |
| Figure 26: Revised SWRC for Mid North 20-30 Greymare.                            | 56 |

|  |    |
|--|----|
| Figure 27: Revised SWRC for Southwest corner 0-10 Greymare.  | 57 |
| Figure 28: Revised SWRC for Southwest corner 20-30 Greymare.   | 57 |
| Figure 29: Revised SWRC for Mid-East 0-10 Armatree.  | 58 |
| Figure 30: Revised SWRC for Mid-East 20-30 Armatree.   | 58 |
| Figure 31: Revised SWRC for Northwest corner 0-10 Armatree.  | 59 |
| Figure 32: Revised SWRC for Northwest corner 20-30 Armatree.   | 59 |
| Figure 33: Revised SWRC for Southwest corner 0-10 Armatree.  | 60 |
| Figure 34: Revised SWRC for Southwest corner 20-30 Armatree.   | 60 |
| Figure 35: Curve fitting of initial SWRC for Mid-East 0-10 Armatree.   | 61 |
| Figure 36: Goodness of fit statistics for initial SWRC for Mid-East 0-10 Armatree.   | 62 |
| Figure 37: Curve fitting of revised SWRC for Mid-East 0-10 Armatree.   | 63 |
| Figure 38: Coefficients, 95% confidence bounds and goodness of fit statistics for revised SWRC for Mid-East 0-10 Armatree. | 63 |
| Figure 39: Permeability plot for Greymare Mid North 0-10.  | 68 |
| Figure 40: SWRC for sandy loam under conventional tillage practices.   | 73 |
| Figure 41: SWRC for different soil types using pressure plate methods.   | 75 |
| Figure 42: Estimation of SWCC using estimated points from pedotransfer functions and Fredlung and Xing equation.           | 76 |
| Figure 43: First page of Risk Assessment for the project.  | 87 |
| Figure 44: Second page of Risk Assessment for the project.   | 88 |
| Figure 45: Soil samples collected from Greymare, Queensland.   | 91 |
| Figure 46: Opened soil samples collected from Greymare, Queensland.  | 91 |
| Figure 47: Soil samples collected from Armatree, New South Wales.  | 92 |
| Figure 48: Opened soil samples collected from Armatree, New South Wales.   | 92 |
| Figure 49: Sieve shaker used for sieve analysis and soil classification.   | 93 |
| Figure 50: Equipment used for liquid limit test (Cone Penetrometer).   | 94 |
| Figure 51: Example of plastic limit test procedure.  | 95 |

|  |     |
|--|-----|
| Figure 52: Vacuum pump used for specific gravity testing.  | 96  |
| Figure 53: Standard Proctor compaction test equipment.   | 97  |
| Figure 54: Vertical permeability test equipment.   | 98  |
| Figure 55: Soil consolidation test set up with consolidation cells loading and weights applied.                      | 99  |
| Figure 56: Complete recording set up for soil consolidation tests including LVDT and Vishay system 5000 data logger. | 100 |
| Figure 57: LVDT (Linear variable displacement transformer) connected to soil consolidation testing equipment.        | 101 |
| Figure 58: Particle size distribution for Mid North 0-10 Greymare.   | 102 |
| Figure 59: Particle size distribution for Mid North 20-30 Greymare.  | 102 |
| Figure 60: Particle size distribution for SW corner 0-10 Greymare.   | 103 |
| Figure 61: Particle size distribution for SW corner 20-30 Greymare.  | 103 |
| Figure 62: Particle size distribution for Mid-East 0-10 Armatree.  | 104 |
| Figure 63: Particle size distribution for Mid-East 20-30 Armatree.   | 104 |
| Figure 64: Particle size distribution for NW corner 0-10 Armatree.   | 105 |
| Figure 65: Particle size distribution for NW corner 20-30 Armatree.  | 105 |
| Figure 66: Particle size distribution for SW corner 0-10 Armatree.   | 106 |
| Figure 67: Particle size distribution for SW corner 20-30 Armatree.  | 106 |
| Figure 68: Example of plastic limit calculations in Excel.   | 108 |
| Figure 69: Example of liquid limit graph for Mid-East 0-10 Armatree.   | 108 |
| Figure 70: Example of liquid limit graph for Mid-East 20-30 Armatree.  | 109 |
| Figure 71: Example of specific gravity calculations for Southwest corner 0-10 Greymare.                              | 109 |
| Figure 72: Standard compaction test results for Mid North 0-10 Greymare.   | 110 |
| Figure 73: Standard compaction test results for Mid North 20-30 Greymare.  | 110 |
| Figure 74: Standard compaction test results for Southwest corner 0-10 Greymare.                                      | 111 |
| Figure 75: Standard compaction test results for Southwest corner 20-30 Greymare.                                     | 111 |
| Figure 76: Standard compaction test results for Mid-East 0-10 Armatree.  | 112 |

|   |     |
|---|-----|
| Figure 77: Standard compaction test results for Mid-East 20-30 Armatree.  | 112 |
| Figure 78: Standard compaction test results for Northwest corner 0-10 Armatree.   | 113 |
| Figure 79: Standard compaction test results for Northwest corner 20-30 Armatree.  | 113 |
| Figure 80: Standard compaction test results for Southwest corner 0-10 Armatree.   | 114 |
| Figure 81: Standard compaction test results for Southwest corner 20-30 Armatree.  | 114 |
| Figure 82: Vertical permeability test results for unsaturated Mid-East 0-10 Armatree using both constant and variable head. | 115 |
| Figure 83: Vertical permeability test results for saturated Mid-East 0-10 Armatree using both constant and variable head.   | 116 |
| Figure 84: Deformation graph for Mid North 0-10 Greymare.   | 117 |
| Figure 85: Deformation graph for Mid North 20-30 Greymare.  | 117 |
| Figure 86: Deformation graph for Southwest corner 0-10 Greymare.  | 118 |
| Figure 87: Deformation graph for Southwest corner 20-30 Greymare.   | 118 |
| Figure 88: Deformation graph for Mid-East 0-10 Armatree.  | 119 |
| Figure 89: Deformation graph for Mid-East 20-30 Armatree.   | 119 |
| Figure 90: Deformation graph for Northwest corner 0-10 Armatree.  | 120 |
| Figure 91: Deformation graph for Northwest corner 20-30 Armatree.   | 120 |
| Figure 92: Deformation graph for Southwest corner 0-10 Armatree.  | 121 |
| Figure 93: Deformation graph for Southwest corner 20-30 Armatree.   | 121 |
| Figure 94: Curve fitting for initial SWRC Mid North 0-10 Greymare.  | 122 |
| Figure 95: Curve fitting for initial SWRC Mid North 20-30 Greymare  | 122 |
| Figure 96: Curve fitting for initial SWRC Southwest corner 0-10 Greymare.   | 123 |
| Figure 97: Curve fitting for initial SWRC Southwest corner 20-30 Greymare.  | 123 |
| Figure 98: Curve fitting for initial SWRC Mid-East 0-10 Armatree.   | 124 |
| Figure 99: Curve fitting for initial SWRC Mid-East 20-30 Armatree.  | 124 |
| Figure 100: Curve fitting for initial SWRC Northwest corner 0-10 Armatree.  | 125 |
| Figure 101: Curve fitting for initial SWRC Northwest corner 20-30 Armatree.   | 125 |

|   |     |
|---|-----|
| Figure 102: Curve fitting for initial SWRC Southwest corner 0-10 Armatree.  | 126 |
| Figure 103: Curve fitting for initial SWRC Southwest corner 20-30 Armatree. | 126 |
| Figure 104: Curve fitting for revised SWRC Mid North 0-10 Greymare.         | 127 |
| Figure 105: Curve fitting for revised SWRC Mid North 20-30 Greymare.        | 127 |
| Figure 106: Curve fitting for revised SWRC Southwest corner 0-10 Greymare.  | 128 |
| Figure 107: Curve fitting for revised SWRC Southwest corner 20-30 Greymare. | 128 |
| Figure 108: Curve fitting for revised SWRC Mid-East 0-10 Armatree.          | 129 |
| Figure 109: Curve fitting for revised SWRC Mid-East 20-30 Armatree.         | 129 |
| Figure 110: Curve fitting for revised SWRC Northwest corner 0-10 Armatree.  | 130 |
| Figure 111: Curve fitting for revised SWRC Northwest corner 20-30 Armatree. | 130 |
| Figure 112: Curve fitting for revised SWRC Southwest corner 0-10 Armatree.  | 131 |
| Figure 113: Curve fitting for revised SWRC Southwest corner 20-30 Armatree. | 131 |



## NOMENCLATURE

|                    |                                      |                 |
|--------------------|--------------------------------------|-----------------|
| A                  | Cross Sectional Area of Soil Chamber | mm <sup>2</sup> |
| a                  | Fitting Parameter                    | -               |
| B                  | Fitting Parameter                    | -               |
| C <sub>c</sub>     | Coefficient Of Gradation             | -               |
| C <sub>u</sub>     | Uniformity Coefficient               | -               |
| e                  | Void Ratio                           | -               |
| G <sub>s</sub>     | Specific Gravity                     | -               |
| H <sub>1</sub>     | Initial Head Height                  | mm              |
| H <sub>2</sub>     | Final Head Height                    | mm              |
| H <sub>s</sub>     | Height Of Solids                     | mm              |
| H <sub>v</sub>     | Height Of Voids                      | mm              |
| h <sub>d</sub>     | Air Entry Pressure                   | kPa             |
| K <sub>sat</sub>   | Saturated Permeability               | mm/s            |
| K <sub>unsat</sub> | Unsaturated Permeability             | mm/s            |
| L                  | Length Of Soil Chamber               | mm              |
| LS                 | Linear Shrinkage                     | -               |
| M <sub>s</sub>     | Mass Of Solids                       | g               |
| m                  | Soil Water Potential                 | kPa             |
| n                  | Pore-Size Distribution               | -               |
| S                  | Degree Of Saturation                 | -               |
| t                  | Drop Time of Water                   | Sec             |
| V                  | Volume Of Sample                     | mm <sup>3</sup> |
| V <sub>a</sub>     | Volume Of Air                        | mm <sup>3</sup> |
| V <sub>s</sub>     | Volume Of Solids                     | mm <sup>3</sup> |
| V <sub>v</sub>     | Volume Of Voids                      | mm <sup>3</sup> |
| V <sub>w</sub>     | Volume Of Water                      | mm <sup>3</sup> |
| α                  | Inverse Of Air Entry Suction         | -               |
| ΔH                 | Change In Head                       | mm              |
| θ                  | Volumetric Moisture Content          | -               |

|            |                         |      |
|------------|-------------------------|------|
| $\theta_R$ | Residual Soil Moisture  | -    |
| $\theta_S$ | Saturated Soil Moisture | -    |
| $\lambda$  | Curve Shape Parameter   | -    |
| $\rho_d$   | Density Of Dry Soil     | g/mm |
| $\rho_s$   | Density Of Water        | g/mm |
| $\Psi$     | Suction Pressure        | kPa  |

## **GLOSSARY**

|      |  |
|------|--|
| ATSM | American Society for Testing and Materials |
| DFE  | Degrees of Freedom for Error               |
| LVDT | Linear Variable Displacement Transformer   |
| RMSE | Root Mean Squared Error                    |
| SSE  | Sum of Squares due to Error                |
| SWRC | Soil Water Retention Curve                 |
| USCS | Unified Soil Classification System         |

# **CHAPTER 1 INTRODUCTION**

## **1.1 BACKGROUND**

The lifting and raising of soil in agriculture refers to the use of mechanical tillage equipment to provide an ideal seedbed to foster the growth and development of crops. Agricultural soils that are used to prepare the soil for planting, in other words preparing a seedbed, require the correct soil density and pore structure constructed by the process of tillage to ensure the correct balance is achieved. This in turn produces a seedbed that can give the most optimum crop yield. Further important and relevant soil characteristics that are affected through the tillage process include aggregation, bonding, density, strength, and stability, which are all key to a soil structure (Victoria Agriculture, 2020).

The main benefits of using this technique of seedbed management include weed control, soil aeration, water infiltration, mixing organic matter into the soil as well as soil decompaction (Dexter, 1997). While tillage has these advantages, it does come with some environmental issues when the soil is mismanaged by surface runoff, soil erosion, soil structure breakdown, loss of nutrients such as nitrogen and soil compaction (Dexter, 1997).

Plant's root suction of water is measured by a parameter called soil matric potential, which is a function of soil moisture content and void ratio. It is a pressure potential that arises from the interaction between the soil retained water and the matrix of the solid soil particles. Soil water retention curves are a basic hydraulic curve that provides information surrounding the amount of matric potential or energy required at different moisture content levels to hold water within the voids of a soil (Assouline, 2021). This curve is influenced by the state of which the soil in question is in, with factors such as tillage, compaction, swelling and shrinking affecting the amount of energy required to hold the same amount of water (Assouline, 2021). This curve provides critical information on a range of agricultural soil properties, ranging from field capacity, water holding capacity, wilting point and many others. There are a range of ways to determine the curve, using

both experimental and inferential techniques, which can be both complex to complete and requiring large amounts of time and resources.

A possible way to determine this curve that will be explored in this project is indirectly through soil consolidation, using the connection between void ratio and volumetric moisture content to derive the curve itself. At this stage there has been little to no work completed in relation to connecting soil consolidation and the soil water retention curve. This project will look to investigate this research gap through both laboratory experiments and the development of analytical and numerical tools to simulate the curve within agricultural soils. Soil will be retrieved from private property located in Greymare, QLD as well as property currently being used for Soil CRC research in Armatree, NSW.

## **1.2 PROJECT AIMS AND OBJECTIVES**

The main aim of this research project is to simulate tilled agricultural soils soil water retention curves using one-dimensional soil consolidation experimental results in a laboratory setting. This will be completed based off a range of soil parameters such as void ratio, moisture content and density. This research looks to use past knowledge and studies to gain an understanding of whether the use of soil consolidation is practical in determining soil water retention curves. With the use of different soil types from different environments in Australia, calculations and results will be able to be compared with similar soil types in past research.

The objectives of this project are as follows:

1. Completion of initial research in tillage, water retention and soil water retention curves and the factors that affect the soils' ability to withhold moisture.
2. Establishment of a connection between void ratio and volumetric moisture content through a derived equation.
3. Conduct standard soil mechanic tests such as sieve analysis, specific gravity, Atterberg limits, compaction, permeability and soil consolidation.

4. Explore the results of both the initial and revised soil water retention curves created using the conversion equation and the different data each created.
5. Compare the results with other research both within the agricultural industry as well as other relevant industries.
6. Draw conclusions on the viability and future improvements of the methodology followed and the results obtained from the revised soil water retention curves.

Appendix A – Project specification.

Appendix B – Risk Assessment.

Appendix C – Resources and Timeline.

## **1.3 PROJECT SIGNIFICANCE**

Water retention in the agricultural industry is critical for the health of the soil as well as the surrounding environment. High water retention promotes soil health, reduced irrigation needs, erosion prevention, consistent crop yields, climate resilience and much more sustainable farming methods. The concept of the soil water retention curve is important not only in the agricultural industry but also environmental, geotechnical, construction, waste management, resource management and others due to its ability to describe the movement of water and the distribution of soil moisture. In agriculture, the soil water retention curve can be used to determine a range of important parameters, such as soil water storage, field capacity, required irrigation, drainage and others that are key to a sustainable and long-term industry. This makes the curve important in understanding what is occurring in the soils in all forms of agriculture, from arable farming to grazing and livestock farming. This is described through the relationship between volumetric water content and soil water potential, which is constantly changing due to many different factors, meaning management is key in maintaining soil stability.

## 1.4 OVERVIEW OF DISSERTATION

The dissertation is as follows:

**Chapter 1** introduces the research project topic, provides background information to the project's development, underlines the significance and defines the aims and objectives.

**Chapter 2** contains the literature review portion of the dissertation, outlining the advantages and disadvantages of tillage, what soil retention is, the importance of soil water retention curves and how these curves are created through both experimental results and modelling.

**Chapter 3** covers the methodology of the project, including both the experimental and the theoretical analysis that will be covered later in the project.

**Chapter 4** presents the experimental results uncovered throughout the laboratorial experiment stage, covering sieve analysis, Atterberg limits, specific gravity, compaction, permeability and soil consolidation.

**Chapter 5** discusses the findings of the experimental results, as well as the creation of both initial and revised soil water retention curves. These curves are also compared to known research in the field to determine whether the results are appropriate and within the criterion.

**Chapter 6** concludes the dissertations with a summary of the findings presented throughout the project and presents some further work to be completed in regard to soil water retention curves.

# **CHAPTER 2 LITERATURE REVIEW**

## **2.1 TILLAGE OPERATIONS**

### **2.1.1 Advantages and Disadvantages of Conventional Tillage**

The use of tillage in agriculture provides producers with the opportunity to create a virtually ideal seedbed for a crop to establish itself in using mechanical manipulation through different types of machinery (University of Nebraska, 2018). This process allows changes to the existing soil structure to occur along with weed prevention and management of crop residue from previous crop cycles, which is important in disease prevention. Whether the tillage equipment used is aggressive or reserved in terms of its impact on the soil, all tillage types produce results that have their advantages and disadvantages for soil health.

The advantages of tillage within agriculture are well known, with the idea of creating the perfect seedbed for a crop being at the forefront of the concept, in other words creating the best possible tilth. The process looks to create an ideal soil aggregate size distribution to suit the specific seed size, with the pore space created by the cultivation allowing larger seed sizes to develop strong root structure and produce high yielding plants (Bayer, 2023). Furthermore, by changing the pore space size and connectivity in the soil structure, there is improved soil aeration as well as water infiltration, which is key in promoting optimum plant conditions. The pore space connectivity is pivotal in allowing this to occur, allowing water and air to move freely through the connected pore structure, reducing surface runoff, promoting groundwater recharge and is significant in allowing plant roots access to water for growth and nutrient uptake. Water conservation within the soil can also be promoted through the manipulation of soil structure and crop-residue retention depending on the methods used (Bayer, 2023). In regard to weed control, tillage is able to reduce overall weed density and stop different weed types from germinating, which was why the technology was so widely used before herbicides were developed and implemented. Different types of tillage can control most weeds, ranging from seedlings to established annual or biennial weeds.



Some soils are known to require more or less tillage depending on the climate and conditions. Examples of requiring more tillage are cool and wet soils, high clay or sand content soils or soils with poor permeability, allowing either infiltration or drainage and drying for the soil depending on the conditions (Bayer, 2023). This is important especially when there is excess water in the subsoil, with deep tillage reducing waterlogging and leaching of nutrients through soil draining. Soils known to require low amounts of tillage include soils that can regenerate soil structure naturally, through the use of soil drying and wetting as well as freezing and thawing processes (Bayer, 2023).

In terms of the disadvantages of tillage in agriculture, there are a wide range of issues that can occur. The main issues include long lasting effects on soil structure, soil biological life and residue cover. In terms of soil structure in the agricultural world, soil should be made up of one-half solid materials that include sand, silt, clay, nutrients, minerals, organic matter and biological life, while the other half is made up of pores spaces, filled with air and water (University of Nebraska, 2018). The biological life and organic matter found within the soil provides the binding factor to create different sizes aggregates and the overall soil structure. A well-structured soil has a good aggregation, with strong pore structure connected from the surface deep into the subsoil, allowing water infiltration, root penetration and air exchange to occur (University of Nebraska, 2018).

Tillage breaks up the soil's structure, changing pore space and connectivity, allowing new pores to be created. If the soil was already ideal for crop growth, tillage will lead to a loss of soil strength and the soil becoming susceptible to compaction and the reduction of pore sizes (University of Nebraska, 2018). Furthermore, tillage destroys the biological life within the soil, and with structure relying on biological life to develop, the structure suffers, and nutrients are less available to plants. Different biological life plays diverse roles within the soil, such as roots acting like rebar in concrete, providing structural stability within the soil, and decaying roots providing a path for water to penetrate and roots to grow into (University of Nebraska, 2018). Microorganisms act as the glue for holding the soil particles together, while also allowing the processing of roots and residue from past crops, putting nutrients and carbon back into the soil systems cycle. Finally larger organisms allow further

cycling of materials while also creating paths within the soil structure for water, air and roots (University of Nebraska, 2018).

In terms of residue cover disruption from tillage operations, the loss of residue from the surface removes the protection from raindrop impacts and wind from hitting the surface of the soil. This increases the chances of erosion, surface crusting (increases runoff and sedimentation in waterways) and increases surface evaporation (University of Nebraska, 2018). Residue on the surface also allows for surface temperatures to be reduced, leading to better rooting near the surface and better plant access to water in drought and light rainfall conditions. Heavy crop residue must still be controlled to ensure crop productivity is not impacted though (University of Nebraska, 2018).

Other disadvantages of tillage on agricultural soils include less resistance to different weather and climate conditions, such as less tolerance in drought conditions, bigger than normal wet seasons and abnormal temperatures (Benchmark Labs, 2022). Furthermore, the labour intensiveness of multiple tillage cycles before as well as the overall cost in terms of machinery maintenance, fuel and worker costs (University of Nebraska, 2018). Changing soil management practices can be costly in terms of machinery and knowledge and lead to lowered yields and efficiencies, therefore when considering changing tillage practices, all conditions as well as inputs and outputs must be significantly considered before changing over to more conservational practices (Benchmark Labs, 2022).

### **2.1.2 Different Types of Tillage**

Over the course of the last hundred years, agricultural engineers have designed, developed and manufactured a range of methods and tools that are capable of meeting the main goals of soil tillage, with each type and piece of equipment have different advantages and limitations (Bayer, 2023).

The first type of tillage that is commonly used across the world is primary tillage, which looks to break up the soil to a depth of between 15 and 90 cm, loosening the soil and mixing in fertilizers and plant material, creating a rougher textured soil (Stewart, n.d.). This is the initial stage of tillage, with the goal to achieve softer top layers of soil, incorporating crop residue and allowing air and water to

infiltrate. Examples of equipment used to achieve this include the moldboard, disk, rotary, chisel and subsoil ploughs (Stewart, n.d.). Each plough is designed to achieve the goal of a softer soil, but also provide additional advantages on top of this. The disk plough for instance provides the chance to work fields that have a known plough sole or pan, where each furrow across the field is the same depth (Stewart, n.d.).

Secondary tillage is a vital stage of the soil preparation stage, looking to improve the seedbed created by primary tillage and attain the ideal tilth. The main techniques for completing this are using soil pulverization, destroying weeds and cutting up crop residue, which attempts to maintain the soil moisture levels. As this is the finer part of the tillage process, the equipment used works at a reduced depth, between 10 and 15 cm depending on the soil aggregate sizes and other ground conditions. The main equipment used to achieve this can be grouped into categories such as cultivators, harrows, pulverisers, rollers and mulchers. Weeders can also be placed under primary tillage equipment, pulling weeds directly out of the ground and protecting the low moisture content in the soil.

The final common tillage type is through minimum tillage or no-till systems. This process promotes the protection of the soils structure and reducing the disturbance on the soil (Stewart, n.d.). With excessive tillage management practices leading to soil crusting, lowered permeability, increased runoff, reduction in water holding ability and several other major issues, minimum tillage attempts to reduce these problems through soil structural stability. This type of tillage has led to much innovation and research into the advantages and disadvantages associated with the practice, which goes against the long-term techniques that have been used for thousands of years. With minimum tillage, primary and secondary tillage types are used sparingly, used only to reduce issues such as waterlogging or compaction. In no-till operations, no tillage equipment is used, planting directly into the soil profile using a direct drill planter. These methods produce soils with an undisturbed structure with much better aggregate stability, allowing nutrient cycles to rebuild as well as natural weed and disease controls to develop, which must be fostered in modern agricultural operations.

### **2.1.3 Past Research into Tilled Agricultural Soils**

Over the course of the last hundred years, the research into both agricultural soils and the ways that tillage improves as well as deteriorates them has been key in understanding the most practical way to farm, while decreasing the impact on the soil in the present and future. This research has ranged from the soil structures, climate and environmental impacts on agricultural soils, crop rotations and sequencing, the use of cover crops and pastures, impacts of different types of tillage equipment, soil surveying and mapping, new soil standards and methodologies as well as many more avenues of research undertaken. With this range of research, there has been a distinct change in how soil is understood and managed, as well as what the next era of soil research will look to achieve. One of the core understandings in this research is the knowledge that soil around the globe is all connected with a variety of processes and interactions with the surrounding environment, meaning the soil in one area can have a completely different makeup compared to the soil located a short distance away (Lin, 2012). This is through the surrounding environment, the formation of the soil and the weathering it has faced throughout its life. It is known that agricultural soil management is constantly evolving, driven by socioeconomic, biophysical and technological factors, and soil research must continue to react to further developments (Tehen et al., 2020). This must be done to continue to provide stakeholders with recommendations and support on how to adapt and prevent different situations that can threaten production.

In terms of previous research in relation to the aim of this project, the laboratory simulation of agricultural soil density reduction and pore increase by lifting and raising field soil elevation, there has been large amounts of research into different parts of the research area.

## **2.2 SOIL PROPERTIES**

There are multiple key soil properties within this research related to tillage and agricultural operations. Some of the most notable are the degree of saturation, structure, density, pore

characteristics and hydraulic properties. These properties all impact an agricultural soil's ability to produce high quality crops, and are all disrupted and altered through the process of tillage.

### Soil Structure

Soil structure refers to the arrangement of solid parts of the soil and the pores located throughout it. This formation creates aggregates, with different particles making up an aggregate. A good, structured soil is known to break into aggregate form, which allows water and air to infiltrate into the soil, retaining water while also allowing it to drain away if there is a surplus, and allowing air to move freely through the soil (Queensland Government, 2013). This is all key in how a soil can support plant life, which is vital in the agricultural industry. Another part of this structure is soil horizons, made up of different layers ranging from the topsoil through to bedrock, with each layer of soil having different characteristics. The main sections disturbed through tillage are the organic layer, topsoil and the subsoil, anything below this is usually deep enough to not be disturbed mechanically but can be physically due to changes occurring above it.

### Bulk Density

The concept of bulk density relates to the mass per unit volume of a dry soil, with the volume including both the solids and pore space within the soil sample. The value is always smaller than the samples particle density, with loose soils having very small bulk density compared to heavy compacted soils such as a heavy clay, which has a much higher value (Brown and Wherrett, 2024). Factors that are known to affect bulk density include organic matter, soil texture, compaction of soil, soil structure and the void structure. Generally, soils with a lower bulk density are much more suitable for agriculture, allowing higher permeability, water retention, better drainage and root growth through the network of pores (Brown and Wherrett, 2024). Human factors surrounding soil management (compaction, tillage, irrigation, etc.) have been known to create significant temporal change upwards of 60% on the land surface soil bulk density (Osunbitan et al., 2005). This can also occur naturally, through processes such as precipitation, root growth, drying and wetting cycles and

shrinkage and expansion of soils, affecting both bulk density and soil structures. Furthermore, it was reported that saturated soil hydraulic conductivity has been determined to decrease while increasing soil bulk density over time after cultivation.

#### Pore Characteristics

There is a range of factors that affect the pore characteristics of soil which all have their own application in understanding agricultural soils. Pore characteristics can be confined to porosity, pore path, mean pore size, pore size distribution, pore volume, pore structure, permeability (both liquid and gas) and surface area (Wang and Zhang, 2021). Pores are created through soil particles leaving spaces between themselves due to their irregular shapes. Fine textured soils can pack into a space much tighter than coarse textured soils, leading to more pore spaces as there are more irregular shapes that are required to fit together. Coarse soils on the other hand take up more space themselves, leading to less soil having to fit together and less pore space being left over.

#### Permeability

The idea behind permeability is related to the soils ability to allow fluids to infiltrate through it, in most cases the fluid is water, which is an important property in the agricultural industry. With one of the main reasons for tillage being to break open the ground and allow water and air to infiltrate, permeability is crucial to all agricultural systems. High permeability soils allow water to flow through them easily, usually having larger particles and well-connected pore spaces (Simon, 2023). Low permeability soils, such as clay soils, have much smaller particles and generally have a more compacted structure, hindering the soils capacity to allow water to flow (Simon, 2023).

#### Degree of Saturation

The degree of saturation relates to the amount of water found within the pores or voids of the soil. If all pores are filled with water the soil is considered saturated and if they are empty and filled with air, the soil is considered unsaturated or dry. If the soil has pores filled with both water and air, the

soil is considered partially saturated. The degree of saturation is defined as the volume of liquids over the volume of voids in the soil, with the degree of saturation of any soil falling between 0% and 100%. Within the agricultural industry, the two most important saturation levels include both the field capacity and the wilting point of the soil. The field capacity, also known as the water holding capacity of the soil, is determined to be the maximum amount of water that a soil can hold after any excess water has drained away, which usually takes two to three days naturally (Rai et al., 2017). At field capacity, the air and water contents are optimum for crop growth. The wilting point of the soil is the point where the plant does not have access to water to continue to grow (Rai et al., 2017). There is still some water left in the soil, but it is very difficult for the plant to extract it, and if no water is added to the soil, most plants will be lost. The wilting point is dependent on crop type, with some crops requiring more water than others.

#### Hydraulic Properties

Soil hydraulic properties are incredibly important when it comes to understanding the soil's health as well as the health of the surrounding environment. The main hydraulic properties include hydraulic conductivity, infiltration rate, field capacity and water table depth. These properties all control water retention, movement of nutrients and flow rate, which are key in understanding relationships and management of plants (Indoria et al., 2020). Applications of this include water movement and storage, irrigation practices, leaching, drainage, and models for long term predictions.

## **2.3 SOIL CONSOLIDATION**

The concept of soil consolidation is used across a range of engineering industries, the most notable being geotechnical engineering. The concept allows an understanding of how soil will slowly settle under an applied load placed on top of it, generally a building or structure. This can be used for predicting settlement for foundations as well as understanding what a soil will most likely do in the short term as well as the long term (Simon, 2023). This all occurs due to the expulsion of water from the soil voids as the load is applied. As Simon describes, soil consolidation can be described as a

sponge, water is squeezed out as the load is applied, with the result being a smaller and denser sponge (Simon, 2023). Soil consolidation testing is important when working with any soil, but is critical when dealing with clays and silts, which are known to have smaller pores, making it difficult for water to escape easily.

There are some important assumptions to consider when using soil consolidation theory, the first of which is one-dimensional consolidation. This theory implies that the load the soil is under is coming from above it, in a vertical direction, and that the soil is uniformly consistent in all directions (Simon, 2023). With soils generally having spatial variations in their properties, there can be major differences between experimental results and practical application. Another assumption is that soil properties such as permeability and compressibility remain unchanged throughout the process. However, it is known that soils can exhibit what are considered time dependent behaviours that alter their properties when different levels of stress are applied (Simon, 2023). The theory of consolidation also assumes that all soils act with isotropic behaviour, acting uniformly in all directions. While most soils do act this way, some soils are known to act with anisotropic behaviours, acting along different axes (Simon, 2023). A final assumption relates to a linear elastic behaviour of soils, with the relationship between stress and strain being linear, which is correct for lightly loaded soils. Once soils reach a certain load, the relationship can begin to become nonlinear (Simon, 2023).

Soil consolidation tests are generally completed using a one-dimensional consolidation test, using an incremental loading oedometer. This allows all three stages of the consolidation to occur, including the initial, primary and secondary consolidations. The initial consolidation relates to the reduction in soil immediately after the application of the load, mainly due to the compression of solid saturated particles (Geo Engineer, n.d.). Primary consolidation is due to the settlement as water is squeezed out of the soil, and finally secondary consolidation is associated with the internal changes of the soils structure while under constant load, which is also known as creep (Geo Engineer, n.d.).



## **2.4 SOIL WATER RETENTION**

Soil water retention is essential to all types of life, allowing an ongoing supply of water to plants, allowing continued growth and survival. Once the excess water within the soil has drained away, the water retained by the soil is critical to the plant developing a strong root system, producing higher quality and higher yielding plants and allows plants to stand up against unpredictable weather conditions. Water retention of the soil is at the beginning of the plant cycle, without water within the soil the plants are unable to grow, meaning no crops are grown for consumption by humans or animals and leaving the world without food.

Improved soil water retention in agriculture has a range of benefits. The first of these is the efficiency of water use across a range of applications, the most important being irrigation, which in turn helps to preserve natural water resources. The increased retention also helps to mitigate flood and alleviate the effects of droughts on plants. This is completed through the changing of rate in terms of the hydrological cycle, improving soil infiltration, slowing the overland flow of the landscape, reducing channel velocity as well as increasing evapotranspiration (Collentine & Futter, 2016). This creates a reduction in both the frequency and intensity of flooding events. Meanwhile, it allows drought alleviation for a range of reasons, including higher infiltration rates, retainment of more moisture and effective absorption of moisture, allowing the soil to efficiently support crops during dry weather (Soil Health Institute, 2021). This also allows the reduction of soil erosion due to overland flow across the soil. All of this helps to improve the overall environmental quality of the surrounding ecosystem, improving soil health and quality and helping plants and crops develop and grow.

## **2.5 SOIL WATER RETENTION CURVE**

### **2.5.1 Overview of Soil Water Retention Curve**

The soil water retention curve is a key concept that describes the relationship between volumetric soil water content and the soil water matric potential, or suction. The soil matrix is made up of the solid phase of the soil and is made up of gravel, sand, silt, clay and organic components, which all

have a major impact on the properties of the soil such as hydraulic conductivity and water potential. Matric potential is a criterion that is used to measure the water availability to plants, through the force that the water is held within the soil by the soil matrix or suction (Yadvinder-Singh et al., 2014). The relationship that is created portrays a positive relationship between soil water content and matric potential (Ochsner, 2019). If the potential is close to zero, the soil is close to full saturation, with the water being held within the soil by only capillary forces. As the volumetric water content decreases and closes in on the wilting point, the binding of the water becomes stronger. As this occurs, at small potentials water is bound in the smallest pores, found at contact points between grains and bound by adsorptive forces around particles. An example of a soil water retention curve can be found in figure 1 below.

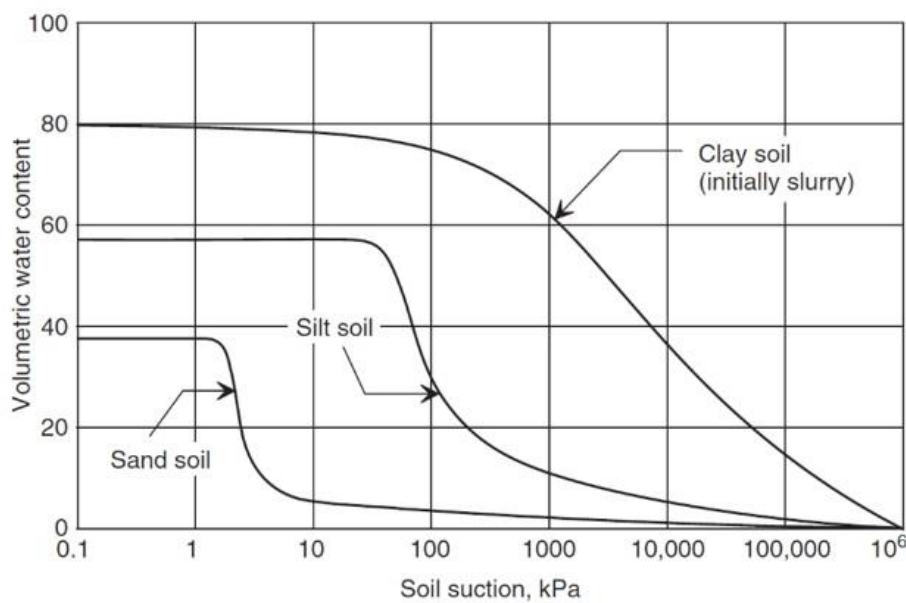


**Figure 1: Typical soil water retention curve (Fredlund and Xing, 1994).**

In terms of specific soil types, sandy soils mainly rely on capillary binding, meaning there is a release of water at higher matric potentials. On the other hand, clayey soils will release water at a much lower potential, due to the adhesive and osmotic binding. The water holding capacity of any soil is reliant on its porosity and the natural bonding of the soil. The differences between soil water retention curves are mainly due to the differences in pore sizes distribution between different soil types.

Furthermore, the curve can be sensitive to changes in soil texture, bulk density and organic matter (Geroy et al., 2011, Ma et al., 2012).

This is one of the basic soil characteristics required for simulation models to determine soil hydraulic properties as well as some mechanical properties such as soil water storage, field capacity and soil aggregate stability. Within the agricultural field, some of the applications include irrigation, runoff, evaporation, transpiration, root water uptake, capillary rise, drainage, salinity, nutrients, pesticides and multiple other increasing important parts of the industry. It is a key piece of information for understanding sustainable land use and soil management for the future (Farooq et al., 2024). Furthermore, water retention curves can also be applied in a wide range of strength problems, most notably geotechnical problems when no experimental data is available for use. There are numerous techniques to determine a SWRC, which can be classified into either directly experimental methods or indirect inferential methods (Han et al., 2010).

### **2.5.2 Experimental Determination of Soil Water Retention Curve**

There are a range of approaches to determining water retention curves for soil through experimentation, with the first of these being proposed by Edgar Buckingham in 1907. A model by Arya and Paris in 1981 was the first physiocoempirical model, which suggested that particles within the soil can be considered spherical and pores can be simplified to cylinders, with each particle size distribution being made up of single particle size fractions which contributes to the pore size distribution (Wang et al., 2017). The water retention curve could then be determined from the particle size distribution using a scaling factor. This has since been developed in terms of both the particle size distribution expressions as well as the scaling factor through research conducted by Hwang and Powers (2003), Haverkamp and Parlange (1986), Tyler and Wheatcraft (1989) and Arya (1999) (Wang et al., 2017). The main issues with this type of approach are that it is focused directly on basic properties of the soil as well as assumptions and theory-based coefficients. It also requires a large number of measured parameters which can be difficult to manage and overall, less applicable. Another technique for determining the water retention curve is through statistical methods based off

soil gradation parameters based on regression analysis (Wang et al., 2017). These methods are both based off theoretical methods to calculate the curve, while there are possible ways to determine the curve through experimental processes.

The first of these experimental methods is the pressure plate test which is the most popular method for finding the curve. This involves an enclosed steel pressure vessel with a soil sample placed within on a saturated ceramic disc (Gaspar et al., 2019). This allows the control of both air pressure and pore water pressure in the sample, with suction then being controlled imposing a known air pressure into the vessel. A flow of water from the sample in the water reservoir is created and this is continued until equilibrium is reached between water content and applied matric suction. This method overall is considered very reliable but is time consuming (Gaspar, et al., 2019). The second method is the filter paper method, which has been used since 1937 by Gardner, and is based on hydraulic equilibrium between the soil water and the dry filter paper. From this method, both the total and matric suction can be measured depending on how the initial hydraulic equilibrium is achieved (Gaspar et al., 2019).

The final two methods of finding the water retention curve are through laboratorial equipment, using either a dewpoint hygrometer or a tensiometer. The hygrometer method looks to determine the total suction based on the thermodynamic relationship between suction and a soil sample in a chamber with an exposed mirror (Gaspar et al., 2019). With a reduction of temperature, the dewpoint is considered to have occurred when the mirror has condensation on it. At this point, with temperature equilibrium reached, the relative humidity inside the chamber can be taken which is a direct measurement of the soil suction. This technique is relatively quick, taking only 15 minutes for one measurement to be taken, while also having a high measurement capacity (Gaspar et al., 2019). The tensiometer method, however, is significantly faster again, using both a tensiometer and scales to record changes in moisture content.

There has been much more research and extrapolation into the soil water retention curve models in recently years, ranging from equations for both the main drying and wetting water retention curves, hysteresis modelling and numerous other possible equations that could fit the theoretical curves.

### 2.5.3 Inferential Determination of Soil Water Retention Curve

The three most important inferential models that have been developed in relation to the SWRC are the Gardner, Brooks-Corey and van Genuchten models. The Gardner model (1958) is the simplest of the three, utilising only the volumetric soil moisture content and the soil water potential. The equation is found below.

$$\theta = a|h|^{-b} \quad [2.1]$$

Where  $\theta$  denotes volumetric soil moisture content (%),  $h$  denotes soil water potential (cm) and  $a$  and  $b$  are two fitting parameters (Pan et al., 2010). Other than the equations simplicity, the main advantage of the equation is its ability to linearise Richards Equation.

The second model is the Brooks-Corey model (1964), which combined Corey's earlier work with other previous models such as Burdine (1953) to produce a soil water retention curve model (Brooks and Corey, 1964). The model's equation can be written similarly to what is found below:

$$\frac{\theta - \theta_r}{\theta_s - \theta_r} = \begin{cases} \frac{m^\lambda}{h_d^\lambda}, & h > h_d \\ 1, & h < h_d \end{cases} \quad [2.2]$$

Where  $\theta_s$  and  $\theta_r$  denote saturated soil moisture content (%) and the residual soil water content (%) respectively,  $m$  denotes the soil water potential (cm),  $h_d$  denotes the air entry pressure and  $\lambda$  denotes a dimensionless parameter related to the curve shape (Pan et al., 2019). This work was originally meant to be used in drainage projects but was found to be helpful in determining hydraulic properties in soil both above and below the soil's surface. Furthermore, as the method considers both moisture and aeration, the model is helpful in establishing a soils status above the water table (Brooks and

Corey, 1964). One of the issues with this function is the fact it is a power function, meaning the curve continues to infinity and was cut off at saturation, failing to reach zero matric potential.

The final model that has had a major effect on the understanding of the SWRC curve in the agricultural industry is the van Genuchten model. This model is based on deriving numerical solutions based off the Richards equation (1931) which represents the movement of water in unsaturated soils, which was further based off the Darcy-Buckingham law (1907). Richard's equation represents the movement of water in unsaturated soils, describing the flow of water in the vadose zone, between the atmosphere and aquifer (Xiong, 2014). This equation is found below.

$$\frac{\partial \theta(h)}{\partial t} = \frac{\partial}{\partial z} \left[ K(h) \frac{\partial h}{\partial z} + K(h) \right] \quad [2.3]$$

Using the Brooks-Corey function, van Genuchten was able to remove the continuous slope of the model, providing a model that was smoother and able to describe what occurs near complete soil saturation. The van Genuchten equation can be written as follows:

$$\theta(\psi) = \theta_r + \frac{\theta_s - \theta_r}{[1 + (\alpha|\psi|)^n]^{1-\frac{1}{n}}} \quad [2.4]$$

Where  $\theta(\psi)$  is the volumetric water content,  $|\psi|$  is the suction pressure,  $\theta_s$  is the saturated water content,  $\theta_r$  is the residual water content,  $\alpha$  is related to the inverse of the air entry suction and  $n$  is related to the pore-size distribution (Pan et al., 2019).

The van Genuchten is the most widely used SWRC model due to its ability to precisely describe the SWRC of a diverse range of soil types, which includes both disturbed and undisturbed soils (Han et al., 2010). This model has been continually extended and developed, such as Shao and Horton (1996) developing an integral method to determine model parameters. Van Genuchten's models' ability to work with disturbed soils allowed development towards solving realistic scenarios and problems at the field level, relating to issues such as irrigation and drainage (Han et al., 2010).

# CHAPTER 3 EXPERIMENTAL METHODOLOGY

## 3.1 SOIL SAMPLE COLLECTION

### 3.1.1 Soil Sample Site Locations

There are two site locations where soil samples were taken from agricultural fields, located in Armatree, NSW and Greymare, QLD. The two locations provide two distinctly different sites with various soil types, surrounding environments and soil management practices.

The first of these locations is Armatree in New South Wales, is a part of a current research farm for Soil CRC. The soil collected at this location was spread across three different areas of a selected field, providing two different soil types overall, with topsoil and subsoil collected at all three locations. These locations included a mid-East location, a Southwest corner location and a Northwest corner location, with the mid-East and Northwest corners being from the same soil classification, which is a red sodosol, similar to the surrounding area (McKenzie, 2024). These locations were otherwise selected as they were away from other trails, eliminating the potential for uneven ground close to researchers, as well as limiting frequent foot traffic within the immediate area of these selected areas.

The Armatree field has a diverse history in terms of crop use over the course of the last decade, with the usual aim of the field to produce the most profitable crop. Past crops recently include wheat in 2020, 2022 and 2024, lupins in 2023 and canola in 2021, as well as a fallow year on record. The only tillage used on the field occurs at planting time, using a straight tined planter to complete this work. The climate in Armatree is considered subtropical using the Koppen maps classification, with hot dry summers and cold winters being expected (Bureau of Meteorology, n.d.). The expected rainfall is usually uniform across the year, with the highest average rainfall in January and the lowest in August (Bureau of Meteorology, n.d.). An image of the Armatree field can be found below in figure 2, describing the layout of the area and sample locations.

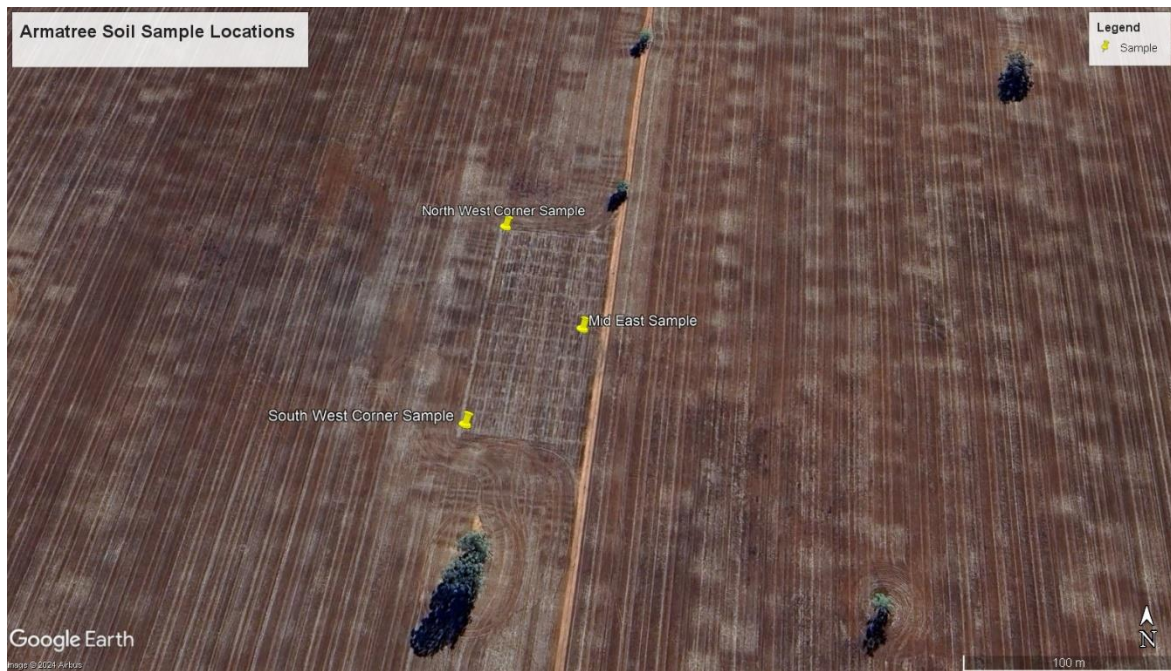


**Figure 2: Armatree site sample locations.**

The second location, found in Greymare Queensland, thirty kilometres west of Warwick, is a part of a cattle grazing farm, with cultivation used for producing oats and lucerne depending on season and conditions. Two locations from the same field were used as collecting locations, being labelled mid-North and Southwest corner. Both locations provide similar soil structure and classification, with the soil being a sandy loam, with a bleached sand topsoil and pale-yellow clay beneath, classified as a texture contrast soil (Maher and Bray, 2014).

The Greymare field is primarily used for growing oats for cattle grazing through winter, but was also planted with lucerne in 2014, as well as being left fallow during 2020 and 2021. The field goes through the different traditional stages of seedbed preparation, with both primary and secondary tillage used. An offset disc harrow is used to initially break up the soil structure and allow air and water to infiltrate into the subsoil. This is optimal for the soil as the area has a clay pan found in the subsoil, allowing the disc set up to easily move over the top without incorporating clay into the topsoil. Following this, a scarifier is used to remove weeds and create a seedbed. Finally, a straight tined planter is used to sow all crops. In terms of the Koppen map, the area of Greymare also falls within the subtropical category, with both hot summers and cold winters (Bureau of Meteorology,



n.d.). In terms of rainfall, the area usually has wet summers and low winter rainfalls expected (Bureau of Meteorology, n.d.). Figure 3 describes the area and the locations of the soil samples in the field.



**Figure 3 : Greymare site sample locations.**

### **3.1.2 Soil Sample Collection Method**

The soil collection method that was used is simple and direct, collecting samples from both the topsoil and the subsoil below. It is important that the soil is not disturbed in both transportation and storage at the lab, meaning all samples taken were to be stored in sealed containers, eliminating any possible contaminations or alterations to the soil that could impact future analysis.

The first step in soil collection is selecting an appropriate area to take a sample from the field. Soil was not collected in impacted zones suffering from erosion, compaction or other related issues that could alter the soil's key properties. These areas can possibly include gateways, animal troughs or feeding areas, washouts as well as soil on fenced boundaries or tree lines.

When collecting the soil, all surface material such as mulch, leaf matter and any other organic matter were removed, eliminating most of the organic matter from the soil sample. Using a spade, a sample

of soil was collected that was considered perpendicular to the surface within the top 10 cm of soil, filling the selected 11L storage container. The container was then sealed using both the supplied lid that comes with the container as well as tape to ensure the box is not disturbed until laboratory experiments commenced. A label is attached to the side of the container denoting the location, date and depth.

Once this was completed, further excavation deeper into the soil was completed, collecting a second sample from this location that was from the subsoil, or 20 to 30 cm deep. Repeating the steps taken previously to ensure all samples have been collected in a similar manner. Soil containers were then transported back and stored safely in the laboratory.

Soil collection was completed on the 22nd of March 2024 in Armatree, with soil collected from three locations found on the tilled section of the farm. These locations were in the Northwest corner, Southwest corner and mid-east sections of the field. This was following high rainfall throughout late February and early March, which lead to wetter soil conditions, but was given approximately a week to dry out before collection. The soil collection in Greymare was completed on 20th of April 2024, taking samples from the sample field. Two samples were taken from the Southwest corner and the centre of the field in the northern end. These locations provided the lowest and highest ground elevations in the field, as well as the biggest difference in soil type. The collection was completed after two weeks of dry weather, leading to much drier soil conditions than those found in Armatree.

## **3.2 INITIAL SOIL EXPERIMENTS**

The collected soil samples were first documented to ensure the soil collected could be returned to the respective areas it was taken from. All soil containers were photographed for documentation and later use. The containers were also weighed with the soil inside as well as after the soil had been removed, giving a total soil weight at the beginning of the experiment phase.

The final experiment that was undertaken in this stage was finding the initial moisture content of the soil, which was completed using a microwave. Firstly, a small porcelain dish is weighed, followed

by a small soil sample being taken and placed on the dish, which is then placed in the microwave for 15 minutes. Once the sample is removed and weighed, the moisture content can be determined. This is to be completed for all ten soil samples that have been collected from both the topsoil and subsoil.

### **3.3 MAIN EXPERIMENTS**

#### **3.3.1 Overview of Soil Experiments**

There was a range of soil experiments that were conducted within this research project that are key to answering the research aims. These tests include sieve analysis and soil classification, specific gravity tests, Atterberg and shrinkage limits, compaction tests with deformation measurements, permeability tests, and saturated one-dimensional soil consolidation tests. These experiments outcomes provided key insights and information which could then be used later within the analysis stage of the research project.

#### **3.3.2 Sieve Analysis and Soil Classification**

The main use of sieve analysis in a soil context is to determine the percentage of grain sizes found within a soil sample, as well as to grade aggregates (Gupta et al., 2021). This can then be used to produce grain size distribution curves and furthermore, classify and predict soil behaviour when faced with different soil conditions (Gupta et al., 2021). The sieve analysis undertaken in this section of the methodology regards the larger grain sizes which are sand and gravel.

The first stage of the sieve analysis was to oven dry the soil sample that would be used within the experiment, which was then pulverised as finely as possible using a mortar and pestle. A 500-gram sample of this pulverised soil could then be used in the experiment, making sure to weigh and record the mass (Gupta et al., 2021). With this stage completed, the second stage included preparing the sieves, making sure all sieves are cleaned, as well as recording all sieves weights and the final pan found on the bottom. The sieves were stacked in order according to the mesh openings, for example a sieve with a 4.75 mm opening will be stacked above a sieve with a 4.00 mm opening (Gupta et al., 2021). The final stage once this was all completed was to pour the 500-gram soil sample into the top

sieve, placing the cover on top. The stack of sieves was placed on the sieve shaker, clamped down and the shaker was run for 15 minutes uninterrupted. After the 15 minutes, the shaker was stopped, all sieves were weighed with the soil still inside them as well as the bottom pan with the soil that managed to pass through all sieves (Gupta et al., 2021).

These values are then used to determine the percentage of soil that passed through each sieve, a grain-size distribution graph, as well as the uniformity coefficient, coefficient of gradation and effective size. Following this, the soils could then be classified using the Unified Soils Classification System, dividing the soils into the four major groups of gravel, sand, silt and clay. The standard used for this experiment was D6913/D6913M – 17: Standard Test Methods for Particle-Size Distribution (Gradation) of Soils Using Sieve Analysis.

### **3.3.3 Atterberg and Shrinkage Limits**

#### **Liquid Limit Test**

The liquid limit of soil is the point where soil changes its state from being free flowing to a plastic state. This is dependent on the clay minerals present in the soil, with the liquid limit also being the point of lowest shear strength of a soil. The liquid limit methodology used in this research uses a cone penetrometer to calculate it.

In this experiment, a soil sample that has been air dried was pulverised using a mortar and pestle and passed through a 0.425 mm sieve (Elementary Engineering, 2019). The experiment requires 150 grams of the sieved soil to be used, which was weighed in an evaporating dish and is then mixed thoroughly with distilled water to create a uniform paste. This uniformed paste was placed in the brass cup underneath the cone penetrometer, with no air pockets inside the cup and the surface was levelled. The cone was then lowered to the level surface of the soil paste, with this point being taken as the initial reading. This was considered the starting point, and once the penetrometer was started the cone will begin to penetrate the soil. The machine was allowed to do this for 5 seconds before the final reading was recorded. The penetration depth was taken as the difference between the initial

and final readings (Elementary Engineering, 2019). Following the experiment, a small sample of the soil paste was taken to determine the moisture content using the microwave method.

This procedure was then repeated three more times to determine a linear trendline of the data. The goal is to determine the moisture content at which the cone penetrates 20 mm in five seconds, which will give the liquid limit. The standard that was followed for this experiment is used by Mainroads Western Australia, test method WA 120.2-2020, Liquid Limit: Cone Penetrometer Method (Mainroads Western Australia, 2020).

#### Plastic Limit Test

The plastic limit refers to the point at which the soil transfers from a plastic state to a semi-solid state. Plasticity allows the soil to be moulded into any shape, with the plastic limit found to be at the moisture content at which it is just able to remain in this state. At any point past this moisture content, the soil will lose plasticity and begin to crumble.

The first stage of this experiment was to take an air-dried sample and put it through a 0.425 mm sieve, taking 30 grams of the sample and placing it into an evaporating dish (Elementary Engineering, 2019). This was then mixed thoroughly with distilled water until a consistency was reached where the soil could be rolled between the palms without it sticking to the hands but does not crack or break apart. This soil was then taken and rolled into a ball, which was placed on a glass plate and gently rolled out into a uniform cylinder. The rolling continues until the thread created is 3mm thick within 2 minutes of rolling, with the desired strokes to be approximately 80 to 90 a minute (Elementary Engineering, 2019). If the thread did not appear to crack at the two-minute mark, this was repeated until the thread began to crack at 3 mm, which was considered the plastic limit, where the moisture content is determined.

This test was completed another two times to determine the liquid limit using fresh soil each time. The average of the three moisture contents would be considered the plastic limit of the soil

(Elementary Engineering, 2019). The standard followed for this experiment is D4318 – 05: Standard Test Methods for Liquid Limit, Plastic Limit, and Plasticity Index of Soils.

Both the plastic and liquid limits could then be used to determine the plasticity index of the soils, which could then be used in the soil classification which was mentioned above.

#### Shrinkage Limit Test

The shrinkage limit is defined as the moisture content at which the soil changes from a semi-solid state to a solid state, with the volume of the soil not changing with further drying past this point.

This was determined using a soil sample of 150 grams of air-dried soil that had passed through a 0.425 mm sieve, which was thoroughly mixed with distilled water to create a paste, with an approximate moisture content of the liquid limit found earlier in the experimental phase (Vickers, 1984). This paste was then placed in a brass mould without trapping air and making sure the surface was level. This soil was oven-dried at 60°C until the paste had shrunk below the mould, and then further dried at 105°C to complete the shrinkage (Vickers, 1984). After the sample had been cooled, the sample length was to be measured. The linear shrinkage could then be calculated using the following equation.

$$LS = 1 - \left( \frac{\text{Length after drying}}{\text{Initial length}} \right) \quad [3.1]$$

The initial length is given as the height of the brass mould that was used in the experiment which was 140 mm (Vickers, 1984).

#### 3.3.4 Specific Gravity Test

The specific gravity tests allow an understanding of the ratio of mass of soil solid to the mass of an equal volume of water at a specific temperature. This generally ranges from 2.60 to 2.90 measured at 20°C and is useful to compare the density of soil solids to the density of water.

The initial stage of this method was to take a specific gravity bottle and determine its weight, followed by filling the bottle with 500 mL of distilled water and again weighing it. The temperature also had to be determined using a thermometer (Gupta et al., 2021). Using an evaporating dish, 100 grams of dried soil was taken, and distilled water was added, continuing this process until a smooth paste was produced. The paste was moved into the specific gravity bottle, adding distilled water until the bottle was approximately two thirds full.

The excess air had to be removed from the soil-water mixture, which was completed using the vacuum method (Gupta et al., 2021). The specific gravity bottle with the soil paste and water mixture inside was attached to a vacuum pump, removing all air from the sample. The sample was also agitated constantly during this period to remove any solid chunks with potential air pockets inside. The bottle was then filled with distilled water until the bottom of the meniscus touched the 500 mL mark (Gupta et al., 2021). A measurement of the combined weight of the bottle, water, and soil was then taken. Finally, the final mass of the dry soil was calculated. This procedure was repeated two further times to get an average specific gravity value (Gupta et al., 2021). The standard used in this experiment is D854 – 02: Standard Test Methods for Specific Gravity of Soil Solids by Water Pycnometer.

### **3.3.5 Standard Compaction Test**

The compaction test that has been chosen to be used in this series of experiments is the proctor test, which is used to determine the optimal moisture content and maximum dry density for a given soil with a certain compaction. The deformation of the soil sample will also be recorded throughout the compaction test for analytical use.

The proctor test used was very basic, providing the required results relatively simply. The first step was to take approximately 3 kg of air-dried soil and sieve it through a 4.75 mm sieve, determining the percentage of soil retained by the sieves (GeoEngineer, n.d.). The weight of both the initial and final soil sample was also recorded. The mould was also weighed without the collar attached. The

soil sample was then brought to the desired moisture content by gradually adding more water. This mixture was placed into the mould in three layers, with each layer receiving 25 blows per layer using a rammer, applied at a steady rate manually. The soil mass inside the mould was added to ensure some of the sample would intrude into the collar, allowing a level surface could be created (GeoEngineer, n.d.).

The collar could then be removed, stripping off the soil that pushed over the top of the mould, leaving the top of the sample level. The mould and soil were weighed together, once this was completed the soil could be removed from the mould using a metallic extruder (GeoEngineer, n.d.). The moisture content was determined for the top, middle and bottom layers of the sample. The soil could then be mixed with further distilled water to reach a higher moisture content, and the method was repeated (GeoEngineer, n.d.). The standard for this experiment is D698 – 07: Standard Test Methods for Laboratory Compaction Characteristics of Soil Using Standard Effort (12 400 ft-lbf/ft<sup>3</sup> (600 kN-m/m<sup>3</sup>)).

### **3.3.6 Vertical Permeability Test**

The vertical permeability test that is used in this research project has been built particularly for this experiment. The basic design of the equipment is a central soil chamber on a stand, with an inlet valve on the top, and an outlet valve on the bottom. Attached to the inlet valve is a 700 mm clear hose with a diameter of 25 mm, which is filled with water, giving the chamber 700 mm of head (H<sub>1</sub>). Attached to the outlet valve, another hose directs water into a container below, capturing the volume of water that flows through the soil chamber. A detailed diagram of the vertical permeability equipment can be found in figure 4.



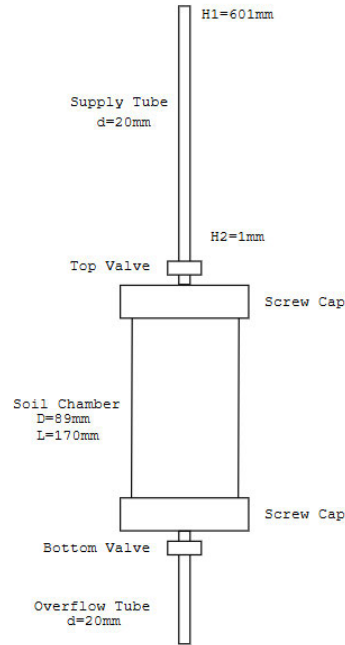


**Figure 4: Simple diagram of vertical permeability equipment used during project.**

#### Unsaturated Test

The unsaturated permeability test was completed with the soil inside the soil chamber considered unsaturated, with the initial water content being the same as when the soil was collected from the field. The first stage of this experiment was to set up the equipment, making sure it was clean and there was no soil blocking the valves or hoses connected. The sponges are also made damp prior to the experiment, meaning the water passing through it is not absorbed. The soil chamber is also filled with the selected soil type, which has not been disturbed. Finally, a second height (H2) was determined which equates to a 600 mm drop in head and was constant throughout the experiments.

The experiment could then begin, filling the supply hose to the maximum mark, giving it 600 mm of head, all while the top valve is closed. The bottom valve is opened for the unsaturated portion of the experiment. Once the top valve was opened, allowing the water into the soil chamber, the stopwatch is started, and is stopped once the head height reaches the second height. This information can then be input into the following permeability variable head equation, found in equation 3.2.

$$K_{unsat} = \left( \frac{V}{A \times \Delta H} \right)^2 \times \Delta \ln(H) \times \frac{L}{t} \quad [3.2]$$

Where  $K_{unsat}$  is the unsaturated permeability, where  $V$  refers to the volume of water in the system,  $A$  is the soil sample cross-sectional area,  $\Delta H$  is the change in head,  $\Delta \ln(H)$  refers to the change in the natural logarithm of head,  $L$  represents the length of the soil chamber and  $t$  stands for the drop time.

#### Saturated Test

The saturated test was completed in a similar manner, with the same preparation of the sample and equipment taking place. Once the 600 mm head was established, the top valve could be opened to allow the soil sample inside to become saturated, while the bottom valve remained closed. Water was continually added to the supply hose over the course of the next ten minutes to adequately saturate the sample, making sure the air bubbles coming from the sample were stopped before beginning the experiment. To begin the experiment, the head was brought to the maximum height with the top valve opened. As the bottom valve was opened, the stopwatch was started and was stopped as the head reached the established  $H_2$ . The information could then be input into the same equation as the unsaturated, which is found below.

$$K_{sat} = \left( \frac{V}{A \times \Delta H} \right)^2 \times \Delta \ln(H) \times \frac{L}{t} \quad [3.3]$$

For both unsaturated and saturated testing, the variable head permeability results were checked using constant head permeability calculations to ensure they were consistent, using equation 3.4 below.

This equation can be used for both unsaturated and saturated permeability.

$$K = \left( \frac{V}{A \times H} \right) \times \left( \frac{L}{t} \right) \quad [3.4]$$

Where  $K$  is the permeability,  $V$  is the volume of water,  $A$  is the area of the soil chamber,  $H$  is the height of head in the supply tube that stays constant,  $L$  is the length of the soil chamber and  $t$  is the time taken.

### **3.3.7 Saturated One-Dimensional Consolidation Test**

The saturated 1D soil consolidation tests that were conducted in this experimental phase were used within the water retention-characteristic analysis later in the project. The experimental procedure that was used to produce this was an oedometer, otherwise known as the consolidometer. The test aims to measure the vertical displacement of the soil sample within the device that has been subjected to a vertical load while being restrained.

The first stage of this process was to pass a soil sample through a 0.425 mm sieve to produce the fine grain particles from the soil. The oedometer's initial dimensions were taken regarding the weight, height and diameter of the mould, as well as the height and diameter of the sample. The cutting-ring was checked using a micrometer and its mass was also determined. The porous disks that will be placed in contact with the sample were boiled in distilled water. These disks were then placed either side of the soil sample within the equipment (Vickers, 1984).

The soil sample could then be added to the apparatus, making sure the two surfaces in contact with the porous disks were plane and level, using the discarded soil to complete moisture content determinations (Vickers, 1984). The complete unit must then be weighed with both soil sample and disks inside. The whole unit was then ready to be placed onto the pedestal in the loading arrangement, with the lever arm being supported and the dial gauge secured to ensure it could vertically travel to record the vertical displacement of the sample. The loading sequence to be used was standardised, starting the loading pressure at 12 kPa until the pressure reaches 200 kPa, where the unloading procedure begins. The loading and unloading procedures changed in 24-hour increments (Vickers, 1984). This test's duration was a complete week, with the water reservoir attached to be constantly refilled to ensure the sample was saturated. Once the experiment was complete, the whole soil sample was weighed and placed in an oven for 24 hours at 110°C, to determine the final moisture content and mass (Vickers, 1984). The international standard that was used for this method is the D2435/D2435 - Standard Test Methods for One-Dimensional Consolidation Properties of Soils Using Incremental Loading.

The two oedometers that were used simultaneously throughout the testing weeks were built by the same manufacturer, but did have different lengths for their lever arms, which were 50 mm long for apparatus 1, while apparatus 2 had a lever arm of length 75 mm. The following tables describe the loading pressures in the experiment, and the weight required to provide the pressure.

| Pressure (kPa) | Mass of Weights (g) |
|----------------|---------------------|
| 12             | 240                 |
| 25             | 500                 |
| 50             | 1001                |
| 100            | 2002                |
| 200            | 4003                |

**Table 1: Mass required for apparatus 1 (50 mm lever arm).**

| Pressure (kPa) | Mass of Weights (g) |
|----------------|---------------------|
| 12             | 540                 |
| 25             | 1126                |
| 50             | 2252                |
| 100            | 4503                |
| 200            | 9007                |

**Table 2: Mass required for apparatus 2 (75 mm lever arm).**

The selected method to complete the conversion from the collected deformation data to void ratio was completed using the height of the solid's method. This method allows the void ratio to be calculated using equation 3.4.

$$e = \frac{H_v}{H_s} \quad [3.4]$$

Where e refers to void ratio,  $H_v$  represents height of voids and  $H_s$  represents the height of solids.

### 3.4 THEORY OF RIEN VAN GENUCHTEN FUNCTION OF SOIL WATER RETENTION BEHAVIOUR

This research is based around the connection between the results of the soil consolidation testing completed and using those results to create a realistic soil water retention curve from the data collected, which can be directly related to Rien van Genuchten's function of soil water retention.

Both soil consolidation and the soil water retention curve use a form of pressure as the constant variable. The pressure in soil consolidation refers to the applied compression pressure that is being forced down onto the saturated soil sample, which initially dissipates the excess pore water pressure, draining the water from the soil's voids, before it is transferred directly to the soil skeleton itself.

In terms of the soil water retention curve, this research will connect the pressure applied in a soil consolidation test and suction as the common variable. With the pressure used being the constant variable, the goal will be to convert the void ratio determined from the results of the consolidation tests to volumetric water content, giving the required information to produce a soil water retention curve. The concept behind this research can be described using a sponge, with soil consolidation the sponge is squeezed, removing all excess water from the pore spaces in the sample. To create the soil water retention curve, the sponge will be acting as if it is sucking water in and attempting to fill the pore spaces, the opposite to what is occurring when consolidation occurs.

The volumetric moisture content of a soil can be given by the following equation.

$$\theta = \left( \frac{V_w}{V} \right) \quad [3.5]$$

Where  $\theta$  represents volumetric moisture content,  $V_w$  refers to the volume of water voids and  $V$  stands for the total volume of soil sample, including the solids, water and air.

Meanwhile, void ratio can be described through the relationship found below.

$$e = \frac{V_v}{V_s} \quad [3.5]$$

Where  $e$  stands for void ratio, while  $V_v$  and  $V_s$  stand for volume of voids and volume of solids respectively. This equation can be expanded further, which is described in the next equation.

$$e = \frac{V_w + V_a}{V_s} \quad [3.6]$$

Using this relationship, the volume of solids can be replaced using mass, specific gravity and density of water. This is found in the following equation.

$$e = \frac{V_w + V_a}{\left(\frac{M_s}{G_s \times \rho_w}\right)} \quad [3.7]$$

Where  $M_s$  refers to mass of solids,  $G_s$  is specific gravity while  $\rho_w$  stands for density of water, which is known to be 1 gram per cubic centimeter (1 g/cm<sup>3</sup>). Further rearrangement and substituting total sample volume ( $V$ ) and dry density ( $\rho_d$ ) in for mass of solids ( $M_s$ ), the following equation is produced.

$$e = \frac{(V_w + V_a) \times G_s \times \rho_w}{\rho_d \times V} \quad [3.8]$$

Rearranging this equation and introducing volumetric moisture content and introducing the degree of saturation  $S = V_w/V_v$ , the void ratio can be given as the following equation.

$$e = \frac{G_s \times \rho_w}{\rho_d} \left( \frac{V_w}{V} \right) = \frac{G_s \times \rho_w}{S \times \rho_d} \times \theta \quad [3.9]$$

So, under any saturation condition, the final rearrangement to be made is to make the volumetric water content the subject of the equation, which can be found in the equation below.

$$\theta = \frac{e \times S \times \rho_d}{G_s \times \rho_w} \quad [3.10]$$

Where  $\theta$  represents volumetric moisture content,  $e$  represents void ratio,  $\rho_d$  represents dry density of the soil,  $G_s$  represents specific gravity and  $\rho_w$  represents the density of water.

For saturated soils, the degree of saturation  $S = V_w/V_v = 1$ , i.e. the volume of air ( $V_a$ ) in the sample is assumed to be zero, as it was the case in all the soil consolidation experiments. Therefore, the final equation is considered to be as follows.

$$\theta = \frac{e \times \rho_d}{G_s \times \rho_w} \quad [3.11]$$

The retention curve that is created will be of a saturated soil, as the consolidation tests are completed under full saturation in the oedometer test rig. Due to the consolidation tests giving a range of pressures from 12 kPa to 200 kPa, there will not be a complete curve created through the analysis. However, this will still give a large enough curve to allow comparisons to be made and to determine whether the function created is viable or not. These comparisons will be completed using past research in the field related to soils similar to those used in this project. That will include soils with a high sand content for both soils, as well as soils with some clay content, providing comparisons for the Armatree soils. There is also potential for full soil water retention curves to be created from the partial curves created through soil consolidation.

# CHAPTER 4 RESULTS

## 4.1 EXPERIMENTAL RESULTS

### 4.1.1 Initial Soil Experiment Results

The initial soil experiment results relate to the amount of soil taken from the respective locations. These values are important to know, as the soil must be returned to the area it was originally taken from. The following tables describe both the weight of the storage containers as well as the moisture content from the field, which were determined on the 28<sup>th</sup> May, 2024.

| Greymare Locations | Depth (cm) | Mass (g) | Moisture Content (%) |
|--------------------|------------|----------|----------------------|
| Mid North          | 0-10       | 12153.8  | 13.20                |
|                    | 20-30      | 11287.1  | 11.46                |
| SW Corner          | 0-10       | 12462.6  | 9.47                 |
|                    | 20-30      | 12083.8  | 8.09                 |

**Table 3: Depth, mass and moisture content for Greymare locations.**

| Armatree Locations | Depth (cm) | Mass (g) | Moisture Content (%) |
|--------------------|------------|----------|----------------------|
| Mid East           | 0-10       | 11103.6  | 8.66                 |
|                    | 20-30      | 9833.0   | 19.89                |
| NW Corner          | 0-10       | 11008.9  | 8.78                 |
|                    | 20-30      | 9461.8   | 15.51                |
| SW Corner          | 0-10       | 9908.5   | 7.50                 |
|                    | 20-30      | 9995.2   | 15.41                |

**Table 4: Depth, mass and moisture content for Armatree locations.**



#### 4.1.2 Sieve Analysis and Particle Size Distribution Curves

The sieve analysis and particle size distribution curves were completed to allow classifications to be made for each of the soil types regarding the amount of gravel, sand and fine material in each sample. Table 5 below describes the results of this test, which was completed on the 4<sup>th</sup> of June. The particle size distribution curves as well as the uniformity coefficient (Cu) and coefficient of gradation (C<sub>c</sub>) can be found in appendix F.1.

| Locations and Depth (cm) | Gravel (%) | Sand (%) | Fine (%) |
|--------------------------|------------|----------|----------|
| Greymare Mid North 0-10  | 0.00       | 64.10    | 35.90    |
| Greymare Mid North 20-30 | 0.02       | 77.59    | 22.39    |
| Greymare SW Corner 0-10  | 0.00       | 82.35    | 17.65    |
| Greymare SW Corner 20-30 | 0.00       | 79.35    | 20.65    |
| Armatree Mid East 0-10   | 0.07       | 77.14    | 22.78    |
| Armatree Mid East 20-30  | 0.23       | 90.94    | 8.83     |
| Armatree NW Corner 0-10  | 0.02       | 78.16    | 21.82    |
| Armatree NW Corner 20-30 | 0.04       | 87.08    | 12.88    |
| Armatree SW Corner 0-10  | 0.04       | 75.62    | 24.34    |
| Armatree SW Corner 20-30 | 1.32       | 89.14    | 9.54     |

**Table 5: Particle size distribution for all locations and depths.**

### 4.1.3 Atterberg and Shrinkage Limits

The Atterberg and Shrinkage limits are important as they give an indication that at a certain moisture content, the soil will go through a phase change, from solid, to plastic and finally liquid. This information will also be used to help classify the soil types using the plasticity index. The results of this experiment can be found in table 6 below, which was completed between the 7<sup>th</sup> and 14<sup>th</sup> of June. The liquid limit graphs used for determining the moisture content can be found in appendix F.2.

| Soil Sample Location and Depth (cm): | Plastic Limit (%) | Liquid Limit (%) | Plasticity Index (%) | Shrinkage Limit (%) |
|--------------------------------------|-------------------|------------------|----------------------|---------------------|
| Greymare Mid North 0-10              | 20.06             | 24.78            | 4.72                 | 2.22                |
| Greymare Mid North 20-30             | 18.05             | 20.55            | 2.05                 | 0.96                |
| Greymare SW Corner 0-10              | 19.75             | 23.56            | 3.81                 | 1.79                |
| Greymare SW Corner 20-30             | 18.51             | 20.05            | 1.54                 | 0.72                |
| Armatree Mid East 0-10               | 17.43             | 22.99            | 5.56                 | 2.61                |
| Armatree Mid East 20-30              | 24.97             | 43.23            | 18.26                | 8.57                |
| Armatree NW Corner 0-10              | 15.67             | 24.10            | 8.43                 | 3.96                |
| Armatree NW Corner 20-30             | 22.29             | 37.92            | 15.63                | 7.34                |
| Armatree SW Corner 0-10              | 15.21             | 20.59            | 5.38                 | 2.53                |
| Armatree SW Corner 20-30             | 21.12             | 35.79            | 14.67                | 6.89                |

**Table 6: Plastic, liquid and shrinkage limit for all locations and depths.**

#### 4.1.4 Specific Gravity Test

The results of the specific gravity tests can be found in table 7 below. This result will be used in later analysis when converting the soil consolidations void ratio to volumetric moisture content. All results are expected to fall between 2.65 to 2.80, which is standard for most soil types. The data was collected between the 9<sup>th</sup> and 12<sup>th</sup> July.

| Soil Sample Location and Depth (cm): | Specific Gravity ( $G_s$ ) |
|--------------------------------------|----------------------------|
| Greymare Mid North 0-10              | 2.70                       |
| Greymare Mid North 20-30             | 2.77                       |
| Greymare SW Corner 0-10              | 2.69                       |
| Greymare SW Corner 20-30             | 2.79                       |
| Armatree Mid East 0-10               | 2.79                       |
| Armatree Mid East 20-30              | 2.74                       |
| Armatree NW Corner 0-10              | 2.71                       |
| Armatree NW Corner 20-30             | 2.70                       |
| Armatree SW Corner 0-10              | 2.75                       |
| Armatree SW Corner 20-30             | 2.67                       |

**Table 7: Specific gravity results for all locations and depths.**

#### 4.1.5 Standard Compaction Test

The compaction test for this research was completed using a standard Proctor soil compaction testing mould. The following test results, completed on the 6<sup>th</sup> of August, describe the optimum dry density and moisture content for each of the soils when compacted, which can be found in table 8 below.

The compaction graphs created can be found in Appendix F.4.

| Soil Sample Location and Depth (cm): | Optimum Moisture Content (%) | Optimum Dry Density (kg/m <sup>3</sup> ) |
|--------------------------------------|------------------------------|--|
| Greymare Mid North 0-10              | 10.523                       | 1885.7                                   |
| Greymare Mid North 20-30             | 9.937                        | 1904.2                                   |
| Greymare SW Corner 0-10              | 8.824                        | 1860.9                                   |
| Greymare SW Corner 20-30             | 8.283                        | 1878.6                                   |
| Armatree Mid East 0-10               | 7.833                        | 1886.4                                   |
| Armatree Mid East 20-30              | 9.649                        | 1743.3                                   |
| Armatree NW Corner 0-10              | 8.767                        | 1963.7                                   |
| Armatree NW Corner 20-30             | 9.736                        | 1821.0                                   |
| Armatree SW Corner 0-10              | 9.128                        | 1884.1                                   |
| Armatree SW Corner 20-30             | 8.509                        | 1881.9                                   |

**Table 8: Optimum moisture content and dry density when compacting for all locations and depths.**

#### 4.1.6 Vertical Permeability Test

The vertical permeability tests were completed between the 16<sup>th</sup> and 19<sup>th</sup> of July, the results of this experiment can be found in table 9 below. The results were determined using the equations discussed in section 3.3.6, using both constant head and variable head permeabilities to ensure the correct result is obtained. An example of the calculations of for both methods of determining the permeability can be found in Appendix F.5

| Soil Sample Location and Depth (cm): | Unsaturated Permeability (mm/s) | Saturated Permeability (mm/s) |
|--------------------------------------|---------------------------------|-------------------------------|
| Greymare Mid North 0-10              | 0.033184285                     | 0.04482911                    |
| Greymare Mid North 20-30             | 0.036987396                     | 0.049366157                   |
| Greymare SW Corner 0-10              | 0.037520868                     | 0.046454408                   |
| Greymare SW Corner 20-30             | 0.039470228                     | 0.048971903                   |
| Armatree Mid East 0-10               | 0.062525671                     | 0.100043988                   |
| Armatree Mid East 20-30              | 0.07570348                      | 0.127370544                   |
| Armatree NW Corner 0-10              | 0.065134861                     | 0.107848928                   |
| Armatree NW Corner 20-30             | 0.067016196                     | 0.090461271                   |
| Armatree SW Corner 0-10              | 0.072752328                     | 0.163239678                   |
| Armatree SW Corner 20-30             | 0.069064961                     | 0.137356394                   |

**Table 9: Unsaturated and saturated permeability results for all locations and depths.**

#### 4.1.7 Soil Consolidation Test

The soil consolidation tests completed between the 2<sup>nd</sup> of July and the 13<sup>th</sup> of August provided results of deformation and void ratio, which will be used in later analysis. The soil consolidation graphs with both loading and unloading cycles are found below in figures 5 to 14. The consolidation graphs were developed using the height of solids method for finding the void ratio. In appendix F.6, further information can be found in terms of deformation vs time graphs for each of the soils.

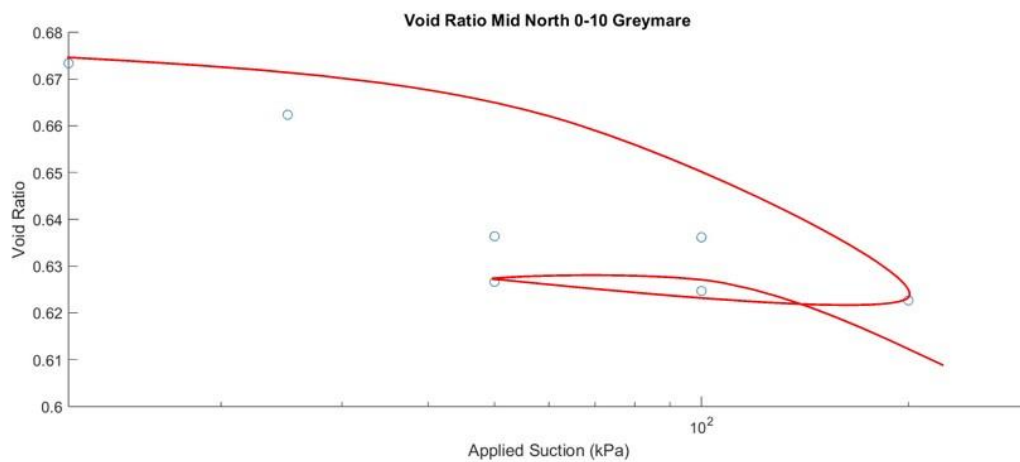


**Figure 5: Void ratio for Greymare Mid North 0-10.**

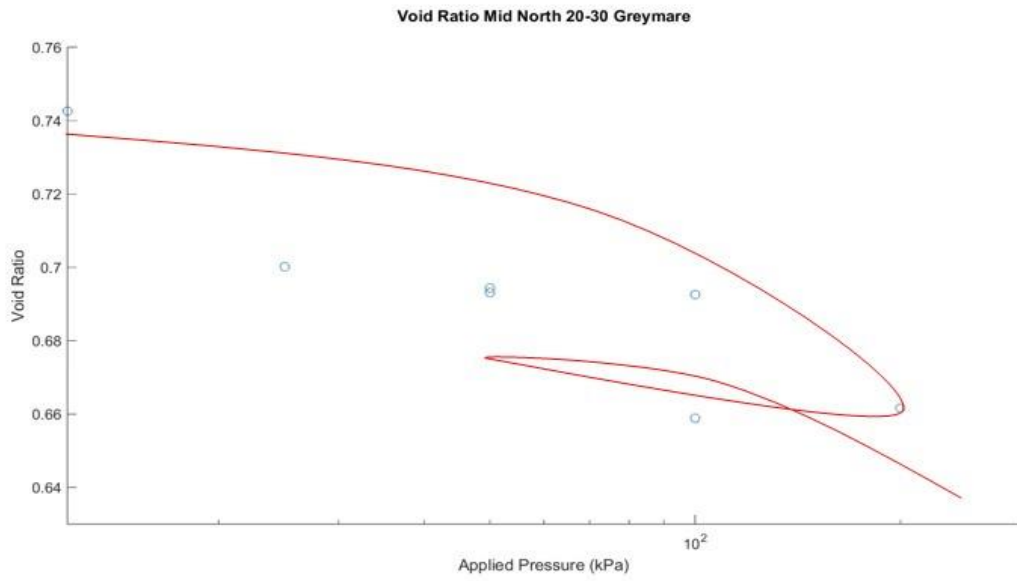


**Figure 6: Void ratio for Greymare Mid North 20-30.**

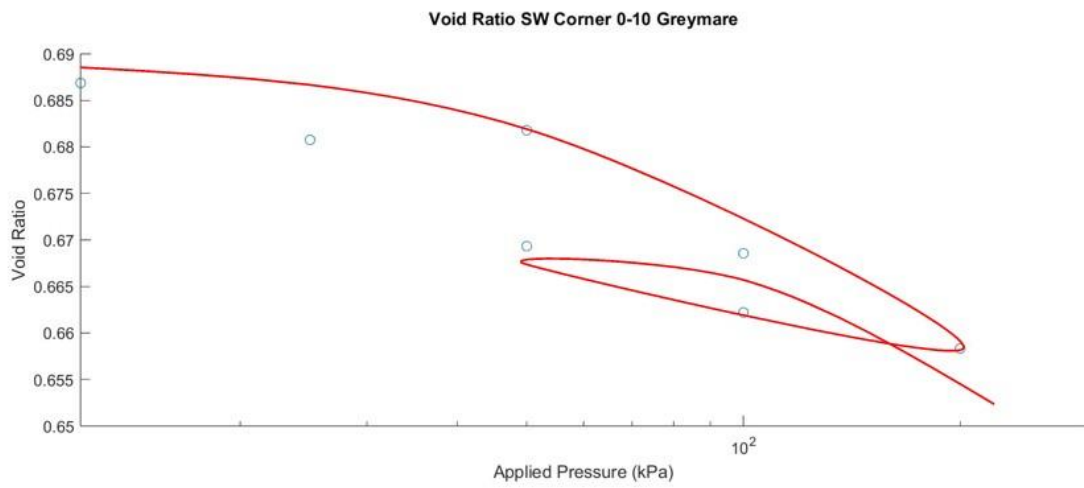


**Figure 7: Void ratio for Greymare SW corner 0-10.**

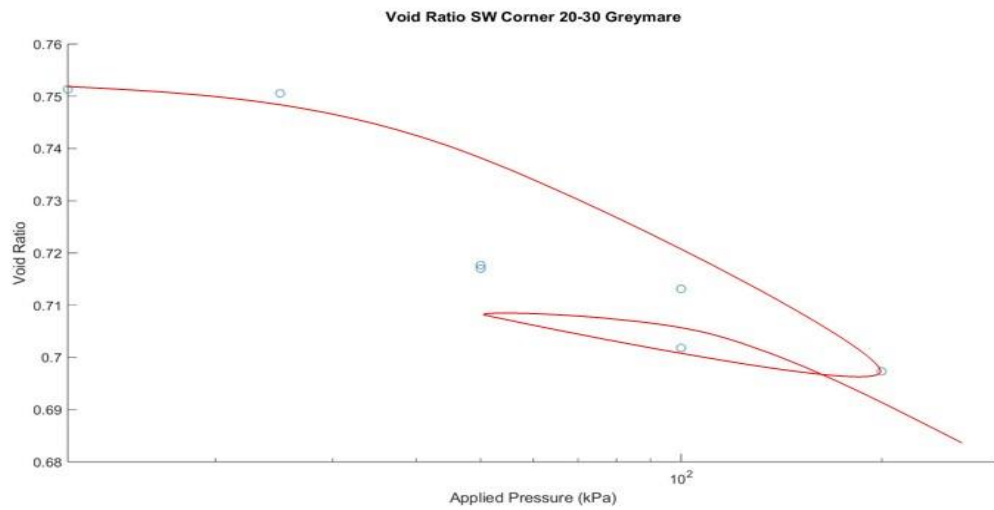


**Figure 8: Void ratio for Greymare SW corner 20-30.**

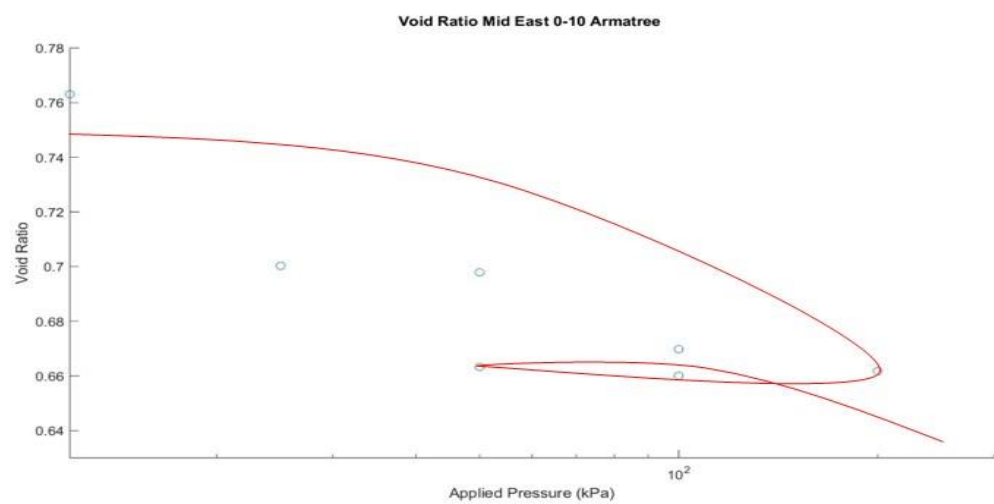


**Figure 9: Void ratio for Armatree Mid East 0-10.**



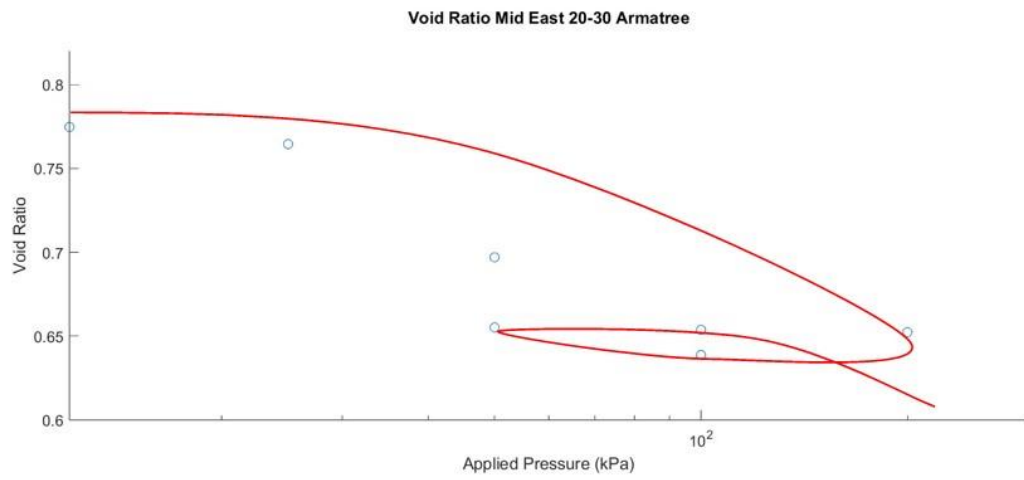


**Figure 10: Void ratio for Armatree Mid East 20-30.**

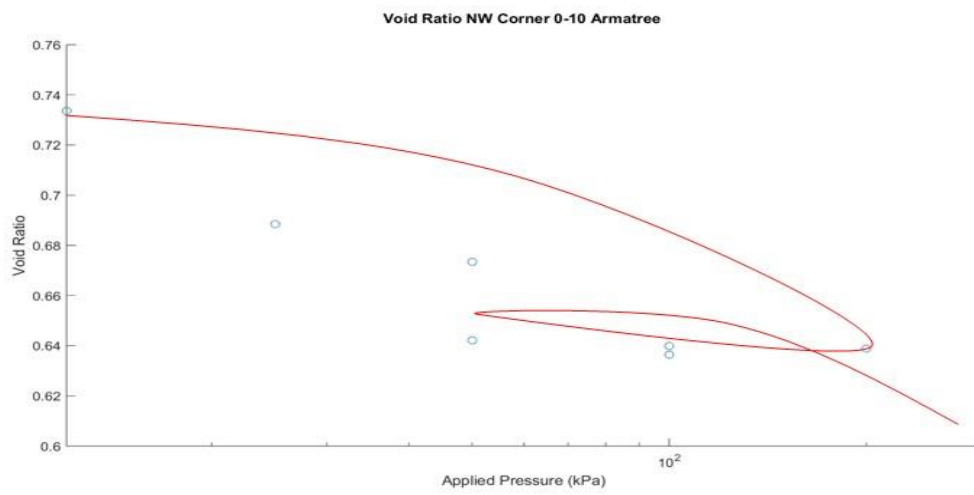


**Figure 11: Void ratio for Armatree NW corner 0-10.**

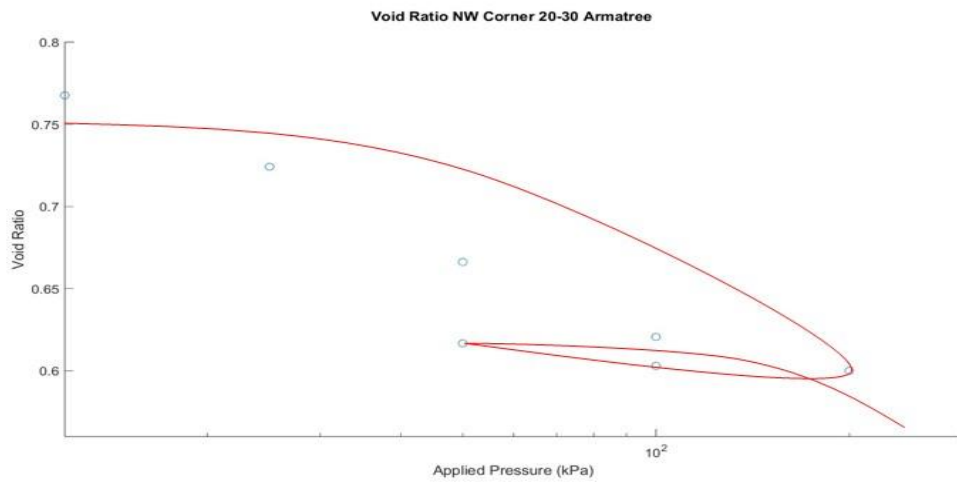


**Figure 12: Void ratio for Armatree NW corner 20-30.**

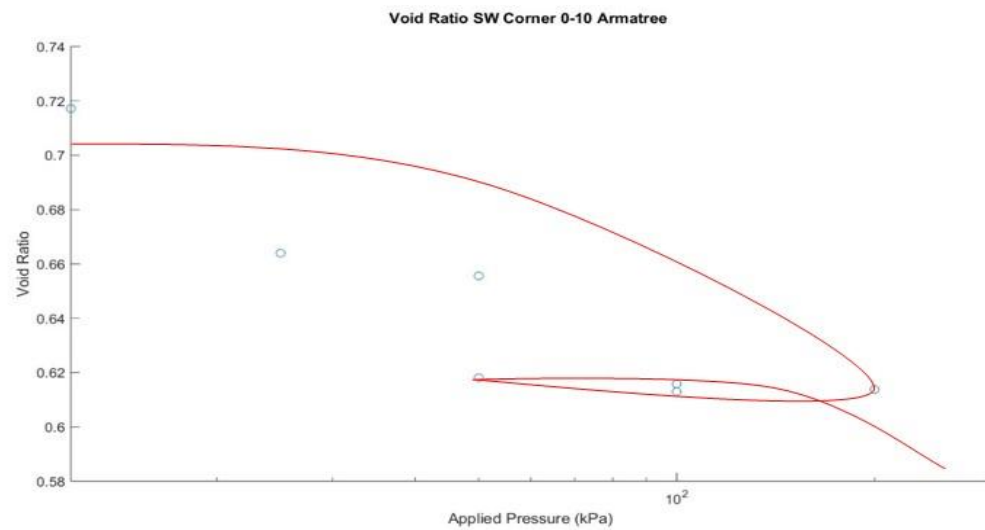


**Figure 13: Void ratio for Armatree SW corner 0-10.**

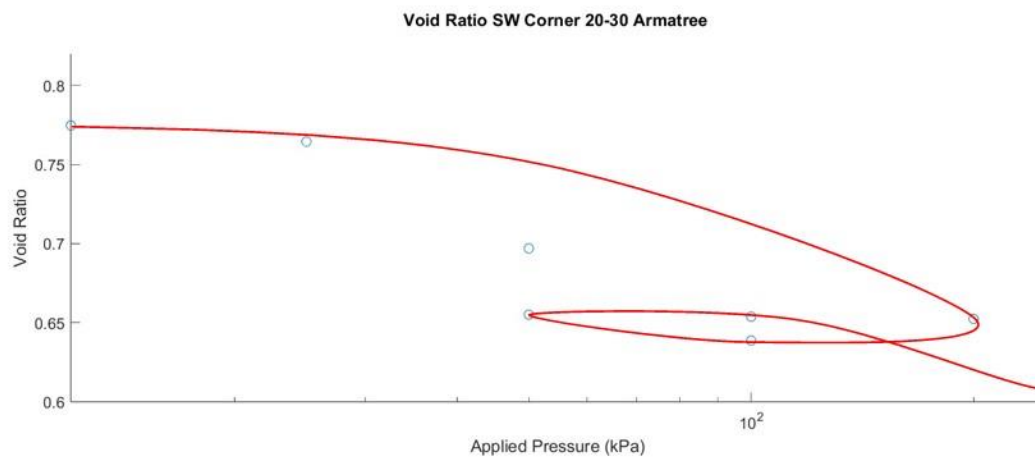


**Figure 14: Void ratio for Armatree SW corner 20-30.**

## 4.2 SOIL CLASSIFICATION

The classification of soil during this project was completed using the Unified Soil Classification System as well as the Australian Standards AS 1726 from 1993, which sorts the soils into the major groups of gravel, sand, silt and clay. Furthermore, the soils are also given a descriptor depending on different parameters. Using the results of the sieve analysis as well as the plastic and liquid limit experiments, the soils were sorted using the criteria from the USCS. The soil groups, descriptors and symbols can be found in table 10.

| Major Soil Group       | Descriptor            |
|------------------------|-----------------------|
| Gravel (G)<br>Sand (S) | Well graded (W)       |
|                        | Poorly Graded (P)     |
|                        | Silty (M)             |
|                        | Clayey (C)            |
| Silt (M)               | Low Plasticity (L)    |
| Clay (C)               | Medium Plasticity (I) |
| Organic (O)            | High Plasticity (H)   |

**Table 10: USCS soil groups, descriptors and symbols.**

All soils from both Armatree as well as Greymare returned results from the sieve analysis stating the sand content was between 64.10% and 90.94%, with the topsoil sample from the Mid North region in Greymare having the least and the highest sand percentage coming from the subsoil in the Mid East sample from Armatree. This information represents that all soils will be considered a part of the sand category in the USCS order.

To continue to classify the soils further, the plasticity index of the soils was used to determine the descriptors. For the Greymare soils, all soils except for the Mid North 20-30 sample were considered a silty sand (SM), which was a clayey sand (SC) due to its slightly higher plasticity index. The Armatree soils had much more varied soil classifications, with some soils falling between two categories. The Southwest corner 20-30 and Northwest corner 0-10 samples were considered clayey sand due to the fines content being greater than 12% and the plasticity index being greater than 7. Both the Mid East 0-10 and Southwest corner 0-10 samples were silty, clayey sands (SC-SM), as both soils plasticity indexes fell between the criteria that satisfies just one descriptor. The final soil type specified was the poorly graded-silty sand soil type (SP-SM), which was given to the Mid East 20-30 sample as well as the Northwest corner 20-30 sample. To obtain the poorly graded descriptor, both soils failed to have more than 12% fines, while having a coefficient of gradation ( $c_u$ ) less than 1. The soil was also considered silty sand as the plasticity index was within the criteria.

### **4.3 INITIAL SOIL WATER RETENTION CURVES**

Using the soil consolidation results found in section 4.1.7, the first section of each soil water retention curve could be established using the derived equation 3.10 to convert the void ratio to volumetric moisture content. The result of this calculation is found below in figures 15 to 24. These results have been determined using the raw void ratio results from the soil consolidation tests.

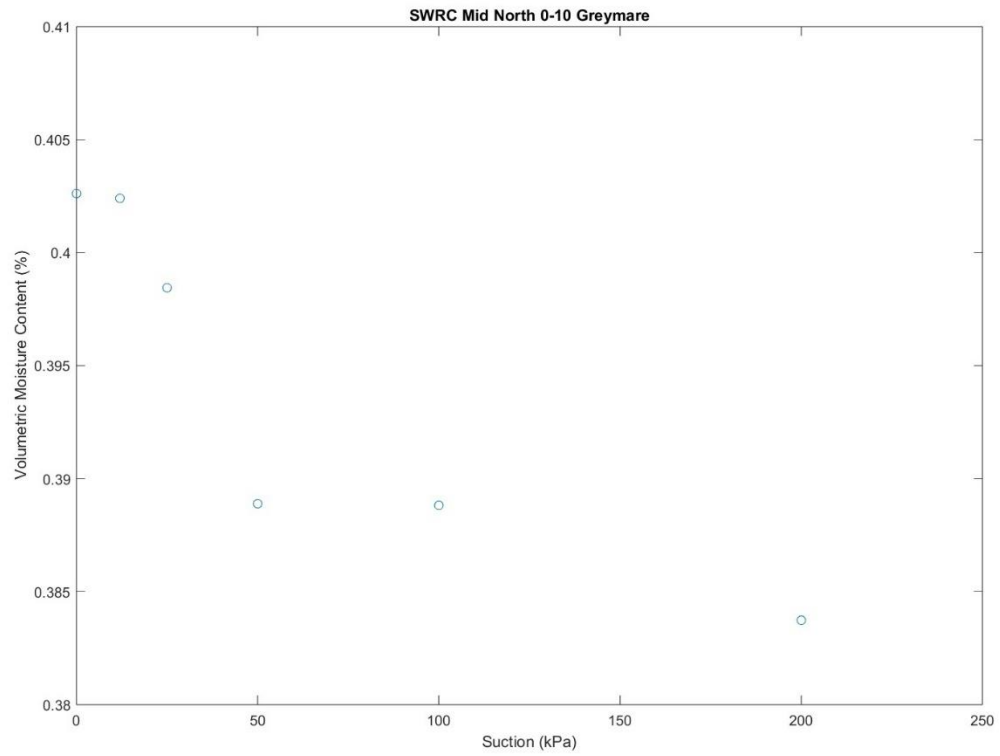


**Figure 15: Initial SWRC for Mid North 20-30 Greymare.**

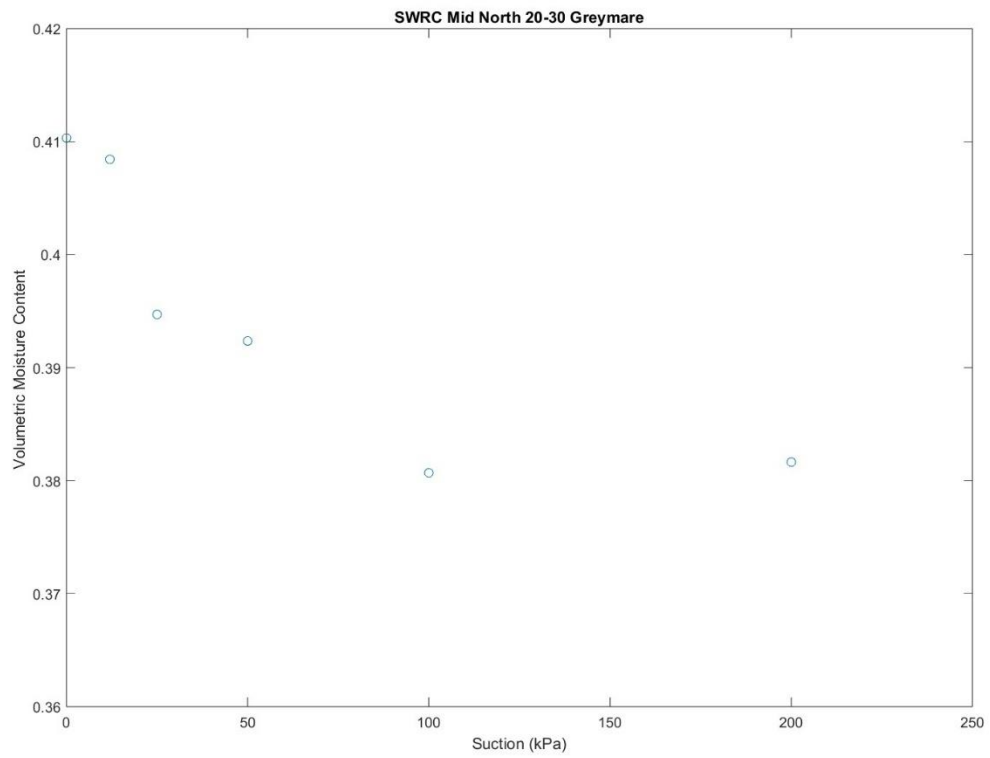


**Figure 16: Initial SWRC for Mid North 20-30 Greymare.**

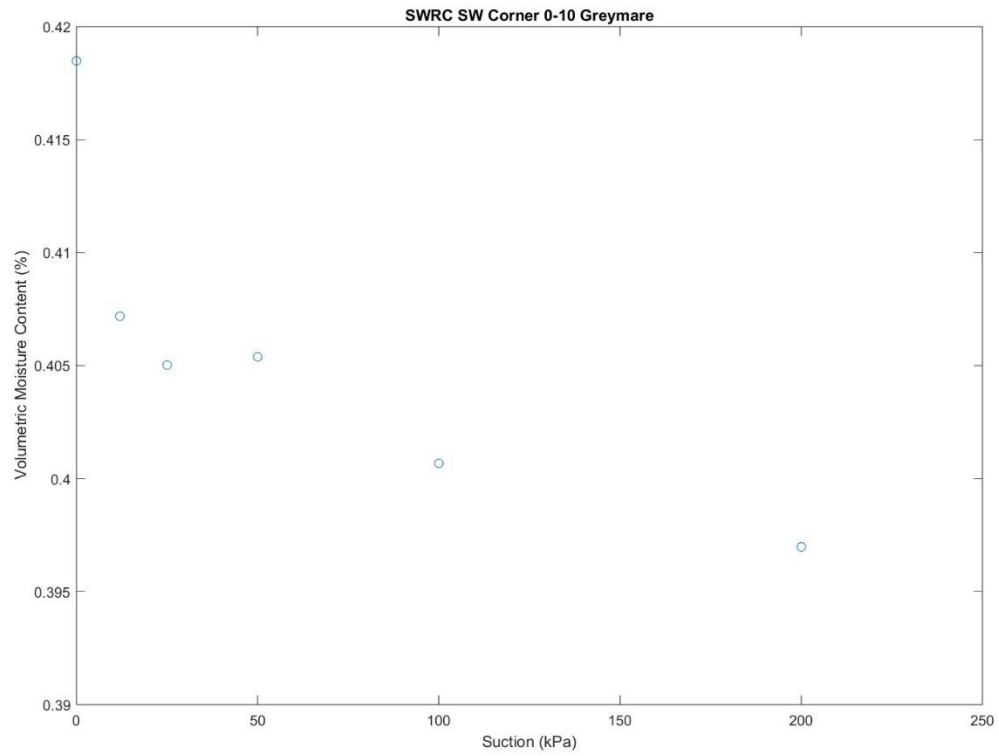


**Figure 17: Initial SWRC for Southwest corner 0-10 Greymare.**

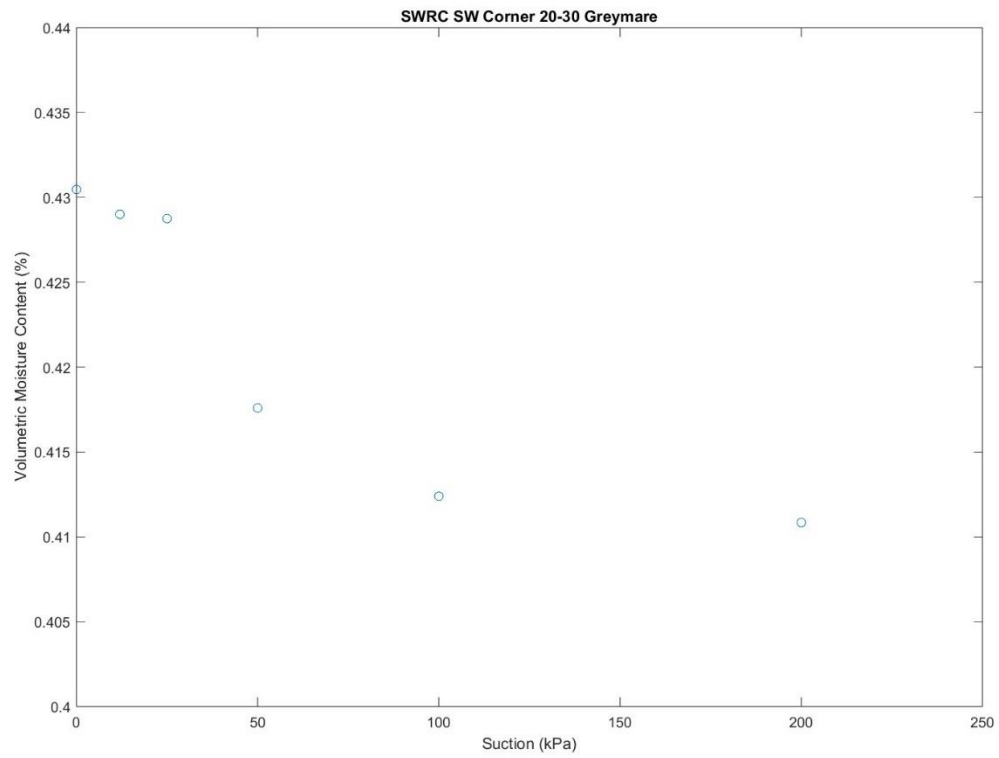


**Figure 18: Initial SWRC for Southwest corner 20-30 Greymare.**

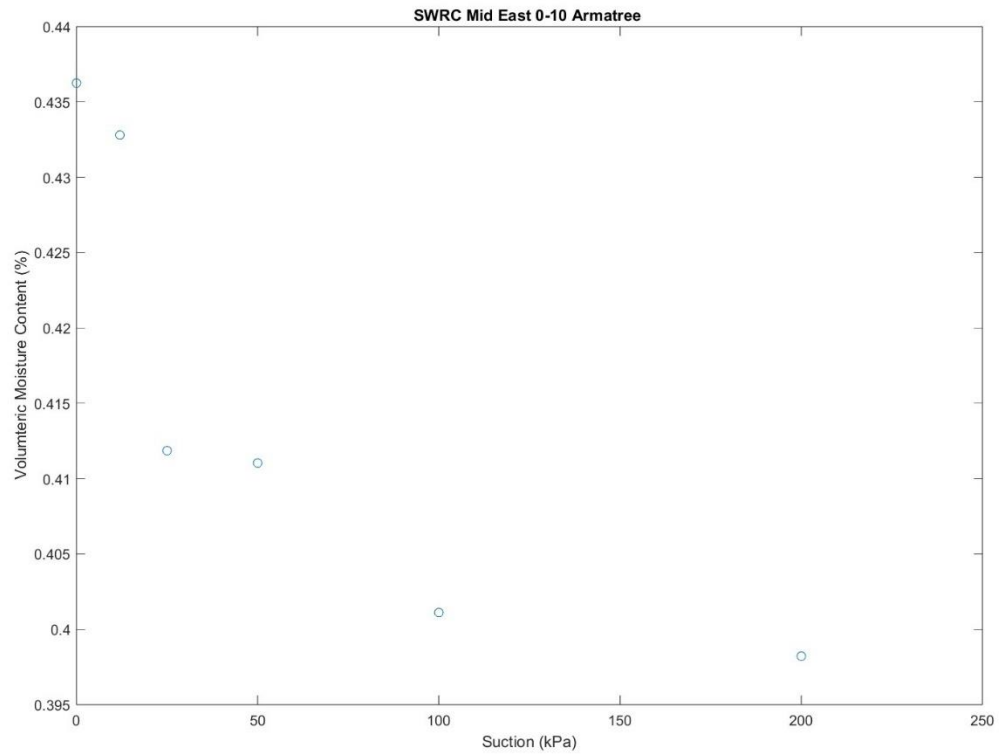


**Figure 19: Initial SWRC for Mid-East 0-10 Armatree.**

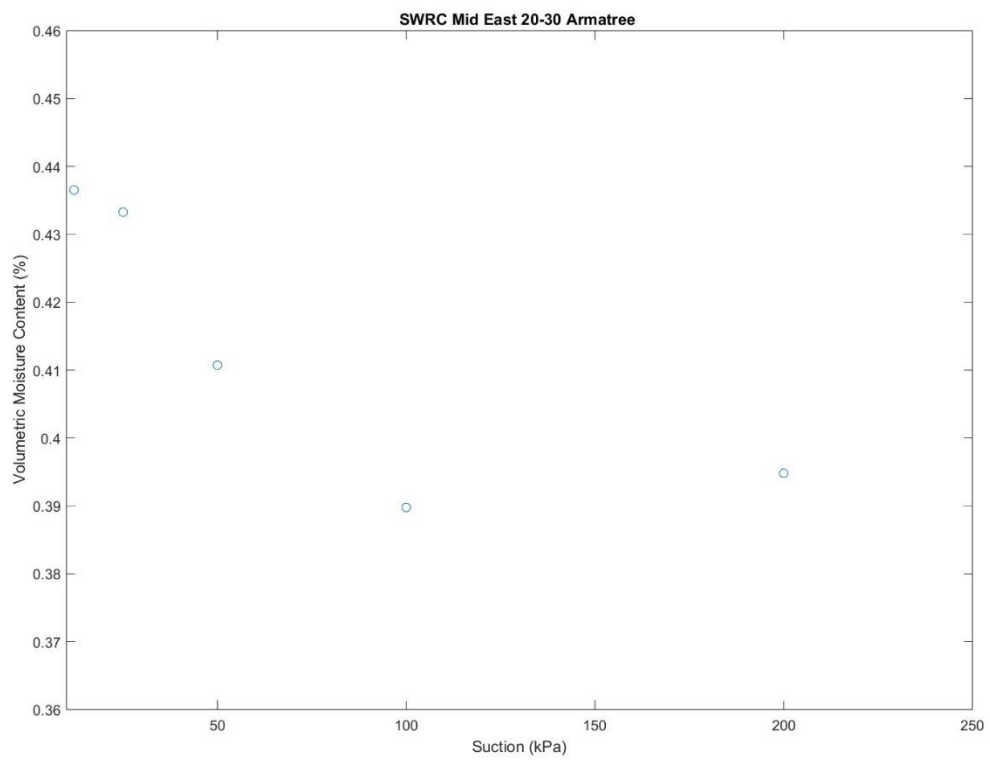


**Figure 20: Initial SWRC for Mid-East 20-30 Armatree.**

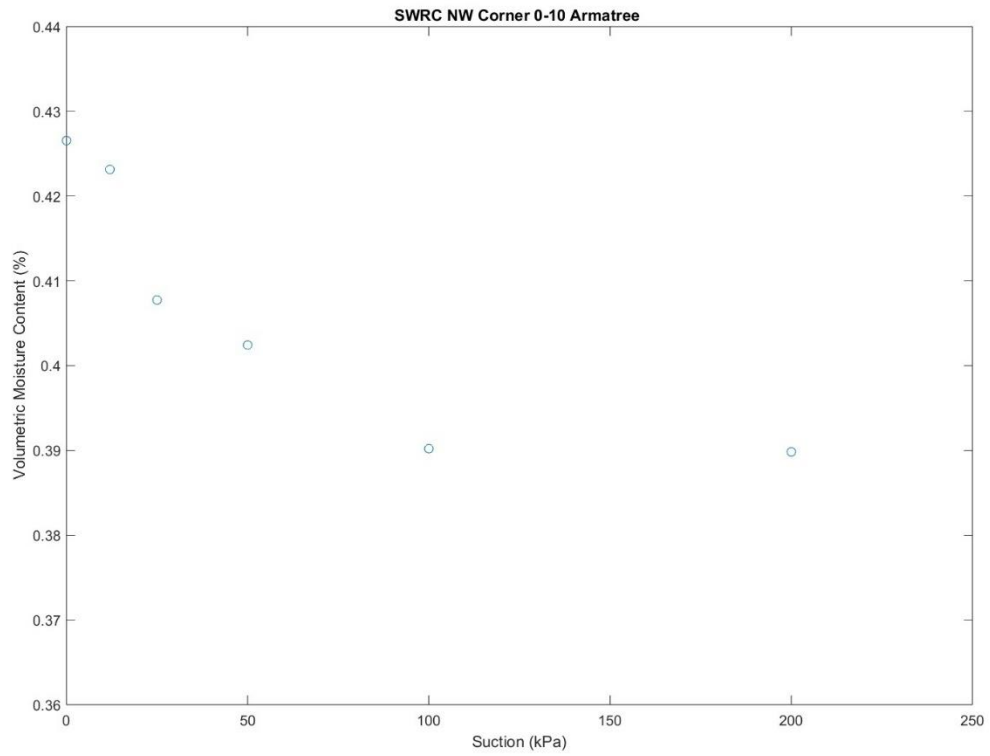


**Figure 21: Initial SWRC for Northwest corner 0-10 Armatree.**

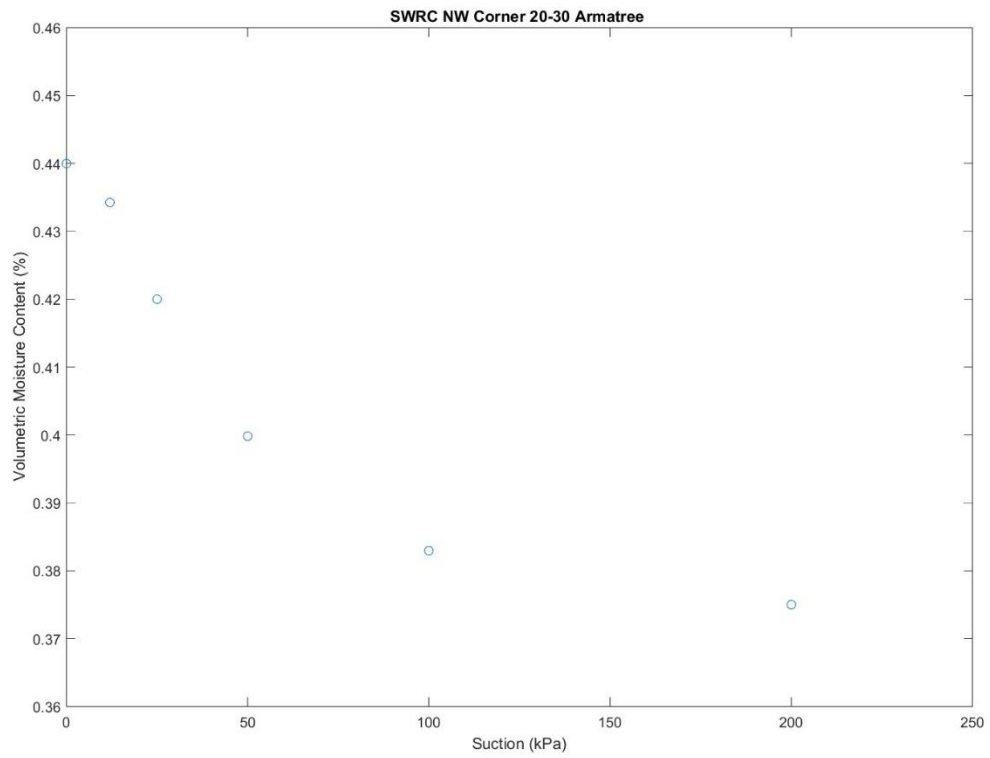


**Figure 22: Initial SWRC for Northwest corner 20-30 Armatree.**



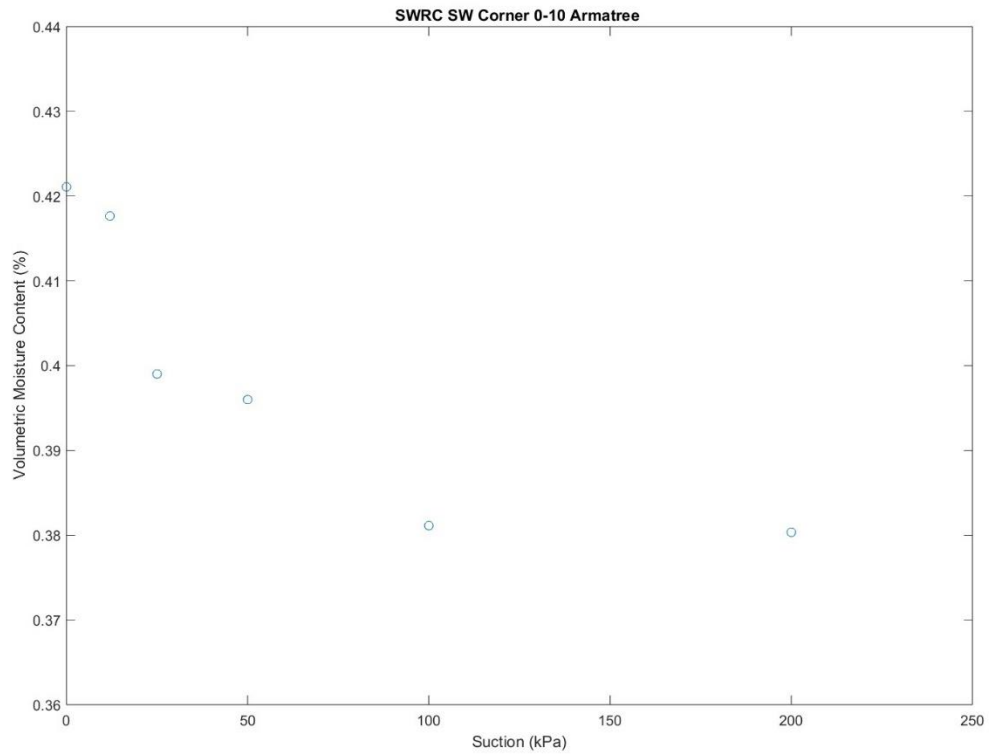


**Figure 23: Initial SWRC for Southwest corner 0-10 Armatree.**

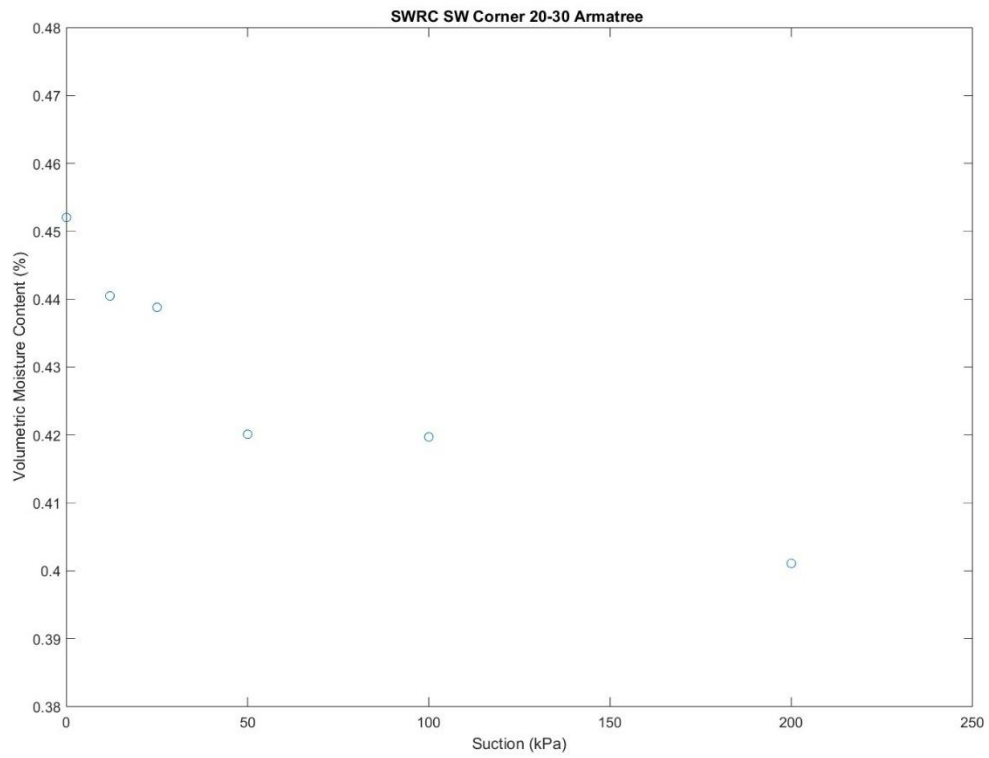


**Figure 24: Initial SWRC for Southwest corner 20-30 Armatree.**

## **4.4 REVISED SOIL WATER RETENTION CURVES**

The soil water retention curves created in section 4.3 were created using the raw data from the soil consolidation tests. The revised soil water retention curves will be created using the void ratio trend lines described in section 4.1.7, which are denoted by the red line through the data. The void ratios that will be used will be the pressure that lines up with the pressures used in this research (12 kPa, 25 kPa, 50 kPa, etc.), allowing comparisons to be made directly to the retention curves created from raw data as well as curves created using other methods from past research.

In this section, the void ratio was used as the starting point, working backwards to determine the sample height within the soil consolidation tests, which is required to find the volume of the sample, the dry density of the sample and finally the volumetric moisture content using the derived equation. By completing it this way, the only variable will be the void ratio that is determined, as all other variables such as height of solids was already determined during the soil consolidation phase. Using this method, the results determined should resemble a standard soil water retention curve to a higher standard compared to the curves created using the raw void ratio data. The results of this work can be found throughout the rest of this section. The graph of this data will be presented in scatterplots, with curve fitting to be completed in the next section using MATLABs curve fitting application.

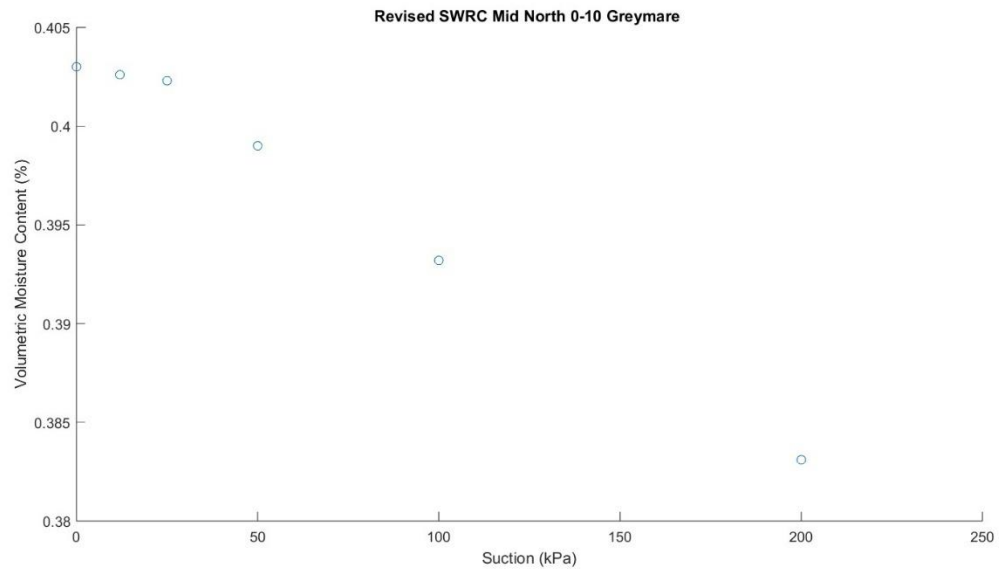


**Figure 25: Revised SWRC for Mid North 0-10 Greymare.**

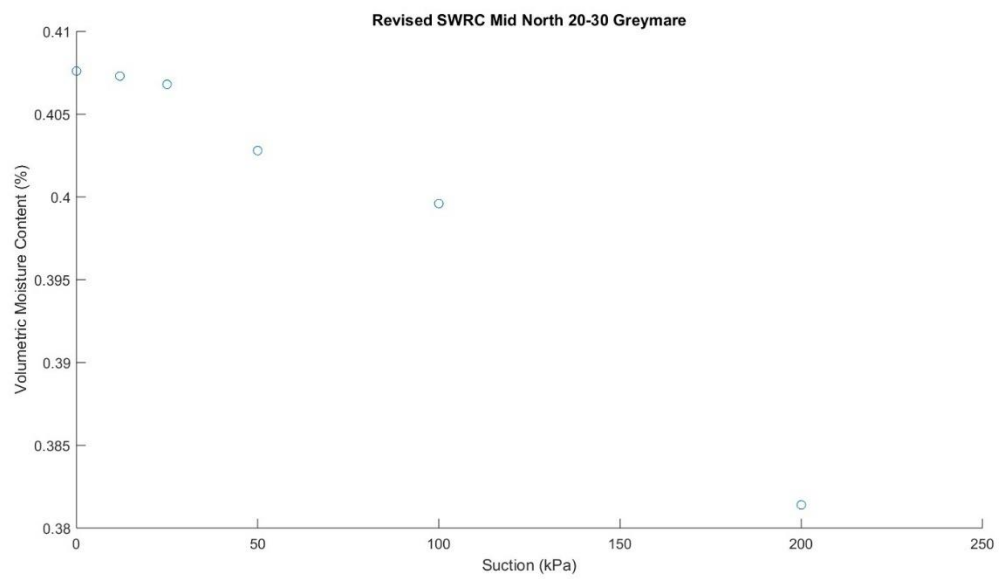


**Figure 26: Revised SWRC for Mid North 20-30 Greymare.**

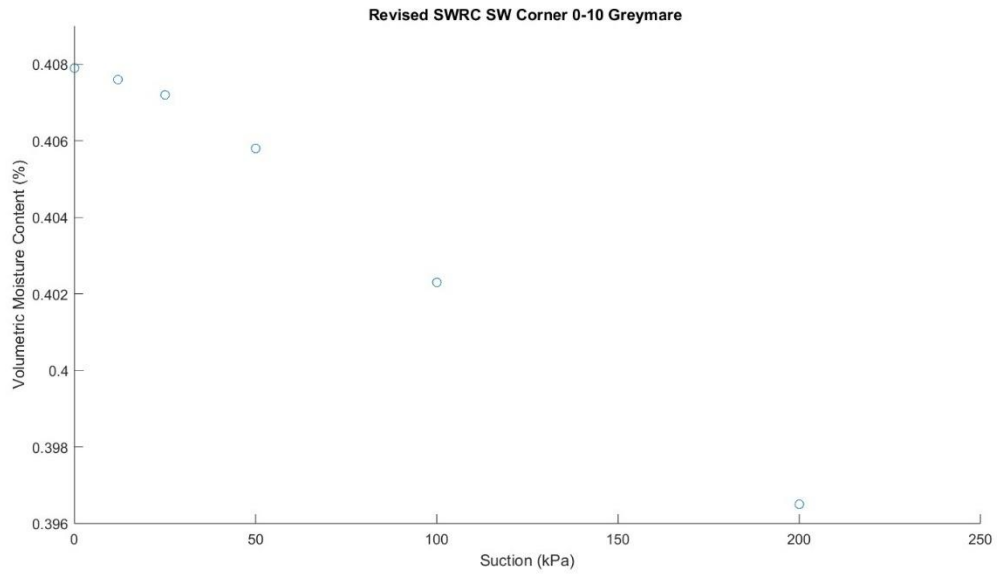


**Figure 27: Revised SWRC for Southwest corner 0-10 Greymare.**

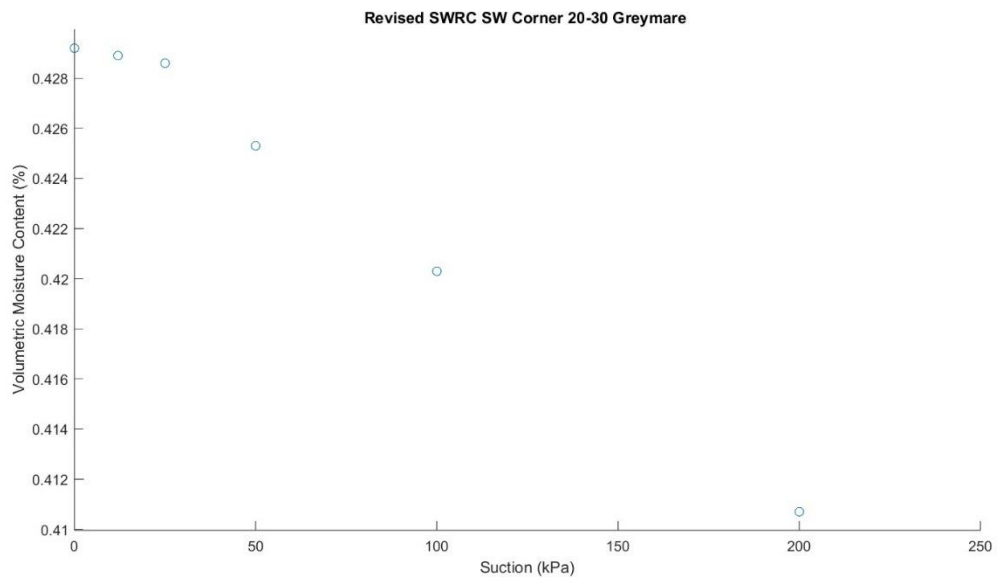


**Figure 28: Revised SWRC for Southwest corner 20-30 Greymare.**

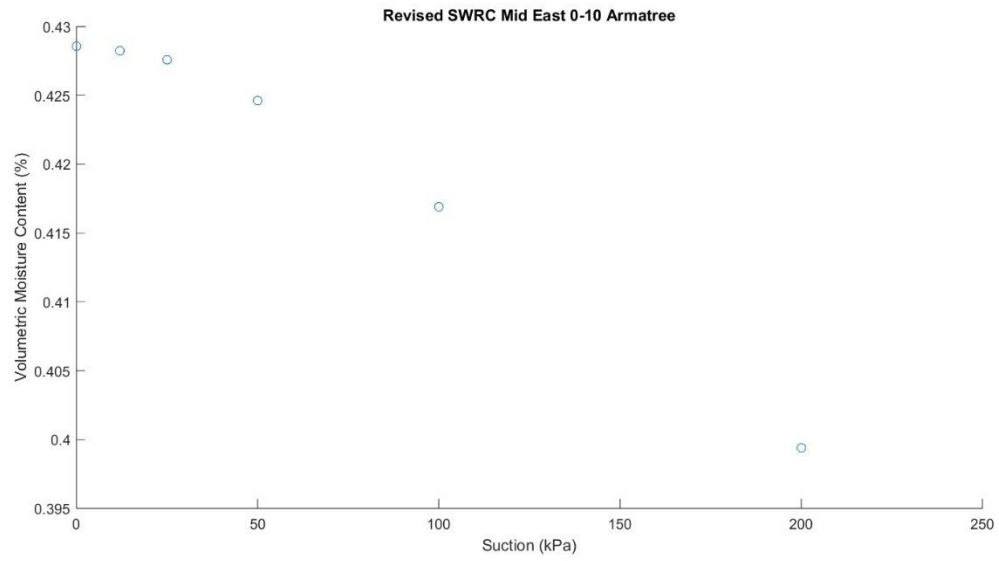


**Figure 29: Revised SWRC for Mid-East 0-10 Armatree.**

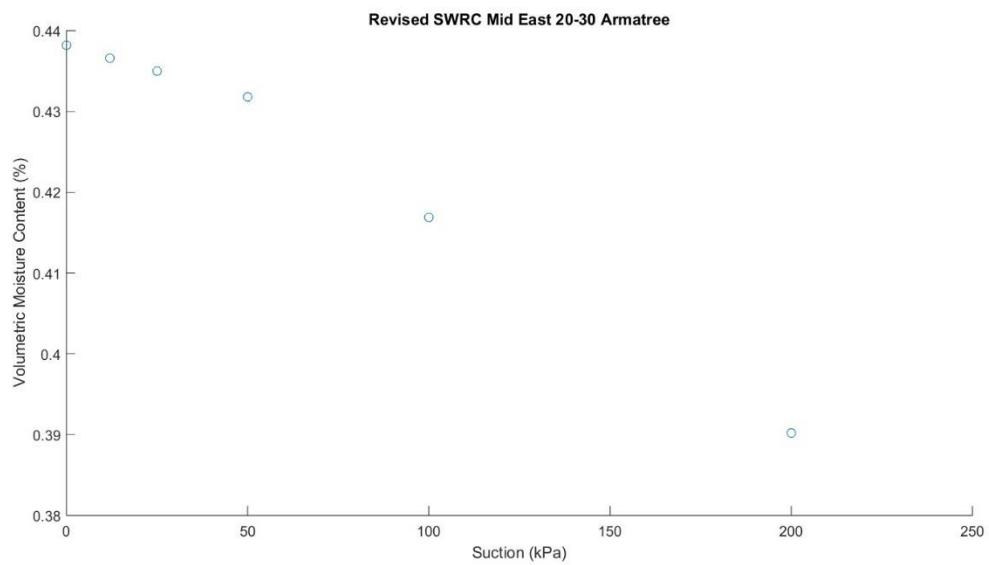


**Figure 30: Revised SWRC for Mid-East 20-30 Armatree.**

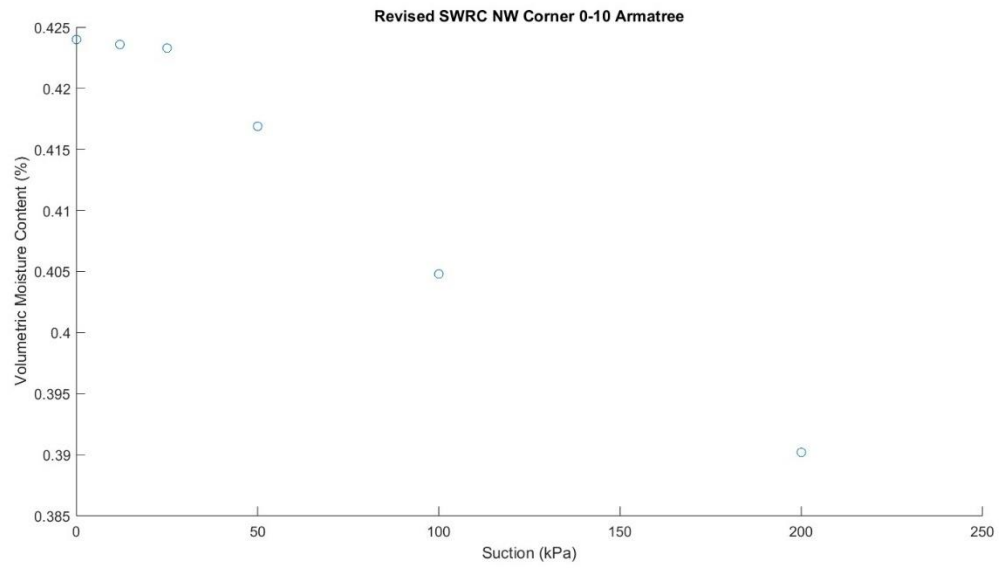


**Figure 31: Revised SWRC for Northwest corner 0-10 Armatree.**

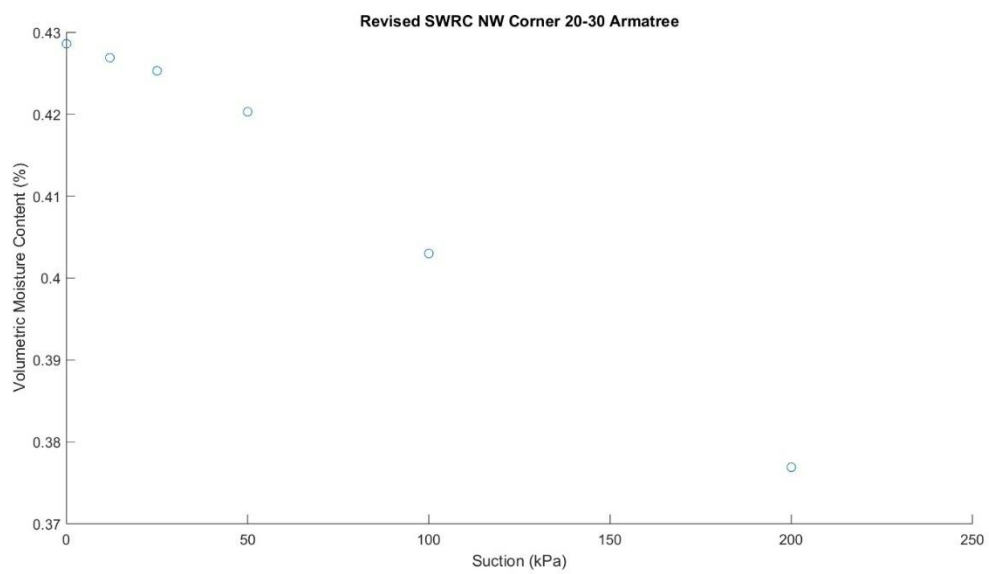


**Figure 32: Revised SWRC for Northwest corner 20-30 Armatree.**

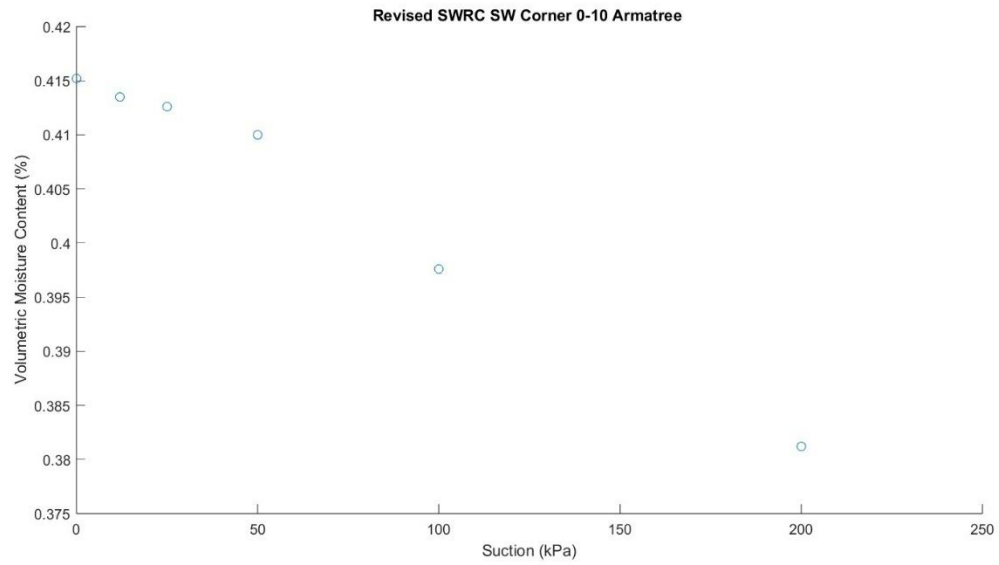


**Figure 33: Revised SWRC for Southwest corner 0-10 Armatree.**

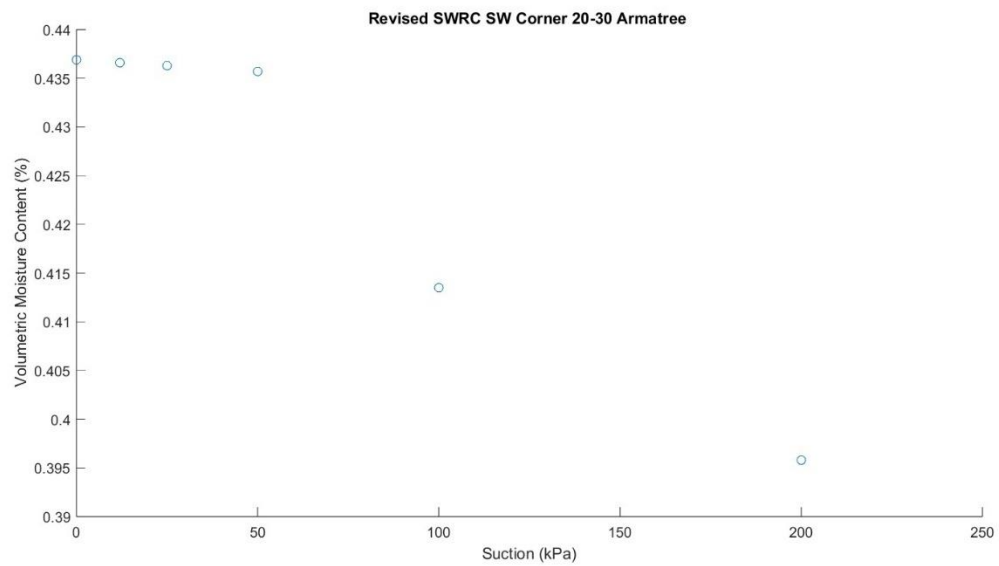


**Figure 34: Revised SWRC for Southwest corner 20-30 Armatree.**

## 4.5 CURVE FITTING FOR SOIL WATER RETENTION CURVES

With the primary section of the soil water retention curves created up until the 200 kPa of suction point, curve fitting can be applied to the data to understand the curve that has been created to a greater extent. Curve fitting allows either interpolation of the data, creating an exact fit of the data required, as well as smoothing of the data, constructing a smooth function that approximately fits the dataset. Within this section, the curve fitting type will be a smoothing function, attempting to create a smooth curve through the dataset to depict the potential soil water retention curve. The curve will allow an understanding of the trends of the data as well as how the data could be extrapolated out to form a complete curve. The curve that will be described in this section will be created for the Mid-East 0-10 soil sample from Armatree. A curve will be created for both the initial and revised soil water retention curves to show the differences between the two and can also be used later to describe why the revised soil water retention curves are much more reliable and comparable to prior research. Found below in figure 35 is the initial retention curve for the Mid-East topsoil from Armatree.

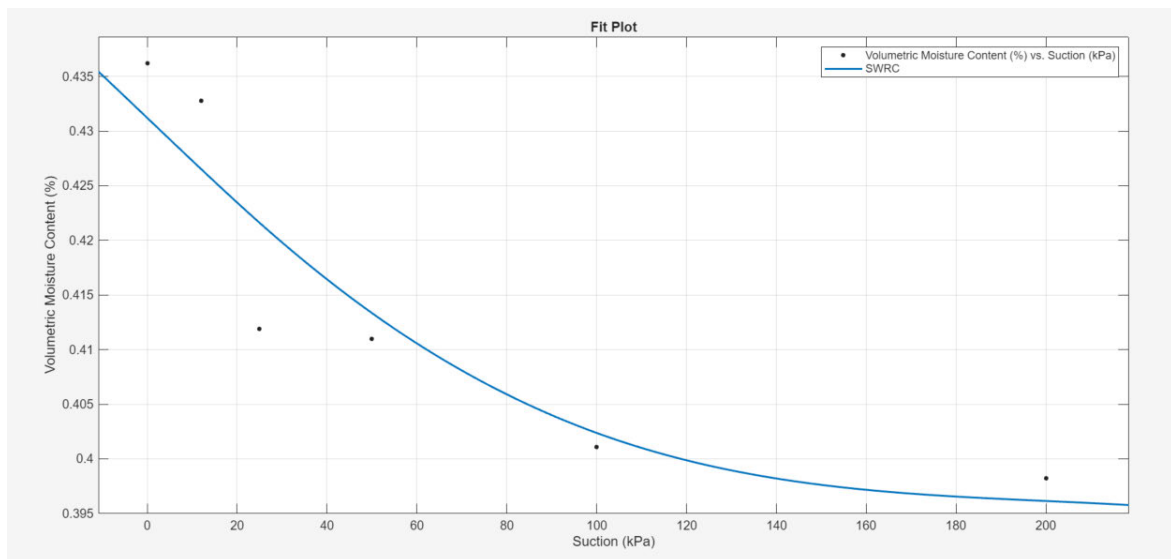
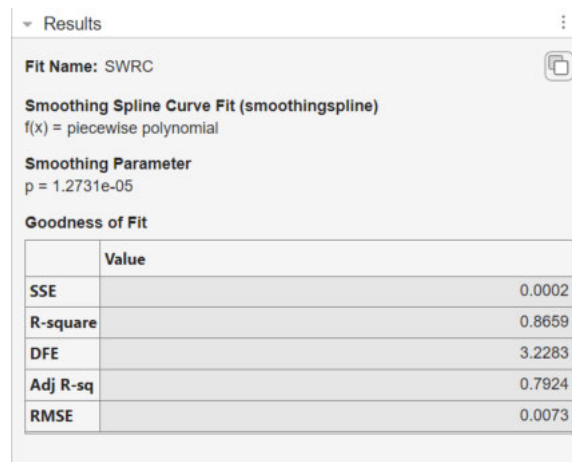


**Figure 35: Curve fitting of initial SWRC for Mid-East 0-10 Armatree.**

This curve is created using the smoothing spline function on the MATLAB curve fitting application, which uses piecewise functions as well as a smoothing parameter to create the best



fitting curve for the data, depending on the roughness or smoothness that is desired. This smoothing spline application also provides what the smoothing parameter is, as well as the goodness of fit for the curve through the use of a range of different measuring techniques. These include SSE (sum of squares due to error), R-square, DFE (degrees of freedom for error), adjusted R-square and finally RMSE (root mean squared error). These results for these different goodness of fit statistics can be found in figure 36 below. The rest of the initial soil water retention curves with the curve fitting application fitted can be found in appendix G.



|          | Value  |
|----------|--------|
| SSE      | 0.0002 |
| R-square | 0.8659 |
| DFE      | 3.2283 |
| Adj R-sq | 0.7924 |
| RMSE     | 0.0073 |

**Figure 36: Goodness of fit statistics for initial SWRC for Mid-East 0-10 Armatree.**

In terms of the revised soil water retention curve for the same sample, the curve fitting function that was best to describe the curve was not the smoothing spline, instead it was a cubic polynomial. This polynomial can be found in figure 37 below. This type of function was selected to describe the data as it provided a much better fit as well as a better understanding of the data presented as well as where the curve is heading compared to other options such as the smoothing spline or an exponential curve.

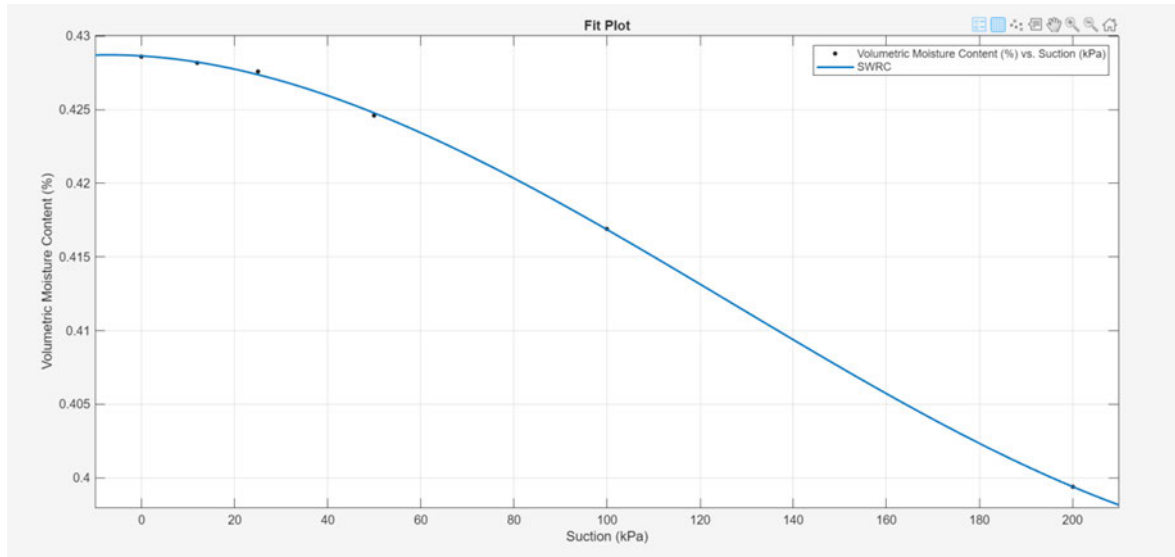


**Figure 37: Curve fitting of revised SWRC for Mid-East 0-10 Armatree.**

This cubic polynomial comprises of four coefficients which is expected, with both lower and upper 95% confidence intervals also provided using the MATLAB application. Also provided is the goodness of fit statistics again for the curve, which is all found in figure 38.

Results

Fit Name: SWRC

Polynomial Curve Fit (poly3)  
 $f(x) = p_1x^3 + p_2x^2 + p_3x + p_4$

Coefficients and 95% Confidence Bounds

|    | Value       | Lower       | Upper       |
|----|-------------|-------------|-------------|
| p1 | 3.4987e-09  | 8.5438e-10  | 6.1429e-09  |
| p2 | -1.3326e-06 | -2.0995e-06 | -5.6573e-07 |
| p3 | -1.9675e-05 | -7.2658e-05 | 3.3308e-05  |
| p4 | 0.4287      | 0.4279      | 0.4294      |

Goodness of Fit

|          | Value  |
|----------|--------|
| SSE      | 0.0000 |
| R-square | 0.9999 |
| DFE      | 2.0000 |
| Adj R-sq | 0.9997 |
| RMSE     | 0.0002 |

**Figure 38: Coefficients, 95% confidence bounds and goodness of fit statistics for revised SWRC for Mid-East 0-10 Armatree.**

By using the cubic polynomial, the goodness of fit statistics are much more reliable and a much closer fit compared to the other curve fitting options, with both the R-square and adjusted R-square

values being basically one, which is the objective. Similarly, both the SSE and RMSE are both considered to be zero or incredibly close, also indentifying a good fit for the curve. The rest of the revised soil water retention curves curve fitting results created can be found in appendix H of this research paper.

# CHAPTER 5 DISCUSSIONS

## 5.1 EXPERIMENTAL RESULTS

Atterberg Limits and Shrinkage Limits:

The Atterberg (plastic and liquid) and shrinkage limits that were determined throughout the experimental phase returned results that were expected. Beginning with the plastic limits, all outcomes fell between 15.67% and 21.12%, and the lower plastic limits were expected due to low amounts of clay in the samples. Silts and mixed sands are expected to have a plastic limit of approximately 20%, which corresponds to the samples within this project. Heavy clays can have plastic limits upwards of 45% due to their overall cohesiveness, while sands and silts produce much lower plastic limit moisture contents.

The liquid limits produced during the experimental phase were also within the desired range. A liquid limit within the range of 20% to 40% indicates a mixture of sand and silt predominantly, with most clay soils having a limit between 50 and 90 per cent. The only soil that did not result in a liquid limit within the range of 20% and 40% was the Armatree Mid East 20-30 soil sample, with a limit of 43.23%, while the other subsoils from the Armatree plot also returning limits of close to 40%. This would be due to the higher clay contents found within the samples, compared to the other topsoils or the Greymare samples. Another interesting finding was that the liquid limit of the Greymare top soils both produced a higher liquid limit compared to the subsoils beneath them. This could be due to higher organic matter content and nutrients found within the top layer of the soil, while the topsoil generally has a higher water-holding capacity as well.

The plastic limits of the soils were also determined, with all soil samples having a plastic limit of between 1% and 10%, except for the subsoil samples retrieved from Armatree. This would be due to the higher clay content found within these soils as discussed previously. These results ranged from 14.67% to 18.26%.

Finally, the shrinkage limits of the soils were also determined, with the results ranging from below 1% moisture content, to being as high as 8.57%. Once again, the subsoil samples from Armatree had much higher limits compared to sandier topsoils from the same area as well as the Greymare samples. This is considered the lowest water content at which there will be no further decrease in the volume of the soil mass. Even though the shrinkage limit is much less used compared to the Atterberg limits, it provides an interesting insight into the lowest moisture content the soil can have while a soil can still be completely saturated.

#### Specific Gravity:

As mentioned in the methodology, specific gravity describes the ratio of the density of a soil sample to the density of a standard substance, which in the experimental stage of this research was water. It is expected that finer soils will return specific gravities that are higher, compared to coarser soils. The specific gravity of the soils that were determined in this project fell between 2.67 and 2.79, with most of the soils resulting in the expected value. However, one thing to note was the fact that the vacuum pump used in the experiment was only able to achieve an average pressure reading of 0.6 bar or 60 kPa. This may have influenced the final results being slightly higher, as the air trapped within the soil voids was not able to escape as desired. However, the results achieved still fell within the acceptable range and could be used for analysis later in the project.

#### Standard Compaction Tests:

The standard compaction tests that were completed using the proctor testing method allowed the maximum dry density to be determined at an optimum water content. This test provides an insight into how the soil compacts over time, as well as the load bearing capabilities of the soils. Out of the soil samples, highest optimum moisture content that was determined was from the Greymare Mid North 0-10 sample, with the moisture content being 10.523%, while having an optimum dry density of 1885.7 kg/m<sup>3</sup>. This was the only soil that was determined to above the 10% moisture content threshold. Meanwhile, the soil with the lowest optimum moisture content was the Armatree Mid East 0-10 sample, with a 7.833% moisture content, however the dry density at this point was

still 1886.4 kg/m<sup>3</sup>. Using this information, the Armatree sample requires much less compactive effort compared to the Greymare sample, with both having a similar dry unit weight, but much more compactive energy required for the Greymare sample due to its higher optimum moisture content.

In terms of optimum dry density, the highest was calculated for the Armatree Northwest 0-10 sample, recorded a 1963.7 kg/m<sup>3</sup> dry density, which occurred at an 8.767% moisture content. Meanwhile, the lowest dry density was the Armatree Mid East 20-30 sample, with was 1743.3 kg/m<sup>3</sup>. This result may be an outlier due to the vast difference between itself and the next lowest dry density being 1821.0 kg/m<sup>3</sup>, from the Armatree Northwest 20-30 sample. However, it is consistent with the fact that the subsoil samples from Armatree all recorded lower optimum dry densities compared to the topsoil samples found above them. This may be due to all the samples unable to have a fourth moisture content to be taken, with any additional water usually creating a slurry that could not be sufficiently compacted. The method followed stated that the dry density should be calculated at moisture contents of 4%, 8%, 12% and 16%, but as stated before at 16%, the sample would turn to sludge. However, results were able to be determined from the experiment, allowing the outcomes to be accurate and reasonable compared to expected results.

The average optimum moisture content for the Greymare topsoil samples were calculated to be 9.674%, while the subsoil samples averaged 9.11%. The Armatree samples had similar results, with the topsoil having an optimum moisture content of 8.576%, while the subsoil samples returned an average of 9.298%. The main difference was the difference in topsoil optimum moisture contents. In terms of optimum dry density, Greymare topsoils had an average of 1873.3 kg/m<sup>3</sup>, while the subsoil had an average of 1891.4 kg/m<sup>3</sup>. For the Armatree samples, the topsoil samples averaged 1911.4 kg/m<sup>3</sup>, while the subsoils were 1815.4 kg/m<sup>3</sup>.

#### Permeability Tests:

The soil permeability tests provide an insight into how quickly water can infiltrate the soil, either saturated or unsaturated. The general idea with the permeability of an unsaturated soil to a

saturated soil is that the permeability increases linearly until the soil reaches complete saturation, where the permeability of the soil becomes constant.

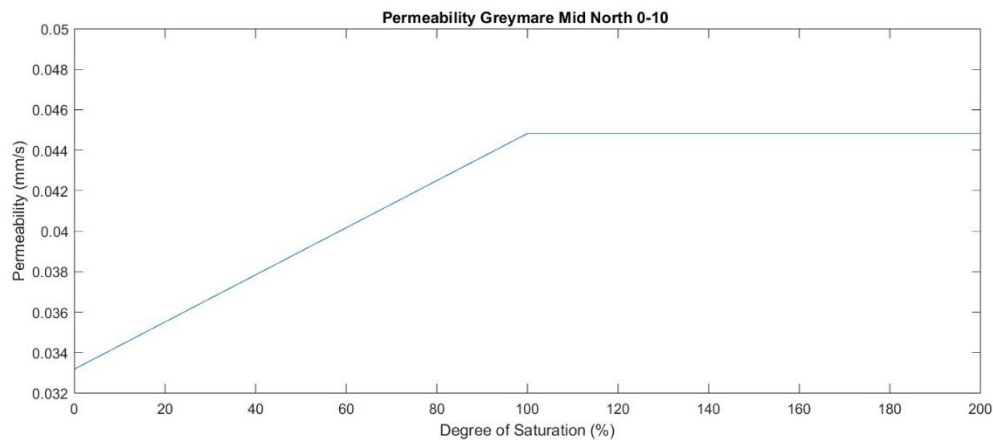


**Figure 39: Permeability plot for Greymare Mid North 0-10.**

As described in figure 39, the unsaturated permeability of the soil will always be lower than the permeability of the saturated soil. This was congruent with the vertical permeability test results, with all unsaturated soils having a lower permeability than when they're saturated. Figure 39 describes this relationship using the results obtained from the soil sample Greymare Mid North 0-10.

The permeability expected for each soil type such as gravel, sand, silt and clay vary drastically, with sand expecting a permeability of 0.1 to  $10^{-4}$  m/s, while clays can have a permeability of below  $10^{-8}$  m/s. The results of the vertical permeability test also fit within these parameters, recording values of permeability between 0.0331 mm/s ( $3.31 \times 10^{-5}$  m/s) to 0.163 mm/s ( $1.63 \times 10^{-4}$ ). The results fall between the sand and silt categories of permeability, which is expected for the high sand contents of each of the soil samples, mixed with the small amounts of finer particles such as silts and clays. The highest unsaturated permeability was calculated for Armatree Mid East 20-30, with a permeability of 0.0757 mm/s, while the highest saturated soil permeability was Armatree Southwest corner 0-10, with an infiltration rate of 0.163 mm/s. Meanwhile, the lowest unsaturated permeability was the Greymare Mid North 0-10 sample, with a rate of 0.0331 mm/s calculated, which also had lowest saturated infiltration rate of 0.0448 mm/s.

The selected method to determine the two results used the variable head equation (equation 3.2 and 3.3), however these results were able to be checked using the constant head method to ensure the results obtained were accurate, using equation 3.4 to check them. Both equations must give the same result, as both constant and variable head permeability tests are just measuring the amount of water that goes through a soil sample in a fixed time interval.

Another thing to note about the vertical permeability test was the inclusion of the sponge, mesh and spacers in the test equipment. The sponge was included to provide a porous medium between the supply hose and the soil chamber, which could then be used to determine the rate of water flow through the sponge. The mesh was used to stop any soil from reaching the sponge, stopping it from becoming filled with soil particles, while still allowing water to pass through the mesh and into the soil sample. The spacers within the equipment were used to make sure the soil sample was unable to move within the whole test rig, being confined to the desired area. They were also used to give the capped ends of the equipment something to seal against, stopping water from leaking either through the removable top or bottom caps.

#### Soil Consolidation Tests:

The soil consolidation tests were completed as per the standards, producing results that were expected in terms of the void ratio. The standard method of converting the deformation data across to void ratio was completed using the height of solid method, first determining the height of voids and solids individually, before using equation 3.4, dividing the height of voids by the height of solids. Alternatively, there are different methods to complete this but would've required further experimentation and data collection. With the chosen method, the values required were simple to either measure or determine.

Most of the consolidation curves produced from the experiments created a typical curve. The loading curves created included both the initial and primary consolidation of the soil samples, which looks to remove pore pressure within the samples. At each loading point, the pore pressure is assumed to be zero as after 24 hours, as it is impossible to completely remove all pore water



pressure within the sample. Another concept that was not considered within this research was the concept of creep, which is known sometimes as secondary consolidation. One strange occurrence was the void ratio at 100 kPa for the Armatree soil sample Mid East 20-30. The void ratio for this pressure was much less than the void ratio at 200 kPa. This could be due to a multitude of reasons, but the main reason would most likely be due to error from the recording equipment or may be due to human error. A similar issue occurred a lower scale for the Southwest corner 0-10 sample from Greymare when the pressure increased between 25 kPa and 50 kPa. Once again this is most likely to some type of error, but the data is still reasonable and can be used to determine an appropriate consolidation curve for the soil sample.

Another area to note is the unloading curves for the subsoils from Greymare. Both unloading curves rebounding steeply, which is unlike all other soil types as well as the expected unloading curve for any soil. As stated, all other soil samples produced results that were consistent and accurate when compared to other research and papers. This could have occurred due to roots or other organic materials found within the sample, which should have been removed during the preparation stage of the experiment. Another reason for this could be due to drastic swelling, however this would be highly unlikely due to the soil's classification. This again could be down to human or instrumental error.

## **5.2 INITIAL SOIL WATER RETENTION CURVES**

The soil water retention curves created using the raw soil consolidation results were within the criteria determined from the research already conducted within the field. The soils all had a slightly higher volumetric moisture content at 1 kPa of suction, which was expected compared to the standard sandy soil curve in figure 1. The subsoils from the Armatree location all had higher initial volumetric moisture contents compared to the corresponding topsoils as well as the Greymare samples, as the subsoils contained slightly more clay particles. The data then initially steeply declined before gradually beginning to smoothen out at the 200 kPa mark. There were some outliers, mainly related to the void ratio data that was already stated as being an error due to human or system influence.

The results produced however were not comparable to many retention curves created through either experimental methods using the discussed approaches or through different models such as Van Genuchten. However, this would mainly be due to the use of the raw results produced by the soil consolidation tests. Knowing this, it was decided that a second set of retention curves would be created using a trendline curve through the void ratio data, smoothening the dataset and producing much more consistent and reliable results.

### **5.3 REVISED SOIL WATER RETENTION CURVES**

The revised soil water retention curves that were created using the fitted curve through the data was much more accurate and useful. Instead of the volumetric moisture content reducing drastically as it had done with the initial set of curves, the curve begins with an almost flat section to begin with, before the data begins to curve down as the suction pressure reaches a point between 25 kPa and 50 kPa. As expected, across the curves the Armatree soils samples produced higher initial moisture contents which would most likely be due to the slightly higher clay percentage found within them. The only Greymare sample to have a higher initial volumetric moisture content was the Southwest corner subsoil sample, which is not that surprising with the clay pan found just below the 20-30 cm depth within that field.

The soil sample that produced the highest initial volumetric moisture content was the Mid-East subsoil sample, with a moisture content of 43.82%. Meanwhile the lowest found was the Greymare Mid-North topsoil sample, with a volumetric moisture content of 40.29%, however both the subsoil at this location as well as the topsoil from the Southwest corner in Greymare had similar moisture contents around the 40% mark. Overall, the initial moisture contents found were similar to what was expected when comparing to other retention curves.

In terms of the remaining sections of the curves that were created, they were as expected. All of the curves were very flat up until approximately 25 kPa of suction, which is where most of the curves began to decline smoothly. An outlier in this phase of the curves was the subsoil sample from the

Southwest corner of the Armatree field, as the volumetric moisture content at 50 kPa of suction continued this flat section of the curve. Other samples such as the Mid East 0-10 and 20-30 samples also had a relatively high volumetric moisture content at 50 kPa, but the Southwest corner 20-30 sample from Armatree was the standout of the curves.

Moving into the higher pressures reached during this simulation of soil water retention curves, there were two distinct ways that the curves finished. For example, many of the curves smoothly transitioned through the pressures, creating a gradual reduction in volumetric moisture content as the pressure increased. On the other hand, there were some samples that produced a fairly rapid decrease in volumetric moisture content. This was produced again by the Southwest corner subsoil sample, with the reduction in moisture content being quick compared to many of the other soil samples.

Overall, the curve shape created by the void ratio equation produced results that could be compared against other similar soils, determining whether the results obtained in this research could be used in the future, which will occur in the next section. Compared to standard models of the soil water retention curve however, such as figure 1, the results are well within the desired range, landing above a completely sand soil, but below a completely silt soil. This is expected as the soils used within this project were sandy loams, having a makeup of varying amounts of silt and clay. There is also a case for some of the soils to also be a loamy sand, with some soils being made up of much more than 75% sand. This would also explain the continuing of the initial flat section of the curves, before decreasing around the 25 kPa mark, and the more gradual decreasing after the 25 kPa mark, due to the clay and silt found within the samples.

## **5.4 COMPARISON BETWEEN REVISED SOIL WATER RETENTION CURVES AND EXISTING RESEARCH**

There is a fairly large range of past research and knowledge that can be drawn upon to compare the results of this project with to understand whether the results are viable or not. This comparison is

being made due to the inability to conduct a known laboratorial experiment due to a range of different constraints to create a soil water retention curve for the given soil samples used within this research. There will be no exact match for the soil types used within this research, with each soil type having its own unique curve due to the characteristics of the soil. Also note that there is not much direct research into the soil water retention curves of tilled agricultural soils, however, there has been a small amount that can be drawn upon. Another note is that much of the research is not completed with the units used within this project, which will also be considered. Finally, the revised soil water retention curves created do fit within the criteria for a standard retention curve, as described by figure 1.

The first of these comparisons is taken from research paper called ‘Soil-water characteristic curves and their estimated hydraulic parameters in no-tilled and conventionally tilled soils’, which was conducted to compare how different tillage techniques impacted a soils soil water characteristic curve and their hydraulic conductivity using Van Genuchten’s modelling (Jabro & Stevens, 2022). The testing produced results for a sandy loam soil at depths of 0-15 cm and 15-30 cm respectively, much like this research. It should also be noted that the sand contents of these soil samples are 71% and 64% respectively, while the silt and clay contents are quite evenly distributed at around 13% each for both soils (Jabro & Stevens, 2022). The result of this research is found in figure 40.

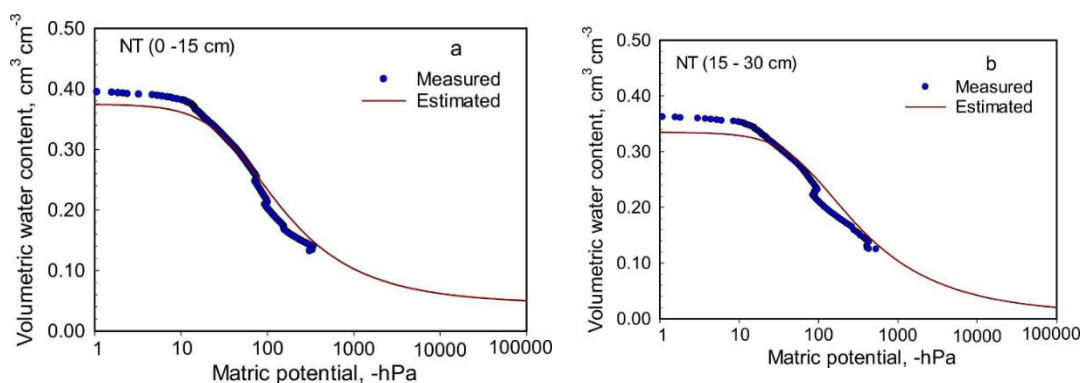


**Figure 40: SWRC for sandy loam under conventional tillage practices.**

The soil water retention curves created in this research compared to these curves are by comparison quite similar, with the experimental volumetric moisture contents being very similar. The experimental equipment used to collect this was the HYPROP assembly, which is a method that uses tensiometers. The moisture content however is dropped when estimated using the modelling function which is to be expected. The drop in volumetric moisture content is also very similar, with the curve slowly decreasing until a point between 25 and 50 kPa where the decrease begins to gradually become steeper. This comparison between the revised retention curves and the curves presented within the study are incredibly similar, which does mean the curves created within this project could possibly be correct or could have at least created reasonable results.

The second comparison between past research and this project is using soil water retention curves created in a research paper called, 'Errors in water retention curves determined with pressure plates: Effects on the soil water balance' (Solone et al., 2012). This research was used to inspect the errors presented when soil water retention curves were created using two different pressure plate techniques. The research produced two curves using the two methods, with one using just Stackman tables and pressure plate apparatus, while the other used the same equipment as well as a dewpoint meter. It was stated that the dewpoint meter method was much more accurate, which is why the results from this project will be directly compared to them (Solone et al., 2012). The soil water potential in this research was recorded in meters of head, meaning the conversion to suction in terms of kilopascals is 9.8 kPa to every meter of head. Found below in figure 41 are the results from the research paper.

The results from this research project compared to the papers is quite similar for the more comparable soil types. The most comparable soil is the loam soil found in the bottom left corner, with the soil water retention curve beginning just below the 40% volumetric moisture content where most of the soil retention curves from this project begun. The curve is also very similar up until the 200 kPa point, which is the only section of curve comparable. The curve seems to drop at a very similar rate

to the curves created in this project as well, which furthers the possibility that the results created through the soil consolidation method could create results that are accurate.

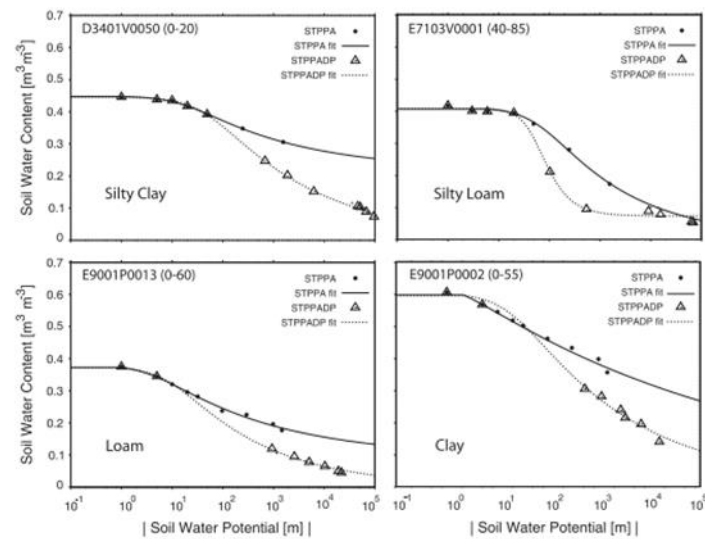


**Figure 41: SWRC for different soil types using pressure plate methods.**

The final comparison that will be drawn upon to compare the results of this project with past research results is found in a paper published under the name, ‘A simple method of estimating soil-water characteristic curve using point pedotransfer functions’ (Zou & Leong, 2019). Within this research paper, pedotransfer functions were used to create soil water characteristic curves for a range of soils, both coarse and fine grained. The results of this research can be found in figure 42 below.

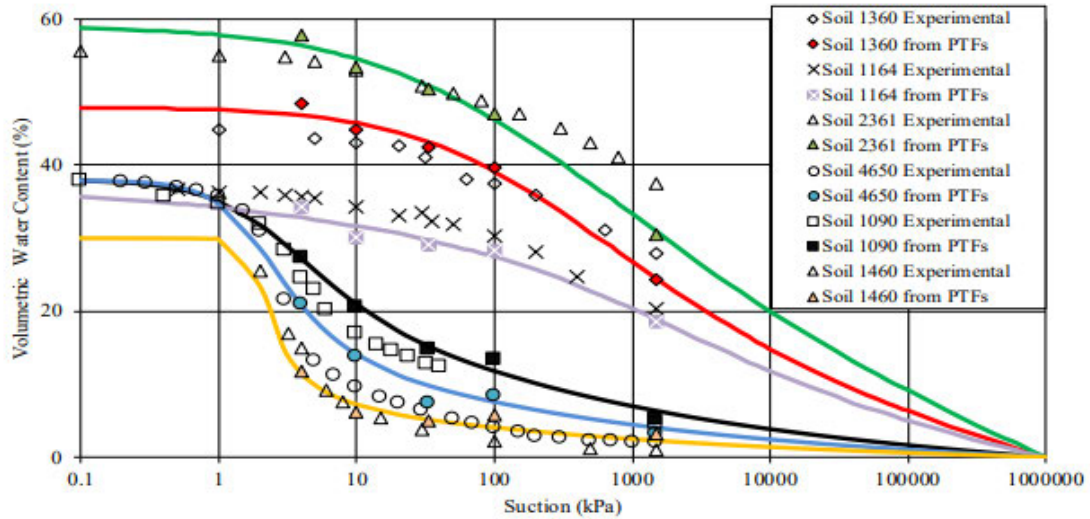


**Figure 42: Estimation of SWCC using estimated points from pedotransfer functions and Fredlund and Xing equation.**

As described by the range of soil types, the soil water retention curves that can be created are very different and unique, based on a range of different parameters. The curve that most likely resembles the soils used from Armatree and Greymare within this research would be soil 1090, except the clay content found within these samples is only 5%, which is considerably less than what is found in the soil samples in this research project. With the higher clay contents, the curve would continue in an initial flat section for much longer like the curves created in this project. However, figure 42 does allow an understanding of the variety of soil water retention curves that can be created just from having slightly different soils. For example, soil 2361 has a clay percentage of 56%, describing the effect that a heavy clay percentage has on the retention abilities of the soil (Zou & Leong, 2019). Soil 1360 also has a higher clay percentage of 44%, with a very low percentage of sand. On the other end of the scale, soil 1460 had a sand percentage of 98%, describing what an almost complete sand sample would react during a soil water retention curve test (Zou & Leong, 2019). Overall, the soil samples provided within this research paper are very different to the samples within this project, with the soil types either having a very high clay content, or having almost no clay at all, which does not cover any of the soil samples within this research. However, this does give an indication of where the retention curves should be, which is helpful.

# **CHAPTER 6 CONCLUSIONS**

## **6.1 SUMMARY OF FINDINGS**

The goals of this research were to conduct standard soil mechanic tests such as permeability, compaction and soil classification tests as well as determining an agricultural soils water retention curve. This revolved around the use of void ratio determined using soil consolidation equipment to create soil water retention curves for a range of soil types. This was completed using a conversion equation between void ratio and volumetric moisture content. This could then be considered and compared with current research to determine whether the results are in fact reasonable and within a select criterion.

A summary of key findings of the research is as follows;

- The results obtained using the raw soil consolidation results created soil water retention curves that were not optimal compared to past research and knowledge.
- The results obtained using the revised soil consolidation results provided soil water retention curves that were much more comparable and reasonable with current research.

The results of the project were promising in providing a close fit to what would have been expected using traditional methods or modelling. However, further research needs to be conducted surrounding different soil types as well as further development in this field.



## 6.2 PROJECT OUTCOMES

The project aims to investigate the connection between void ratio and volumetric moisture content and the possibility to connecting the two to create soil water retention curves. These curves are dependent on a range of different factors and characteristics of the soil, ultimately impacting the soil retention capabilities of the soil. The following points achieved this.

1. Completion of initial research in tillage, water retention and soil water retention curves and the factors that affect the soils' ability to withhold moisture.

Initial research into the effects of tillage and water retention in agricultural soils gave a great insight into not only the importance of the practices undertaken by many agricultural industries but also the importance of retaining as much water within the soil as possible to navigate dry spells. Furthermore, research into soil water retention curves gave a greater visible understanding of water retention, as well as the applications it has across the industry, such as soil water storage, water flow, plant available water and irrigation applications.

2. Establishment of a connection between void ratio and volumetric moisture content through a derived equation.

The establishment of the derived equation that could be used to connected both void ratio and volumetric moisture content allowed a further connection to be made between soil consolidation and the soil water retention curve. This would allow retention curves to be created in a much easier way compared to many of the difficult and time-consuming experimental methodologies that currently exist.

3. Conduct standard soil mechanic tests such as sieve analysis, specific gravity, Atterberg limits, compaction, permeability and soil consolidation.

Through conducting standard soil mechanics tests, a much greater understanding of the soil could be made, such as its permeability under saturated and unsaturated conditions, its optimum dry density

and moisture content under compaction as well as simple soil classifications to be made under the USCS system (Unified Soil Classification System). With many of these factors influencing the results of the project, it was important to determine these parameters.

4. Explore the results of both the initial and revised soil water retention curves created using the conversion equation and the different data each created.

The initial curve created using the raw void ratio data described a characteristic curve that did not resemble a soil water retention curve, almost having an opposite shape to the expected curve. This may have been due to some human and systematic error throughout the data collection phase while conducting the soil consolidation testing. Using the general shape of a consolidation curve, a trendline could be developed that described the data much clearer. This in turn created a revised soil water retention curves that resemble a standard curve as described in figure 1.

5. Compare the results with other research both within the agricultural industry as well as other relevant industries.

Comparing the results of the revised soil water retention curves with other curves for similar soils both within the industry as well as other industries allowed assessments of the curves and evaluations to be made. The final curves created resembled the expected characteristic curves generated using other known methodologies and models for very similar soil types, meaning the soil water retention curves created using this projects approach is at least reasonable to a certain extent.

6. Draw conclusions on the viability and future improvements of the methodology followed and the results obtained from the revised soil water retention curves.

The methodology employed to create the soil water retention curves ended up being viable for this soil type, however there are many improvements to be made. The first of which would be to increase the applied pressure within the testing, allowing a much greater and significant curve to be developed. Furthermore, an automatic computerised oedometer could be used to retrieve much more

accurate results, aiding the reliability of the final results. Closer increments could also be helpful in determining the initial section of the curve as well. There also a range of other improvements that could be undertaken to improve the overall experimental procedure undertaken in this project.

## **6.3 FURTHER RESEARCH**

This project has been preliminary research into the laboratorial simulation of soil water retention curves as well as other standard soil experiments including permeability and compaction. There are several avenues of research that could stem from this that could be investigated, great benefiting the knowledge gained from this research surrounding water retention. The following research streams could be investigated in the future:

- The experimentation on the same or very similar tilled soil types to determine whether the retention curves created were within a reasonable tolerance of the correct curves.
- Refinement of methodology (different increments for pressure measurements, moisture contents, different soil consolidation apparatus used, etc.)
- Higher pressure placed upon the soil samples within the experimentation phase of the project, creating a larger soil water retention curve
- The introduction of further variables within the equation that was derived, possibly with the addition of the voids of air within the soil consolidation sample.
- Using more advanced modelling to analyse the curves, whether that is using existing models such as Van Genuchten, Brooks and Corey or Gardners, or a new model.
- Further research into the retention curves when the soil sample has organic materials within them, such as root structures, leaves or mulch.

## CHAPTER 7 REFERENCES

- Assouline, S., 2021. What can we learn from the water retention characteristic of a soil regarding its hydrological and agricultural functions? review and analysis of actual knowledge. *Water Resources Research*, 57(12).
- Bayer, 2023. *Tillage effects on weed management*. [online] Tillage Effects on Weed Management | Crop Science US. Available at: <[https://www.cropscience.bayer.us/articles/bayer/tillage-effects-weed-management](https://www.cropsscience.bayer.us/articles/bayer/tillage-effects-weed-management)> [Accessed 26 Jul. 2024].
- Benchmark Labs, 2022. *Advantages and disadvantages of conservation tillage methods*. [online] Benchmark Labs. Available at: <<https://www.benchmarklabs.com/blog/advantages-disadvantages-of-conservation-tillage-methods/>> [Accessed 27 Jul. 2024].
- Brooks, R., and Corey, A., 1964. Hydraulic Properties of Porous Media and Their Relation to Drainage Design. *AMERICAN SOCIETY OF AGRICULTURAL ENGINEERS*, 7(1), pp.0026–0028.
- Brown, K., and Wherrett, A., 2024. Bulk density – on farm use. [online] Bulk Density - On Farm Use | Fact Sheets. Available at: <<https://www.soilquality.org.au/factsheets/bulk-density-on-farm-use>> [Accessed 16 Mar. 2024].
- Bureau of Meteorology, n.d. Climate Classification Maps. [online] Climate classification maps, Bureau of Meteorology. Available at: <<http://www.bom.gov.au/climate/maps/averages/climate-classification/>> [Accessed 28 Jul. 2024].
- Collentine, D., and Futter, M.N., 2016. Realising the potential of natural water retention measures in Catchment Flood Management: Trade-offs and matching interests. *Journal of Flood Risk Management*, 11(1), pp.76–84.
- Elementary Engineering, 2019a. Liquid Limit - Cone Penetration Method. [online] Elementary Engineering Library. Available at: <<https://elementaryengineeringlibrary.com/civil-engineering/soil-mechanics/liquid-limit-cone-penetration-method>> [Accessed 23 May 2024].
- Elementary Engineering, 2019b. Plasticity and plastic state and plastic limit of soil and its determination. [online] Elementary Engineering Library. Available at: <<https://elementaryengineeringlibrary.com/civil-engineering/soil-mechanics/plasticity-and-plastic-state-and-plastic-limit-of-soil-and-its-determination>> [Accessed 10 May 2024].
- Farooq, U., Ajmal, M., Li, S., Yang, J., and Ullah, S., 2024. Evaluation of pedotransfer functions to estimate soil water retention curve: A conceptual review. *Water*, 16(17), p.2547.
- Fredlund, D.G., and Xing, A., 1994. Equations for the soil-water characteristic curve. *Canadian Geotechnical Journal*, 31(4), pp.521–532.
- Galvín, P., and Romero, A., 2014. A MATLAB toolbox for soil–structure interaction analysis with finite and boundary elements. *Soil Dynamics and Earthquake Engineering*, 57, pp.10–14.
- Gaspar, T., Jacobsz, S., Schulz-Poblete, M., and Toll, D., 2019. Measurement of the soil water retention curve: practical considerations.

GeoEngineer, n.d. [online] Soil Compaction Test | [geoengineer.org](https://www.geoengineer.org/education/laboratory-testing/compaction-test). Available at: <<https://www.geoengineer.org/education/laboratory-testing/compaction-test>> [Accessed 10 May 2024].

Geo Engineer, n.d. *Soil consolidation and Oedometer Test*. [online] Geo Engineer. Available at: <<https://www.geoengineer.org/education/laboratory-testing/soil-consolidation>> [Accessed 11 Sep. 2024].

Geroy, I.J., Gribb, M.M., Marshall, H.P., Chandler, D.G., Benner, S.G., and McNamara, J.P., 2011. Aspect influences on soil water retention and storage. *Hydrological Processes*, 25(25), pp.3836–3842.

Gupta, A., Gupta, N., Dola, M.M., MD Sahadat Hossain, Ph.D., Islam, M.A., Badhon, F.F., and Imtiaz, T., 2021a. Sieve analysis. [online] Properties and Behavior of Soil Online Lab Manual. Available at: <<https://uta.pressbooks.pub/soilmechanics/chapter/sieve-analysis/>> [Accessed 6 May 2024].

Gupta, A., Gupta, N., Dola, M.M., MD Sahadat Hossain, Ph.D., Islam, M.A., Badhon, F.F., and Imtiaz, T., 2021b. Specific gravity test. [online] Properties and Behavior of Soil Online Lab Manual. Available at: <<https://uta.pressbooks.pub/soilmechanics/chapter/55/>> [Accessed 7 May 2024].

Han, X.-W., Shao, M.-A., and Horton, R., 2010. Estimating van Genuchten model parameters of undisturbed soils using an integral method. *Pedosphere*, 20(1), pp.55–62.

Hannam, I., 2020. Soil legislation in Australia. *Legal Instruments for Sustainable Soil Management in Africa*, pp.181–212.

Indoria, A., Sharma, K., and Reddy, K., 2020. Hydraulic properties of soil under warming climate. *Climate Change and Soil Interactions*, pp.473–508.

Jabro, J.D., and Stevens, W.B., 2022. Soil-water characteristic curves and their estimated hydraulic parameters in no-tilled and conventionally tilled soils. *Soil and Tillage Research*, 219, p.105342.

Lin, H., 2012. Understanding Soil Architecture and Its Functional Manifestation across Scales. *Hydropedology*, pp.41–74.

Ma, K., Lin, Y., and Tan, Y., 2012. The influence of salinity on hysteresis of soil water-retention curves. *Hydrological Processes*, 27(17), pp.2524–2530.

Maher, J., and Bray, D., 2014. Stanthorpe-Rosenthal Region Land Management Manual, South East Queensland. [online] Stanthorpe-Rosenthal Region - Land Types. Available at: <<https://www.publications.qld.gov.au/dataset/land-resource-areas-stanthorpe-rosenthal-srm/resource/9537dfe2-0fb3-413a-a2ba-1b69a87a85ab>> [Accessed 26 Jul. 2024].

Mainroads Western Australia, 2020. Liquid limit - test method WA 120.2 – 2020. [online] LIQUID LIMIT: CONE PENETROMETER METHOD. Available at: <<https://www.mainroads.wa.gov.au/globalassets/technical-commercial/technical-library/materials-engineering/test-methods/100-series-soil/liquid-limit-cone-penetrometer-method.pdf?v=4a9054>> [Accessed 28 Jul. 2024].

McKenzie, D., 2024. Karoona' Armatree: GRDC Soil Amelioration Core Site 'Hassat Moisture Probe' calibration – soil descriptions, 2024, unpublished.

Ochsner, T., 2019. Soil water retention. [online] Rain or Shine. Available at: <<https://open.library.okstate.edu/rainorshine/chapter/3-3-soil-water-retention/>> [Accessed 24 Mar. 2024].

Osunbitan, J.A., Oyedele, D.J., and Adekalu, K.O., 2005. Tillage effects on bulk density, hydraulic conductivity and strength of a loamy sand soil in southwestern Nigeria. *Soil and Tillage Research*, 82(1), pp.57–64.

Pan, T., Hou, S., Liu, Y., and Tan, Q., 2019. Comparison of three models fitting the soil water retention curves in a degraded alpine meadow region. *Scientific Reports*, 9(1).

Queensland Government, 2013. Soil structure. [online] Queensland Government. Available at: <<https://www.qld.gov.au/environment/land/management/soil/soil-properties/structure>> [Accessed 16 Mar. 2024].

Rai, R.K., Singh, V., and Upadhyay, A., 2017. Chapter 17 - Soil Analysis. *Planning and Evaluation of Irrigation Projects*, pp.505–523.

Solone, R., Bittelli, M., Tomei, F., and Morari, F., 2012. Errors in water retention curves determined with pressure plates: Effects on the Soil Water Balance. *Journal of Hydrology*, 470–471, pp.65–74.

Stewart, R., n.d. Tillage. [online] Encyclopædia Britannica. Available at: <<https://www.britannica.com/topic/tillage>> [Accessed 15 Mar. 2024].

Simon, L., 2023. Mastering the underground: A comprehensive guide to soil consolidation and ground improvement techniques. *Ground Improvement*.

Soil Health Institute, 2021. *How does soil health increase resilience to drought and extreme rainfall?*. [online] Soil Health Institute. Available at: <<https://soilhealthinstitute.org/news-events/how-does-soil-health-increase-resilience-to-drought-and-extreme-rainfall-2/>> [Accessed 19 Jul. 2024].

Techen, A., Helming, K., Brüggermann, N., Reinhold-Hurek, B., Lorenz, M., Bartke, S., Heinrich, U., Amelung, W., Angustin, K., Boy, J., Corre, M., Duttman, R., Gebbers, R., Gentsch, N., Grosch, R., Guggenberger, G., Kern, J., Kiese, R., Kuhwald, M., Leinweber, P., Schlöter, M., Weismeyer, M., Winklermann, T., and Vogel, H.-J., 2020. Soil research challenges in response to emerging agricultural soil management practices. *Advances in Agronomy*, 161, pp.179–240.

University of Nebraska, 2018. *Production Considerations*. [online] CropWatch. Available at: <<https://cropwatch.unl.edu/tillage/production>> [Accessed 10 Sep. 2024].

Vickers, B., 1984. Laboratory work in Soil Mechanics. London: Granada.

Wang, J., Hu, N., François, B., and Lambert, P., 2017. Estimating water retention curves and strength properties of unsaturated sandy soils from basic soil gradation parameters. *Water Resources Research*, 53(7), pp.6069–6088.

Wang, N., and Zhang, T., 2024. Soil pore structure and its research methods: A Review. *Soil and Water Research*, 19(1), pp.1–24.

Wolkowski, R., n.d. IMPACT OF TILLAGE ON SOIL PROPERTIES.

Xiong, Y., 2014. Flow of water in porous media with saturation overshoot: A Review. *Journal of Hydrology*, 510, pp.353–362.

Yadvinder-Singh, Kukal, S.S., Jat, M.L., and Sidhu, H.S., 2014. Improving water productivity of wheat-based cropping systems in South Asia for sustained productivity. *Advances in Agronomy*, pp.157–258.

Zou, L., and Leong, E.C., 2019. A simple method of estimating soil-water characteristic curve using point pedotransfer functions. *Japanese Geotechnical Society Special Publication*, 7(2), pp.287–292.

# **APPENDIX A: PROJECT SPECIFICATION**

ENP4111 Research Project

Project Specification

For: Hayden Doherty

Title: Laboratory simulation of agricultural soil density reduction and pore increase by lifting and raising field soil elevation

Major: Agricultural Engineering

Supervisor: Habib Alehossein

Enrolment: ENP4111 – EXT Full Year 2024

Project Aim: To create soil water retention curves by investigating the connection between void ratio and volumetric moisture content through soil consolidation and derived soil mechanics equations.

**Program: Version 1, March 2023**

**Example Below:**

1. Completion of initial research in tillage, water retention and soil water retention curves and the factors that affect the soils' ability to withhold moisture.
2. Establishment of a connection between void ratio and volumetric moisture content through a derived equation.
3. Conduct standard soil mechanic tests such as sieve analysis, specific gravity, Atterberg limits, compaction, permeability and soil consolidation.
4. Explore the results of both the initial and revised soil water retention curves created using the conversion equation and the different data each created.



5. Compare the results with other research both within the agricultural industry as well as other relevant industries.
6. Draw conclusions on the viability and future improvements of the methodology followed and the results obtained from the revised soil water retention curves.

*If time and resources permit:*

7. Conduct a simple suction test or another soil water retention curve experimental method to compare the retention curve results obtained within this research with experimental results using a known method.

## APPENDIX B: RISK ASSESSMENT

As the project has a large amount of laboratory work over the course of multiple weeks, a risk assessment is very important to identify any possible risks and hazards, which could be dealt with before moving forward with the project. The risk assessment also takes into account the collection of the soil samples, but the major of it relates directly to laboratory work. Found below is the risk assessment for this project.

| 4787   | RISK DESCRIPTION   |                    | STATUS   | TREND           | CURRENT               | RESIDUAL |
|--|--|--------------------|--|-----------------|-----------------------|----------|
|  | ENP4111 - Laboratory simulation of agricultural soil density reduction and pore increase by lifting and raising field soil elevation |                    | Draft  | <div></div>     | Low                   | Low      |
| RISK OWNER   |  | RISK IDENTIFIED ON | LAST REVIEWED ON   |                 | NEXT SCHEDULED REVIEW |          |
| Hayden Doherty   |  | 21/05/2024         |  |                 |                       |          |
| RISK FACTOR(S)   | EXISTING CONTROL(S)  | CURRENT            | PROPOSED CONTROL(S)  | TREATMENT OWNER | DUE DATE              | RESIDUAL |
| Laboratorial equipment or soil samples falling   | Control: Wearing PPE such as steel capped boots, safety glasses, long sleeved shirts and long pants.                                 | Low                | Only one person working within the area, isolating the experiments from other ongoing experiments in the laboratory. |                 | 30/06/2024            | Very Low |
| There is a range of moving pieces of equipment found in the experimental methodology, from shaking equipment to loading equipment. | Control: Wearing PPE such as steel capped boots, safety glasses, long sleeved shirts and long pants.                                 | Low                | Remove all experiments and other people from the area while equipment is running.                                    |                 | 30/06/2024            | Low      |
|  | Control: Guidelines for distances from machinery and operating practices.  |                    |  |                 |                       |          |
| Constant moving of soil samples and equipment as well as long periods of standing and monitoring.                                  | Control: Follow general guidelines such as safe lifting practices and working practices in regard to equipment.                      | Low                | Complete experiments in one location, removing the need to walk across laboratory with samples and equipment.        |                 | 30/06/2024            | Very Low |
| The noise potential when operating the sieve analysis and compaction experiments.  | Control: The use of ear plugs for all members within the laboratory.   | Low                | Complete the experiments at a time when a low number of people are within the laboratory.                            |                 | 30/06/2024            | Very Low |
| When collecting soil samples from fields animals may be within the area and could possibly pose a risk.                            | Control: Completely remove all livestock and visually check for any wild animals within the area.                                    | Very Low           | No Control:  |                 |                       | Very Low |
|  | Control: Apply insect repellent and wear steel capped boots, long sleeved shirts and long pants.                                     |                    |  |                 |                       |          |
| Collecting soil samples from farmland poses risks surrounding biological materials related to animals and plants.                  | Control: Apply insect repellent and wear steel capped boots, long sleeved shirts and long pants.                                     | Very Low           | No Control:  |                 |                       | Very Low |
|  |  |                    |  |                 |                       |          |

powered by riskware.com.au

commercial in confidence

powered by riskware.com.au

commercial in confidence

Figure 43: First page of Risk Assessment for the project.

|   |  |          |             |  |  |          |
|---|--|----------|-------------|--|--|----------|
| Potential for wind and high temperatures through the collecting stage in the field. | Control: Wearing broad brimmed hat, long sleeved shirt and long pants. | Very Low | No Control: |  |  | Very Low |
|   | Control: Constant hydration breaks through the collection stage        |          |             |  |  |          |

**Figure 44: Second page of Risk Assessment for the project.**

## APPENDIX C: RESOURCES AND TIMELINE

Listed below are the required resources from UniSQ and Soil CRC.

From UniSQ:

- Use of university laboratory for storage of resources
- Use of laboratory equipment (sieve shaker, vacuum pump, etc.)
- ASTM Standards

From Soil CRC:

- Soil Samples from Armatree Site

From myself:

- Soil samples from Greymare Site

No other resources are required to complete the project other than a computer and excel, which I have access to both of. If any other resources are required, they will be added, as well as any needs of the resources as well. Contact with Habib Alehossein will be roughly fortnightly or whenever necessary, using phone calls and meetings when required. As the experimental phase is on the university campus, contact can also be made there to make sure the project is being completed to a high standard.

A timeline for the project can be found below.

| Month:       | Description and Plan:  |
|--------------|--|
| 1 (February) | <p>Project Initiation and Proposal:</p> <ul style="list-style-type: none"><li>- Develop and submit project plan.</li><li>- Gain approvals and permissions.</li></ul> <p>Literature Review:</p> <ul style="list-style-type: none"><li>- Begin researching relevant papers and further understanding soil mechanics.</li></ul> |

|                            |  |
|----------------------------|--|
| 2-3 (March to April)       | <p>Literature Review:</p> <ul style="list-style-type: none"> <li>- Conduct in depth literature review of the soil water retention curve, different tillage types.</li> <li>- Understand how the soil is affected by tillage and its effects on water retention.</li> </ul> <p>Research Design:</p> <ul style="list-style-type: none"> <li>- Finalise methodology (Sieve analysis, Atterberg limits, specific gravity, compaction, permeability and consolidation tests).</li> <li>- Complete risk management.</li> </ul> <p>Laboratorial Testing:</p> <ul style="list-style-type: none"> <li>- Begin soil testing and collecting data using methodology.</li> </ul> <p>Other:</p> <ul style="list-style-type: none"> <li>- Early during this period, soil will also be collected from both Greymare, Qld and Armatree, NSW.</li> </ul> |
| 4-5 (May to June)          | <p>Laboratorial Testing:</p> <ul style="list-style-type: none"> <li>- Continue collecting data and complete lab methodology.</li> </ul> <p>Analysis:</p> <ul style="list-style-type: none"> <li>- Begin computing data.</li> </ul>   |
| 6-7 (July to August)       | <p>Laboratorial Testing:</p> <ul style="list-style-type: none"> <li>- Finish collecting data (Soil Consolidation).</li> </ul> <p>Analysis:</p> <ul style="list-style-type: none"> <li>- Finish computing basic data .</li> <li>- Begin simulating soil water retention curve.</li> </ul>   |
| 8-9 (September to October) | <p>Further Analysis and Report Writing:</p> <ul style="list-style-type: none"> <li>- Continue simulating.</li> <li>- Begin compiling findings into report.</li> <li>- Prepare a presentation describing the key findings and any recommendations.</li> </ul>   |
| 10 (November)              | <p>Finalising and Presenting Results:</p> <ul style="list-style-type: none"> <li>- Finish, review and finalise report.</li> <li>- Complete any other outstanding requirements.</li> </ul>  |

**Table 11: Timeline for the project.**

## APPENDIX D: SOIL SAMPLE IMAGES



**Figure 45: Soil samples collected from Greymare, Queensland.**



**Figure 46: Opened soil samples collected from Greymare, Queensland.**





**Figure 47: Soil samples collected from Armatree, New South Wales.**



**Figure 48: Opened soil samples collected from Armatree, New South Wales.**

## APPENDIX E: LABORATORIAL EQUIPMENT

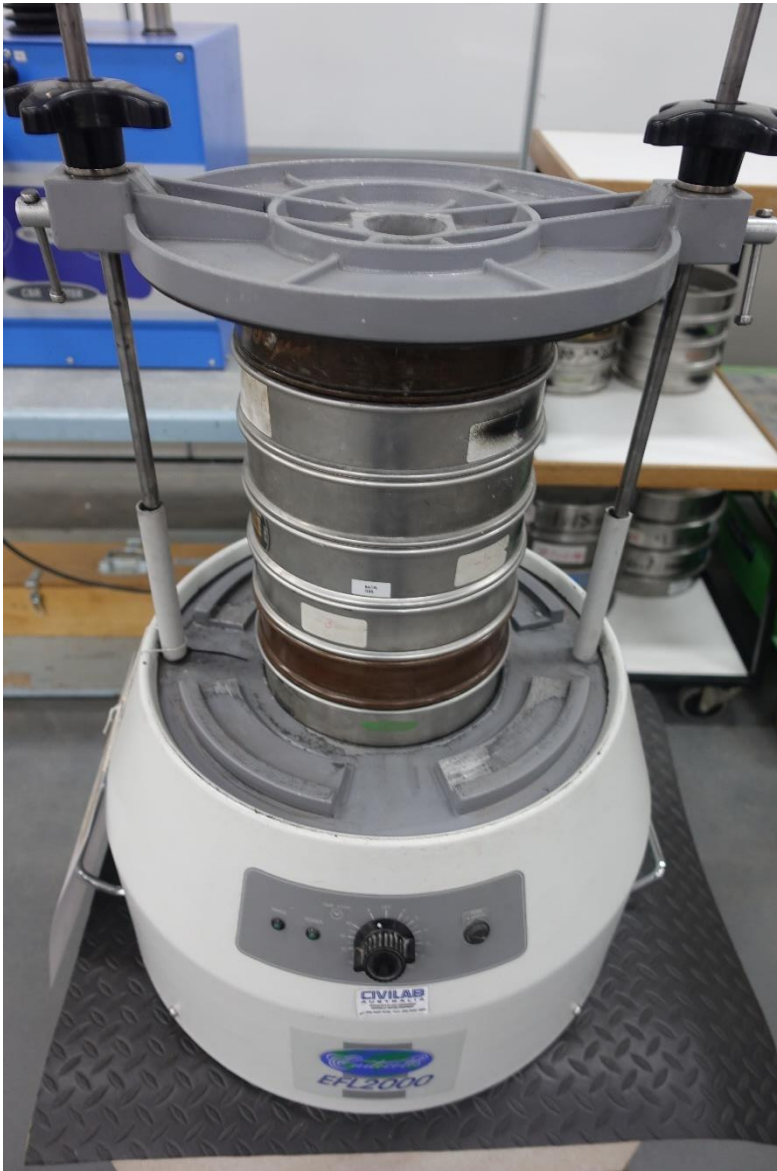


**Figure 49: Sieve shaker used for sieve analysis and soil classification.**





**Figure 50: Equipment used for liquid limit test (Cone Penetrometer).**



**Figure 51: Example of plastic limit test procedure.**



**Figure 52: Vacuum pump used for specific gravity testing.**



**Figure 53: Standard Proctor compaction test equipment.**





**Figure 54: Vertical permeability test equipment.**



**Figure 55: Soil consolidation test set up with consolidation cells loading and weights applied.**



**Figure 56: Complete recording set up for soil consolidation tests including LVDT and Vishay system 5000 data logger.**



**Figure 57: LVDT (Linear variable displacement transformer) connected to soil consolidation testing equipment.**



## APPENDIX F: EXPERIMENTAL ANALYSIS

### F.1: SIEVE ANALYSIS AND PARTICLE SIZE DISTRIBUTION

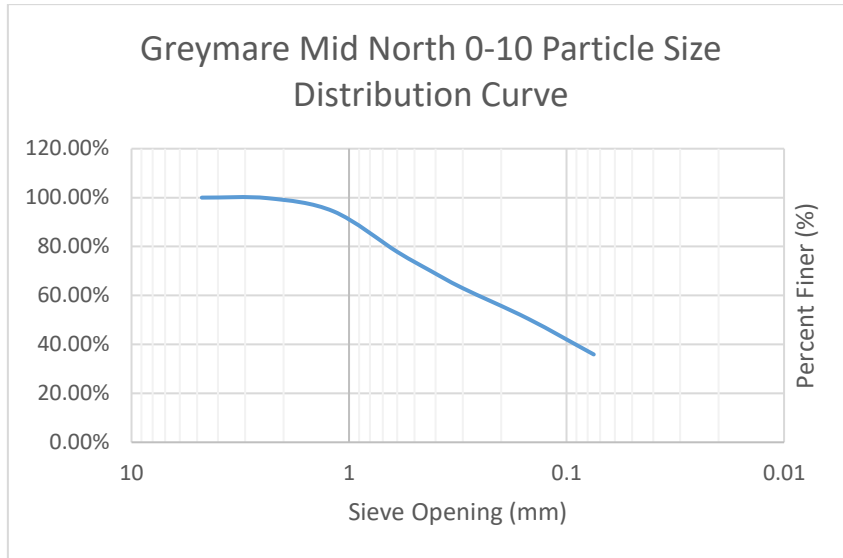


**Figure 58: Particle size distribution for Mid North 0-10 Greymare.**

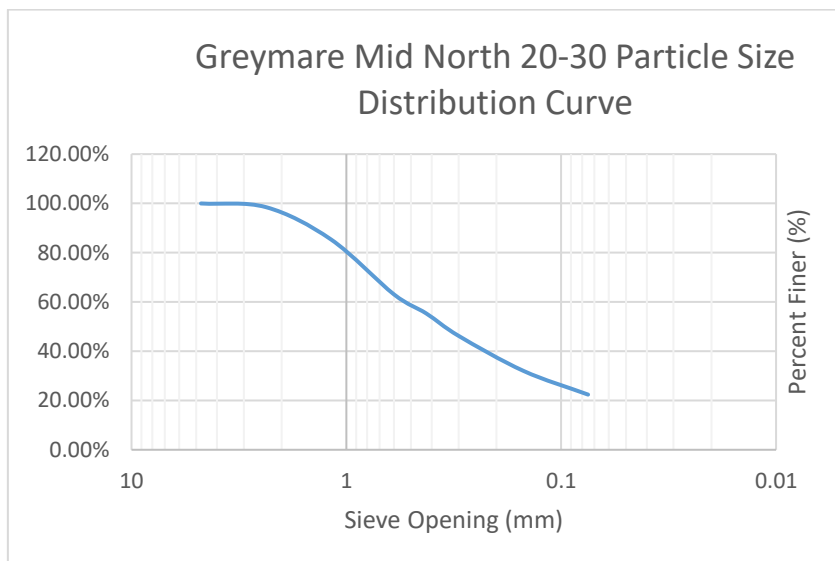


**Figure 59: Particle size distribution for Mid North 20-30 Greymare.**

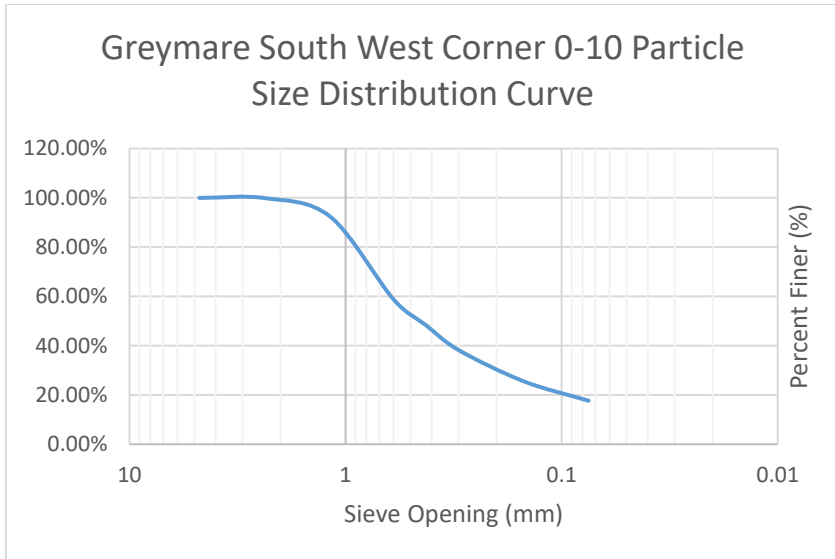


**Figure 60: Particle size distribution for SW corner 0-10 Greymare.**

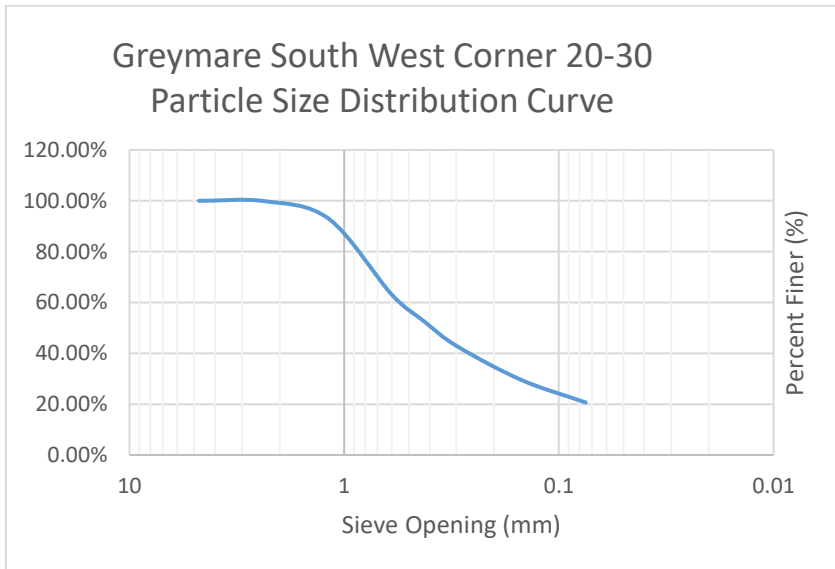


**Figure 61: Particle size distribution for SW corner 20-30 Greymare.**

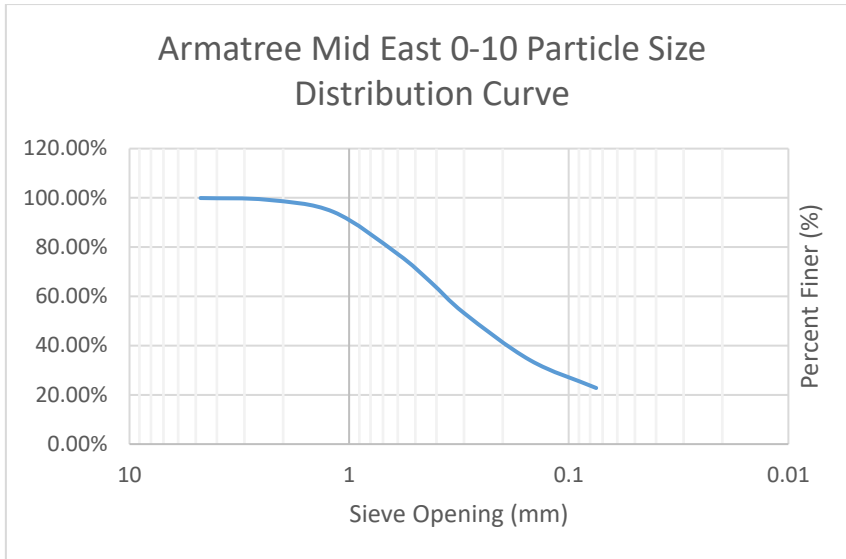


**Figure 62: Particle size distribution for Mid-East 0-10 Armatree.**

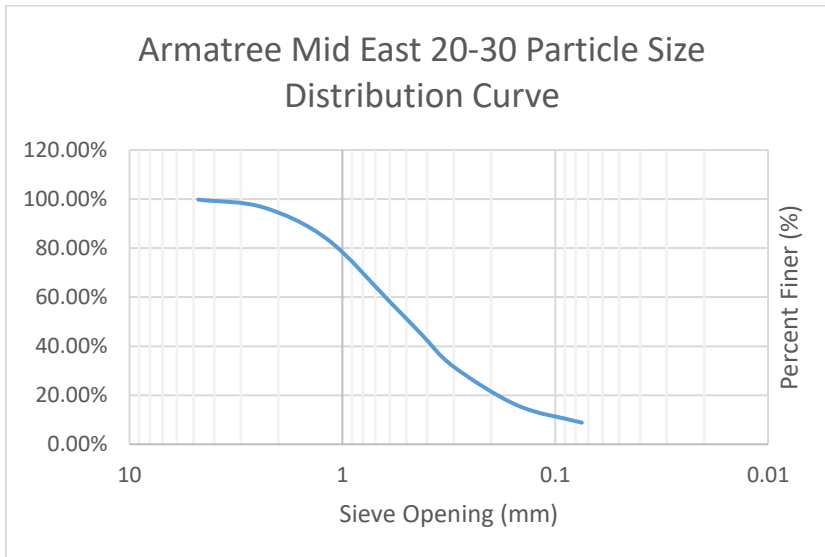


**Figure 63: Particle size distribution for Mid-East 20-30 Armatree.**

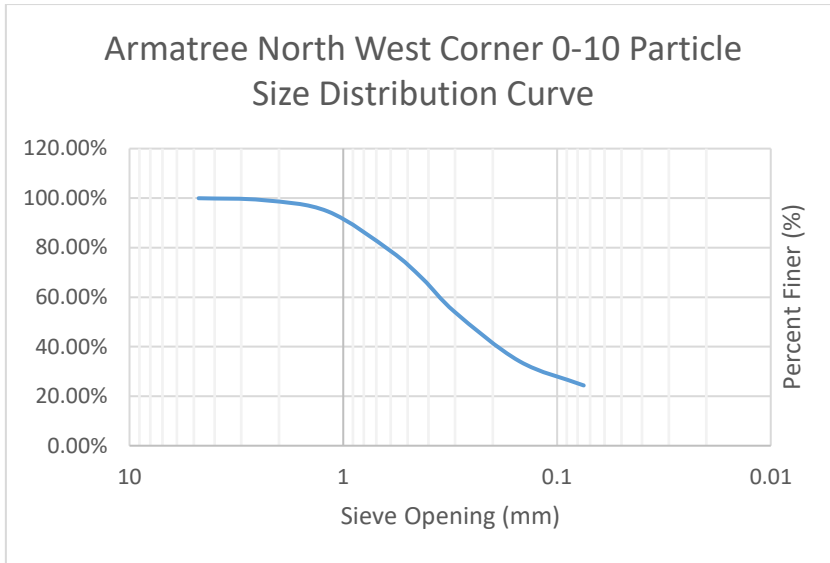


**Figure 64: Particle size distribution for NW corner 0-10 Armatree.**

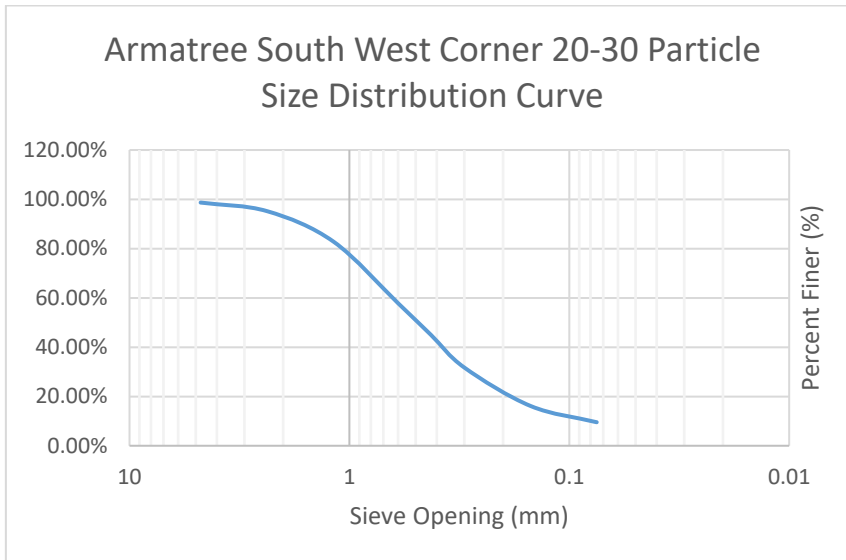


**Figure 65: Particle size distribution for NW corner 20-30 Armatree.**

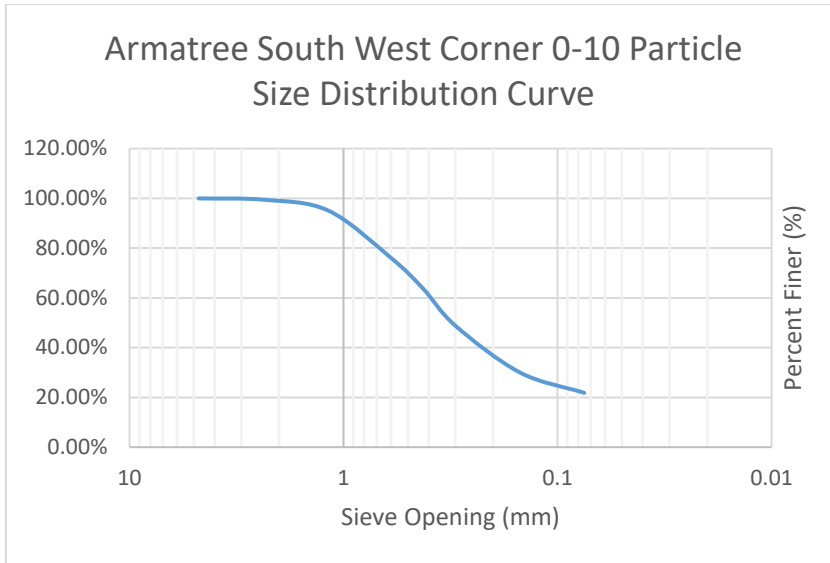


**Figure 66: Particle size distribution for SW corner 0-10 Armatree.**

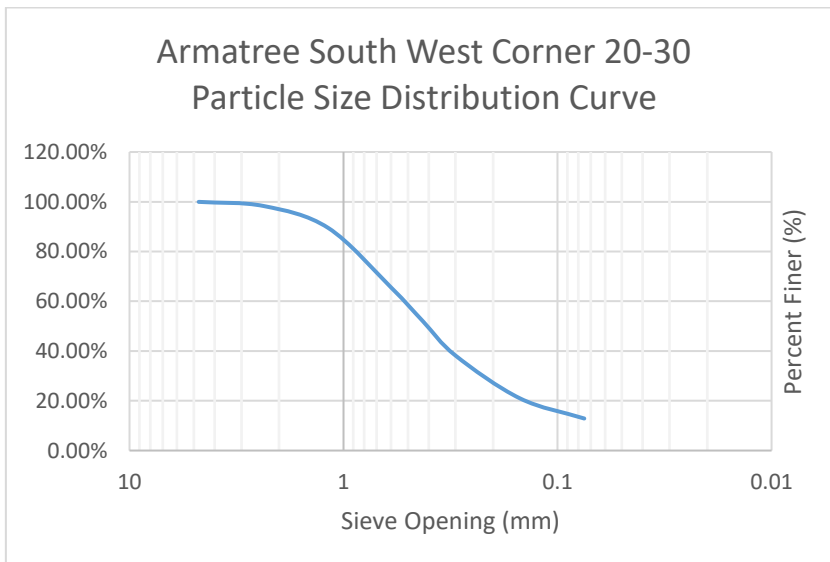


**Figure 67: Particle size distribution for SW corner 20-30 Armatree.**

| Soil Type:               | C <sub>u</sub> : | C <sub>c</sub> : |
|--------------------------|------------------|------------------|
| Mid North 0-10 Greymare  | 12.654           | 0.0252           |
| Mid North 20-30 Greymare | 15.847           | 0.285            |
| SW Corner 0-10 Greymare  | 14.603           | 0.00281          |
| SW Corner 20-30 Greymare | 15.101           | 0.00159          |
| Mid-East 0-10 Armatree   | 11.161           | 0.00135          |
| Mid-East 20-30 Armatree  | 7.308            | 0.0111           |
| NW Corner 0-10 Armatree  | 11.450           | 0.00196          |
| NW Corner 20-30 Armatree | 9.076            | 0.00575          |
| SW Corner 0-10 Armatree  | 11.561           | 0.162            |
| SW Corner 20-30 Armatree | 8.114            | 0.00990          |

**Table 12: Uniformity coefficient and coefficient of gradation for all soil types.**

## F.2: ATTERBERG LIMITS

**Armatree Boxes**  
**Mid East 0-10**

| Number   | Tin Weight (g) | Initial Weight (g) | Final Weight (g) | Moisture Content (%) |
|----------|----------------|--------------------|------------------|----------------------|
| 1        | 110.57         | 143.99             | 138.71           | 18.76%               |
| 2        | 109.32         | 142.95             | 137.99           | 17.30%               |
| 3        | 112            | 145.85             | 141.11           | 16.28%               |
| 4        | 111.06         | 144.29             | 139.37           | 17.38%               |
| Average: |                |                    |                  | 17.43%               |

**Figure 68: Example of plastic limit calculations in Excel.**

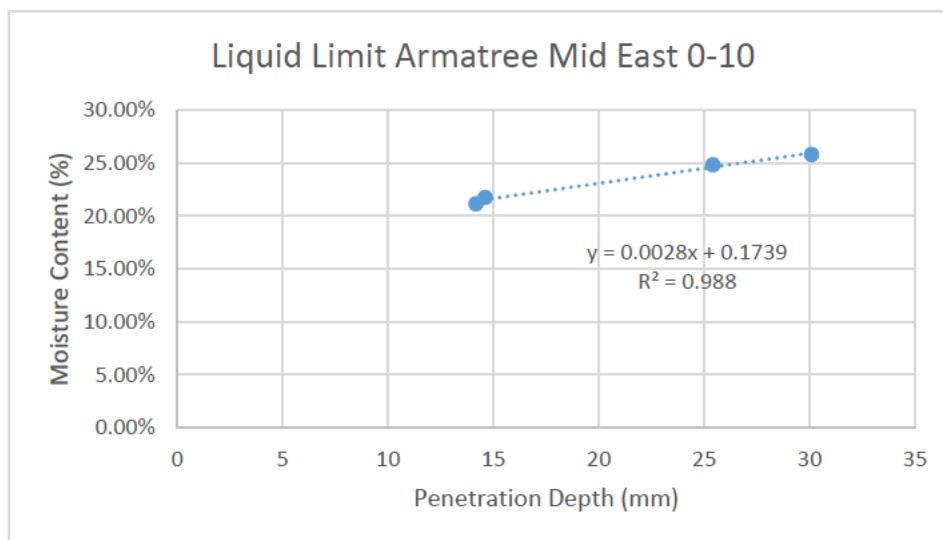


**Figure 69: Example of liquid limit graph for Mid-East 0-10 Armatree.**

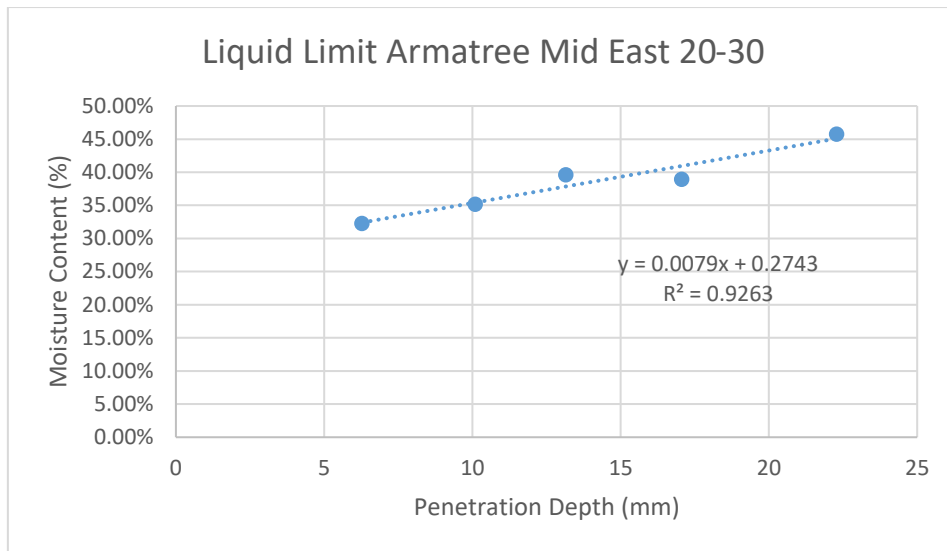


**Figure 70: Example of liquid limit graph for Mid-East 20-30 Armatree.**

### **F.3: SPECIFIC GRAVITY**

**Greymare Boxes:**

**South West Corner 0-10:**

| Test: | Weight1: | Weight2: | Soil Weight: | Weight 3: | Weight 4: | M2-M1: | M3-M4: | Specific Gravity: | Average: |
|-------|----------|----------|--------------|-----------|-----------|--------|--------|-------------------|----------|
| 1     | 189.44   | 680.8    | 51.65        | 241.23    | 713.53    | 51.79  | 32.73  | 2.717208814       | 2.69     |
| 2     | 179.84   | 684.4    | 50.94        | 230.55    | 716.48    | 50.71  | 32.08  | 2.721953838       |          |
| 3     | 190.19   | 682.06   | 52.49        | 243.08    | 714.78    | 52.89  | 32.72  | 2.622211205       |          |

**Figure 71: Example of specific gravity calculations for Southwest corner 0-10 Greymare.**



**F.4: STANDARD COMPACTION TESTS**

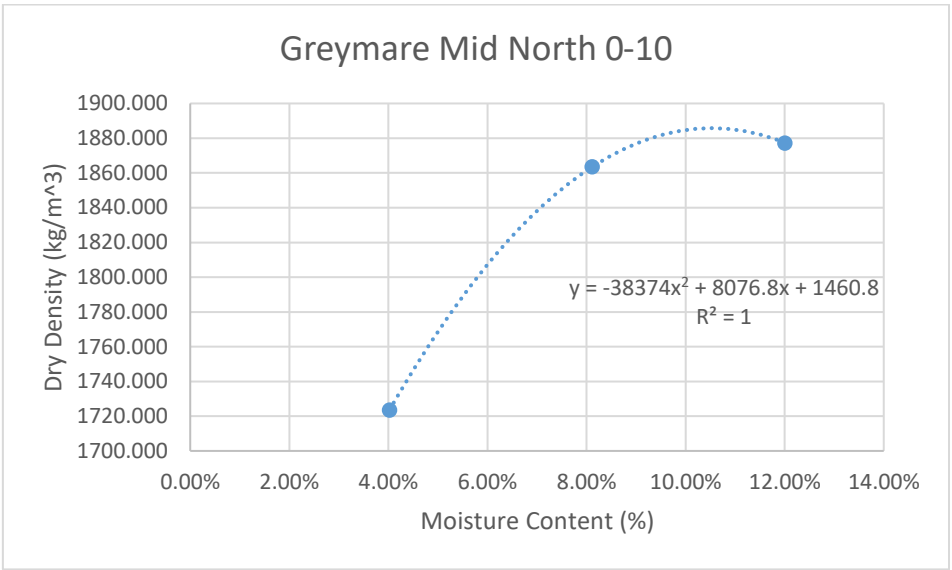


**Figure 72: Standard compaction test results for Mid North 0-10 Greymare.**

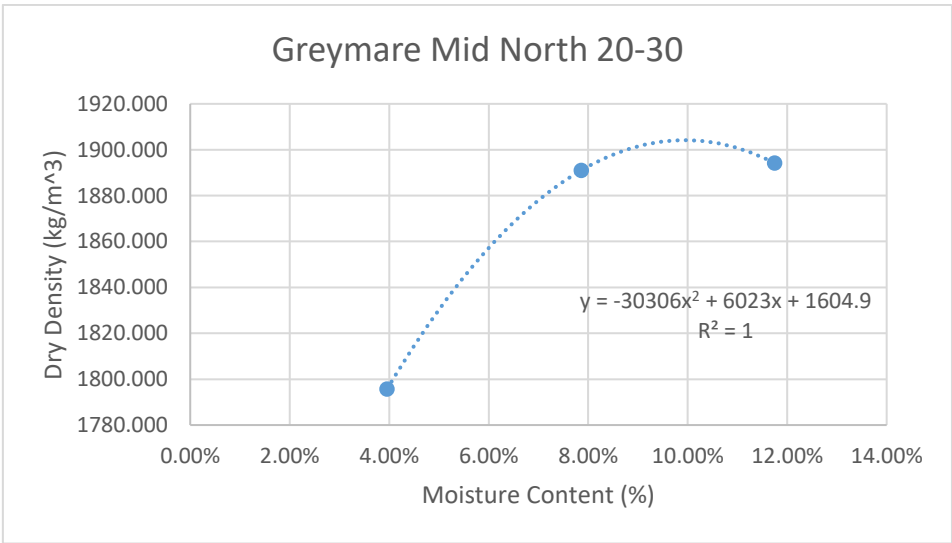


**Figure 73: Standard compaction test results for Mid North 20-30 Greymare.**

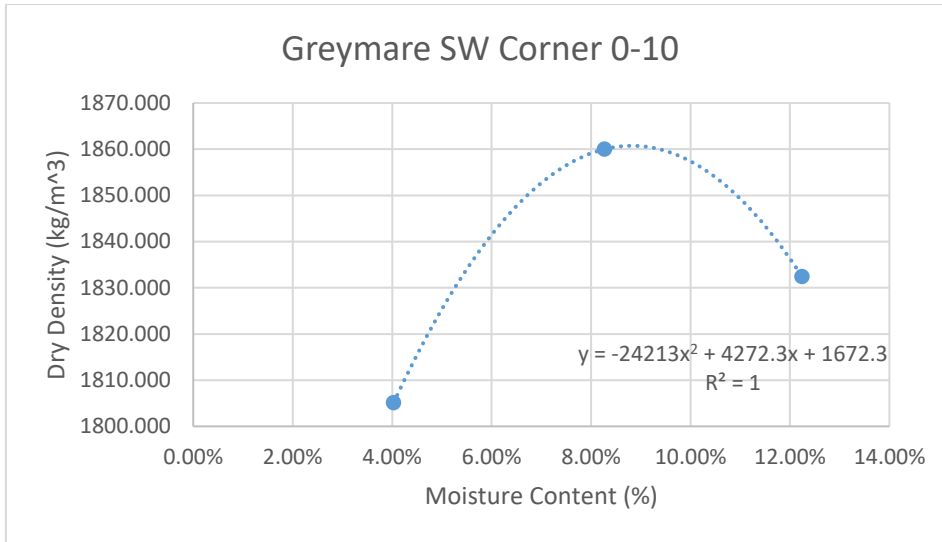


**Figure 74: Standard compaction test results for Southwest corner 0-10 Greymare.**

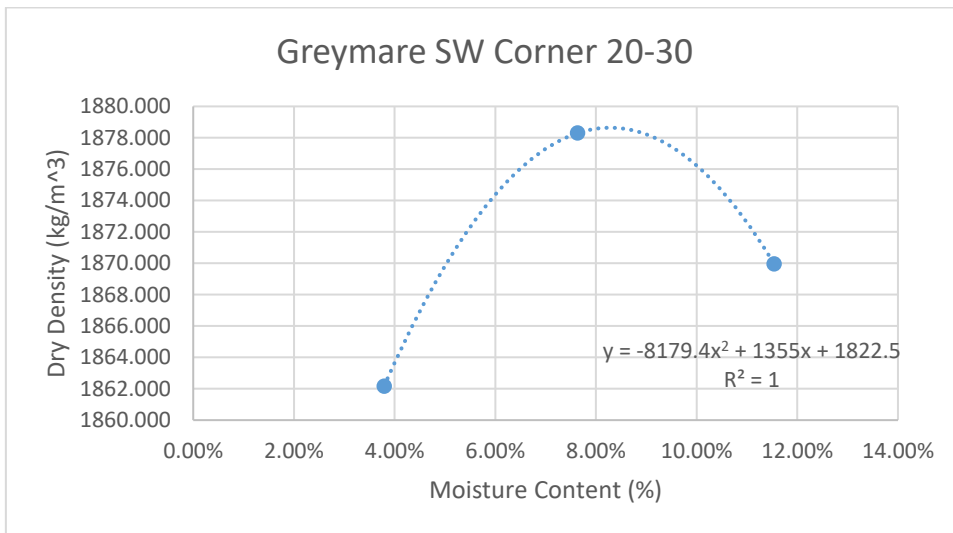


**Figure 75: Standard compaction test results for Southwest corner 20-30 Greymare.**

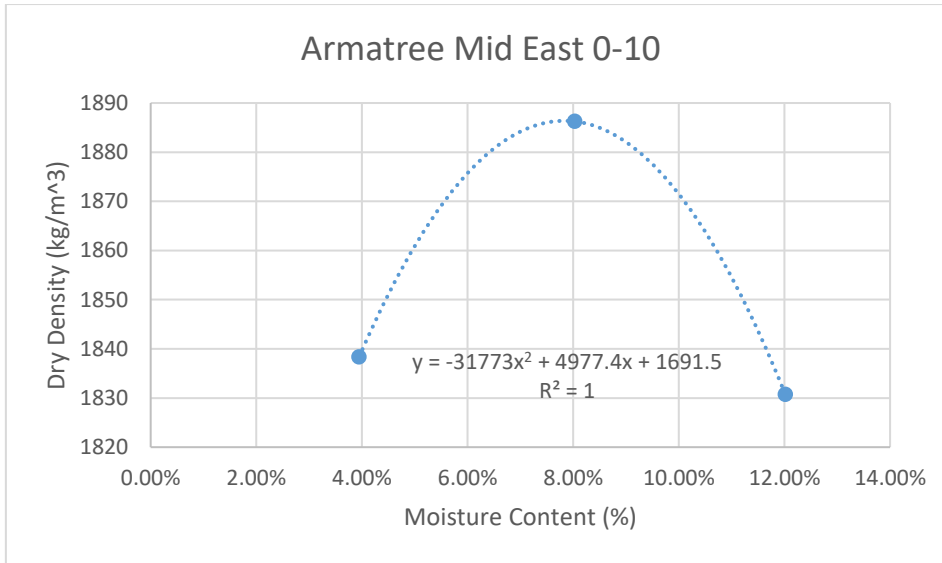


**Figure 76: Standard compaction test results for Mid-East 0-10 Armatree.**

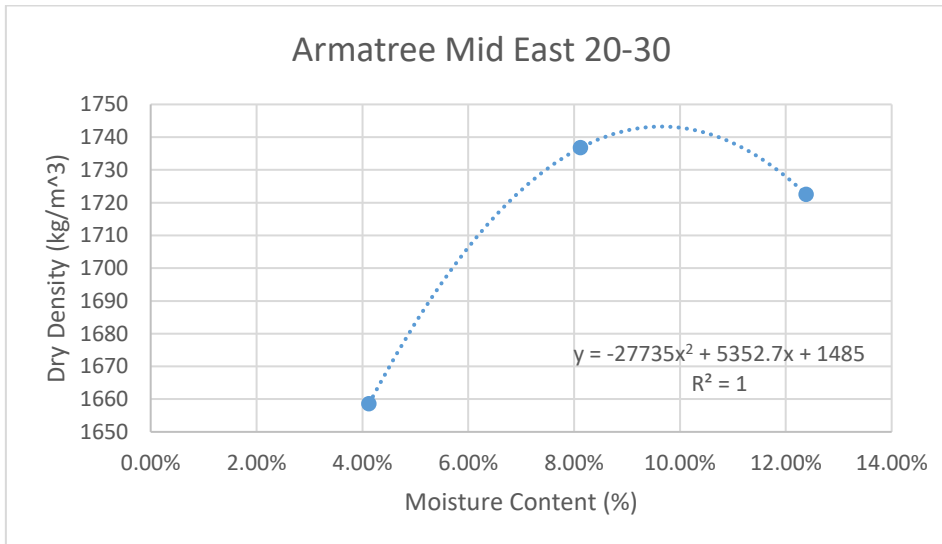


**Figure 77: Standard compaction test results for Mid-East 20-30 Armatree.**

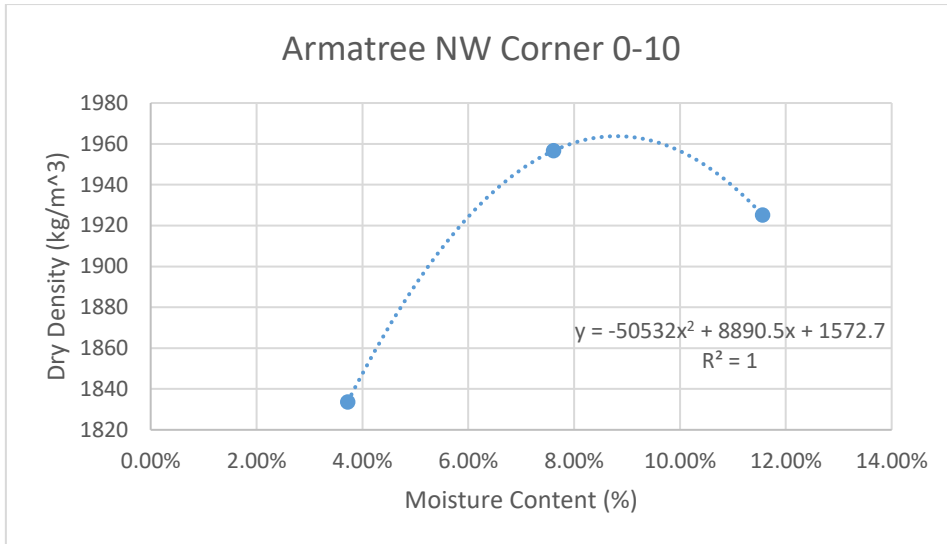


**Figure 78: Standard compaction test results for Northwest corner 0-10 Armatree.**

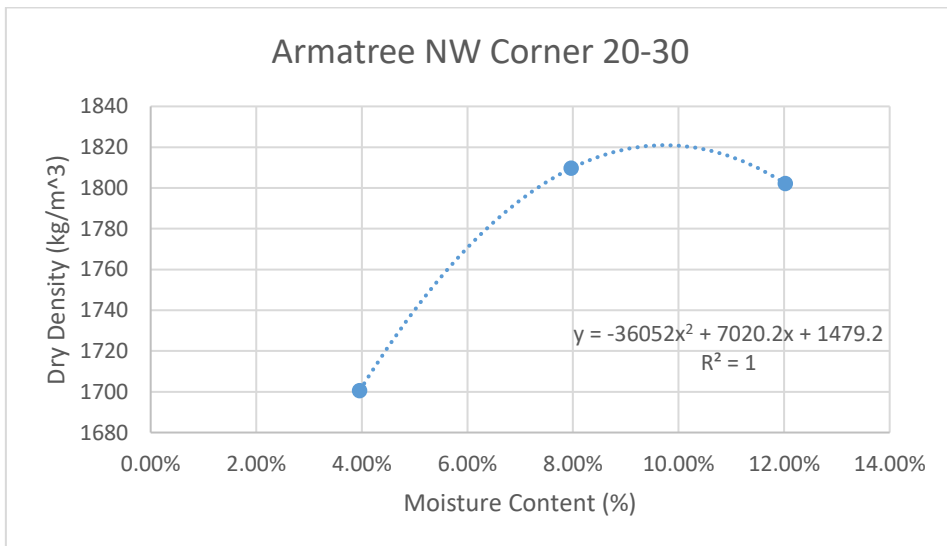


**Figure 79: Standard compaction test results for Northwest corner 20-30 Armatree.**

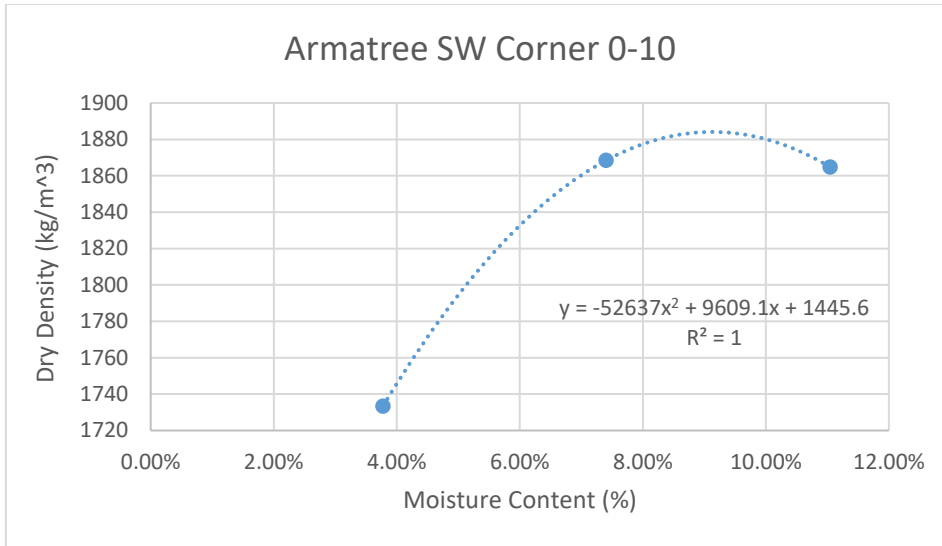


**Figure 80: Standard compaction test results for Southwest corner 0-10 Armatree.**

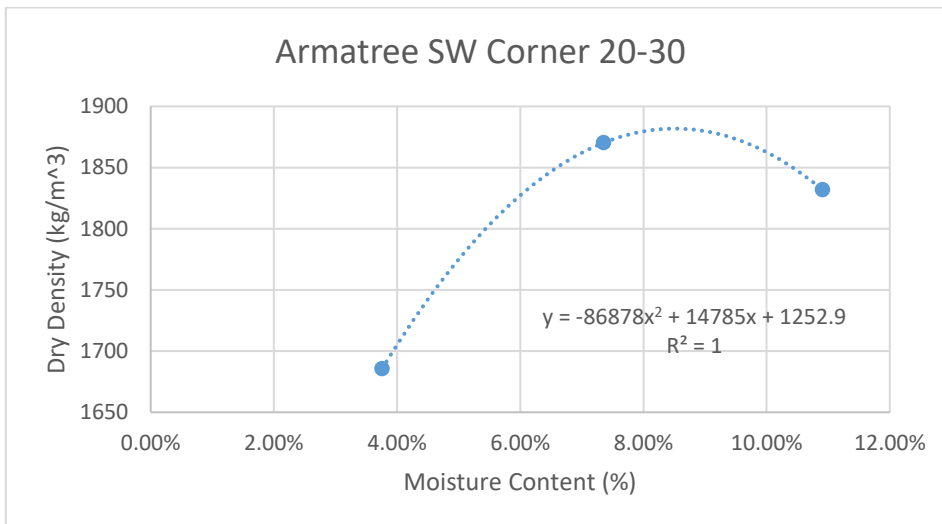


**Figure 81: Standard compaction test results for Southwest corner 20-30 Armatree.**

## F.5: VERTICAL PERMEABILITY TEST

### Mid-East 0-10 Armatree Unsaturated Permeability:

|  |            |                                |
|--|------------|--------------------------------|
| Upstream water tube diameter           | d          | 20 mm                          |
| Head 1                                 | H1         | 601 mm                         |
| Head 2                                 | H2         | 1 mm                           |
| Soil diameter                          | D          | 89 mm                          |
| Soil Length                            | L          | 170 mm                         |
| Water tube area                        | a          | 314.1592654 mm <sup>2</sup>    |
| Soil sample area                       | A          | 6221.138852 mm <sup>2</sup>    |
| Ratio a/A                              | a/A        | 0.050498674                    |
| Head (H)                               | H=H1-H2    | 600                            |
| Volume of water                        | Vw_cal     | 188495.5592                    |
| Volume of water                        | Vw_meas    | 165000 mm <sup>3</sup>         |
| Time T1 for constant head permeability | T1         | 137.3 sec                      |
| Constant head flow rate Q1             | Q1         | 1372.873701 mm <sup>3</sup> /s |
| Constant head permeability K1          | K1         | 0.062525671 mm/s               |
| Time T2 for variable head permeability | T2         | 878.5270845 sec                |
| Variable head Delta LNnH               | DLNH       | 6.398594935                    |
| Variable Head Delta H                  | DH = H1-H2 | 600 mm                         |
| Variable Head Permeability K2          | K2         | 0.062525671 mm/s               |
|  |            | 0.400076443 mm/s               |
|  |            | 0.400076443 mm/s               |

**Figure 82: Vertical permeability test results for unsaturated Mid-East 0-10 Armatree using both constant and variable head.**

Mid-East 0-10 Armatree Saturated Permeability:

|                                       |            |                                |
|---------------------------------------|------------|--------------------------------|
| Upstream water tube diameter          | d          | 20 mm                          |
| Head 1                                | H1         | 601 mm                         |
| Head 2                                | H2         | 1 mm                           |
| Soil diameter                         | D          | 89 mm                          |
| Soil Length                           | L          | 170 mm                         |
| Water tube area                       | a          | 314.1592654 mm <sup>2</sup>    |
| Soil sample area                      | A          | 6221.138852 mm <sup>2</sup>    |
| Ratio a/A                             | a/A        | 0.050498674                    |
| Head (H)                              | H=H1-H2    | 600                            |
| Volume of water                       | Vw_cal     | 188495.5592                    |
| Volume of water                       | Vw_meas    | 165000 mm <sup>3</sup>         |
| Time T1 for constant head permability | T1         | 85.81 sec                      |
| Constant head flow rate Q1            | Q1         | 2196.661918 mm <sup>3</sup> /s |
| Constant head permeability K1         | K1         | 0.100043988 mm/s               |
| Time T2 for variable head permability | T2         | 549.0634313 sec                |
| Variable head Delta LNH               | DLNH       | 6.398594935                    |
| Variable Head Delta H                 | DH = H1-H2 | 600 mm                         |
| Variable Head Permeability K2         | K2         | 0.100043988 mm/s               |
|                                       |            | 0.640140958 mm/s               |
|                                       |            | 0.640140958 mm/s               |

**Figure 83: Vertical permeability test results for saturated Mid-East 0-10 Armatree using both constant and variable head.**

**F.6 SOIL CONSOLIDATION DEFORMATION DATA**

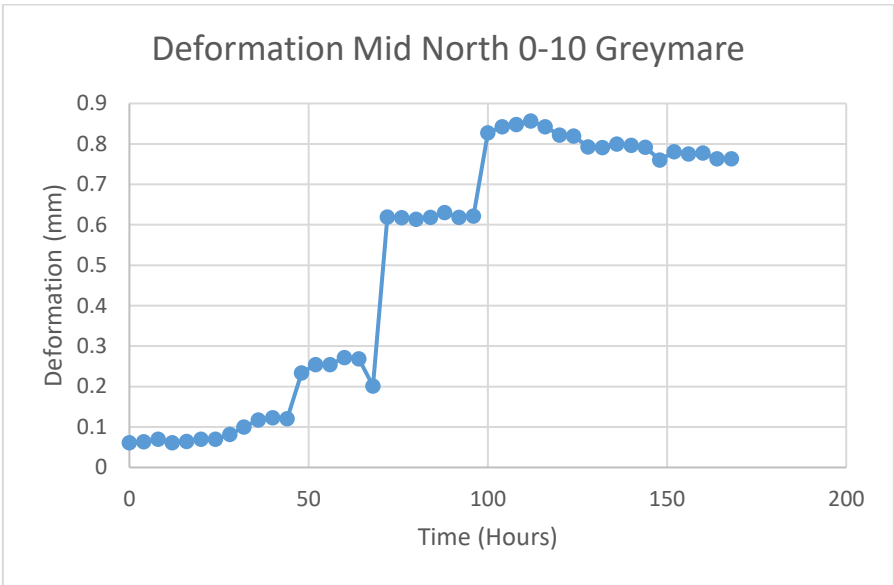


**Figure 84: Deformation graph for Mid North 0-10 Greymare.**

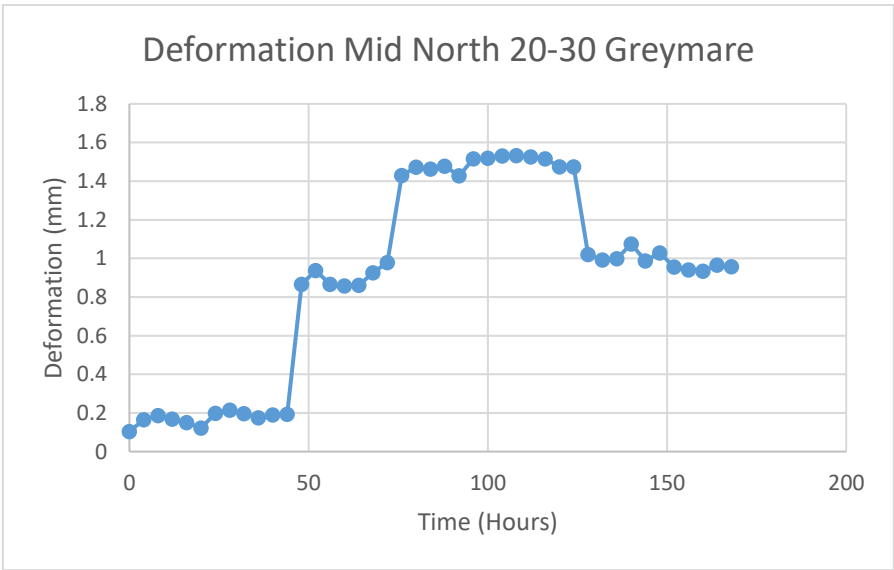


**Figure 85: Deformation graph for Mid North 20-30 Greymare.**



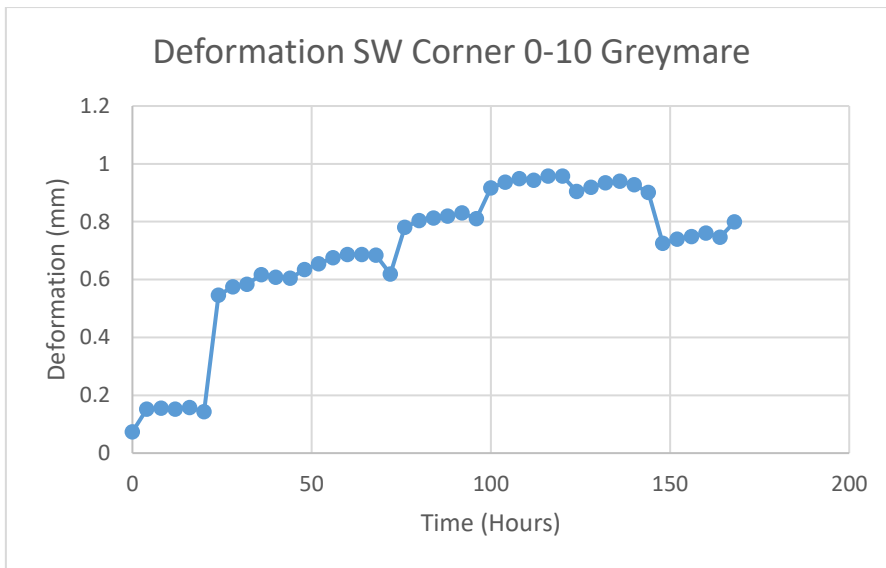


**Figure 86: Deformation graph for Southwest corner 0-10 Greymare.**

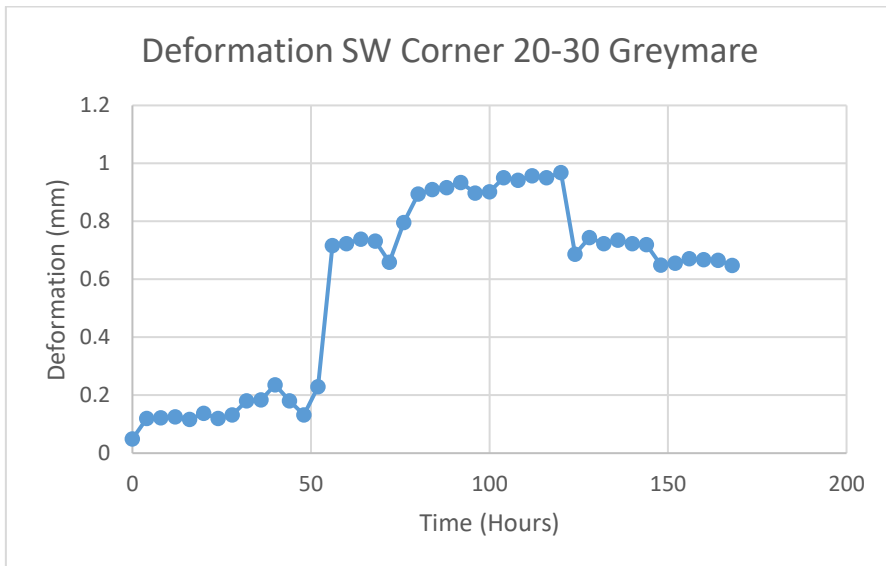


**Figure 87: Deformation graph for Southwest corner 20-30 Greymare.**

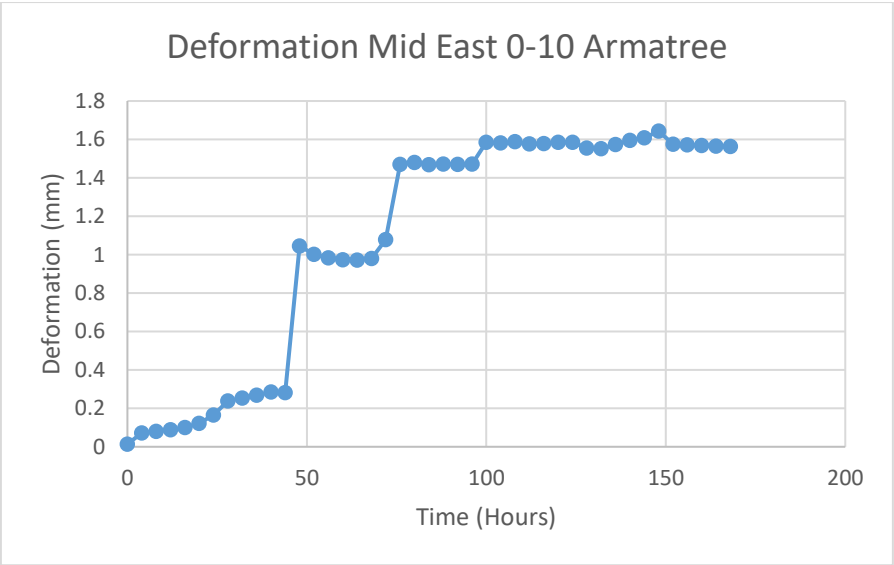


**Figure 88: Deformation graph for Mid-East 0-10 Armatree.**

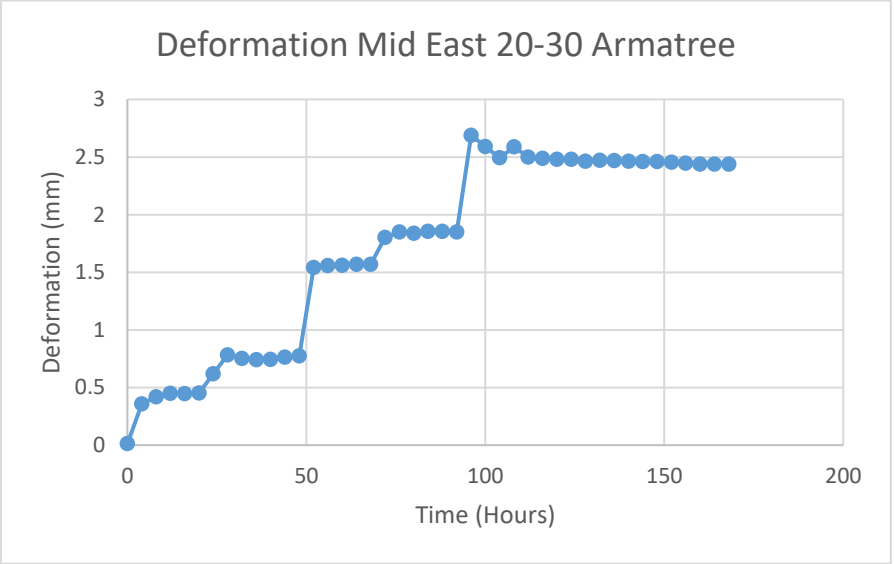


**Figure 89: Deformation graph for Mid-East 20-30 Armatree.**

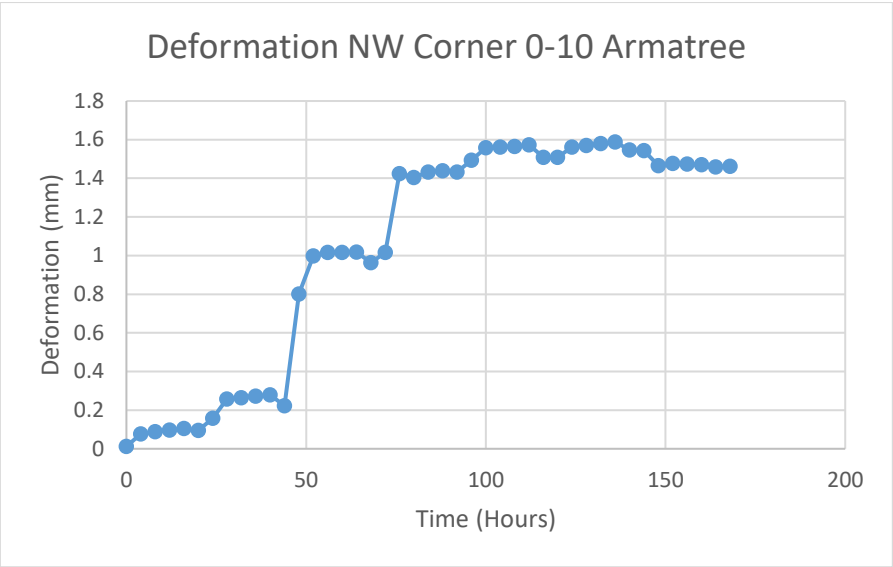


**Figure 90: Deformation graph for Northwest corner 0-10 Armatree.**

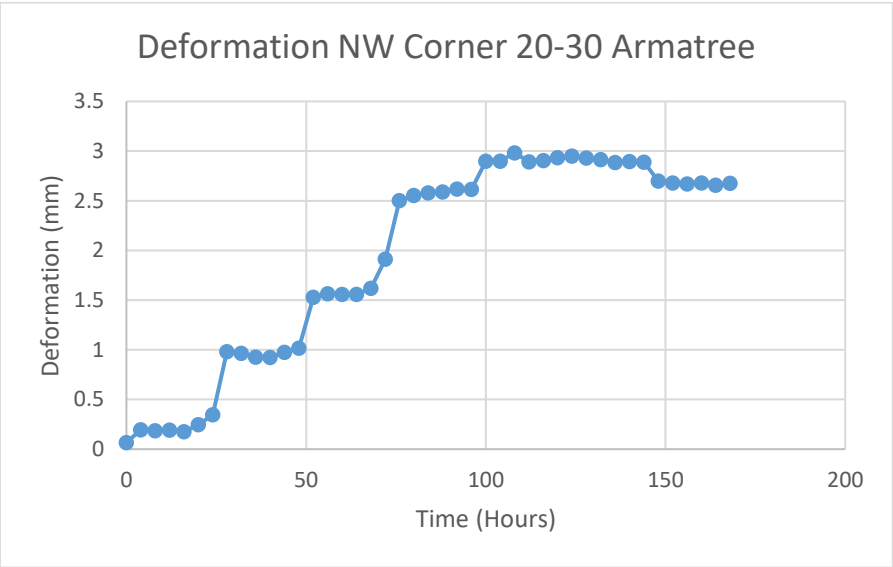


**Figure 91: Deformation graph for Northwest corner 20-30 Armatree.**

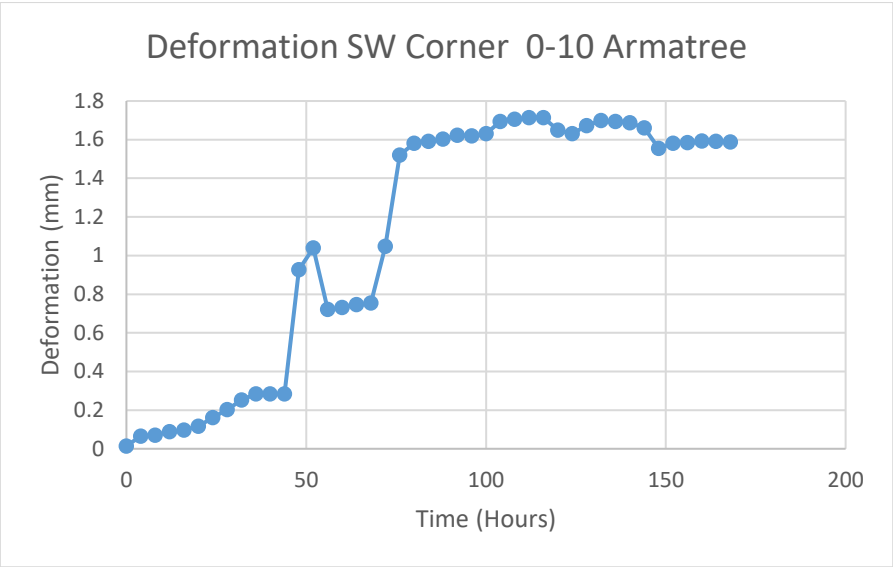


**Figure 92: Deformation graph for Southwest corner 0-10 Armatree.**

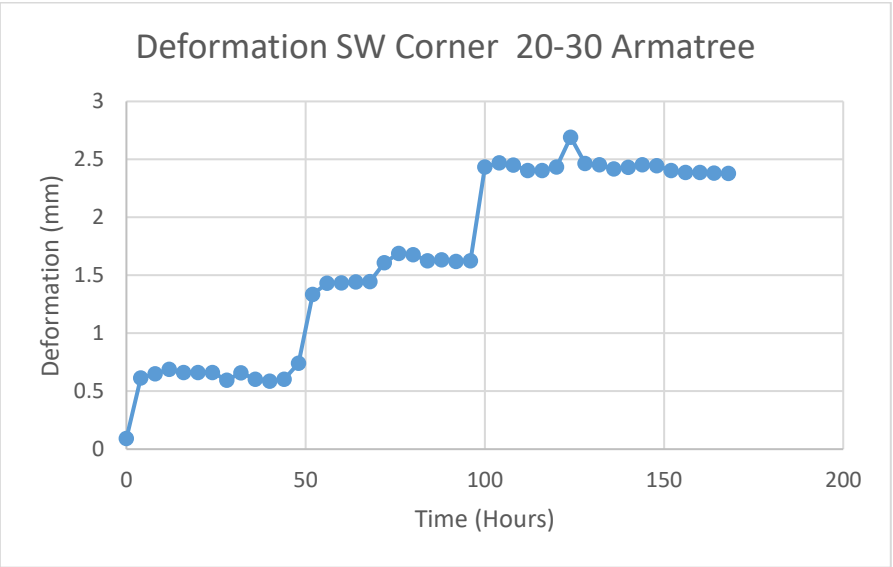


**Figure 93: Deformation graph for Southwest corner 20-30 Armatree.**

# APPENDIX G: CURVE FITTING FOR INITIAL SOIL WATER RETENTION CURVES

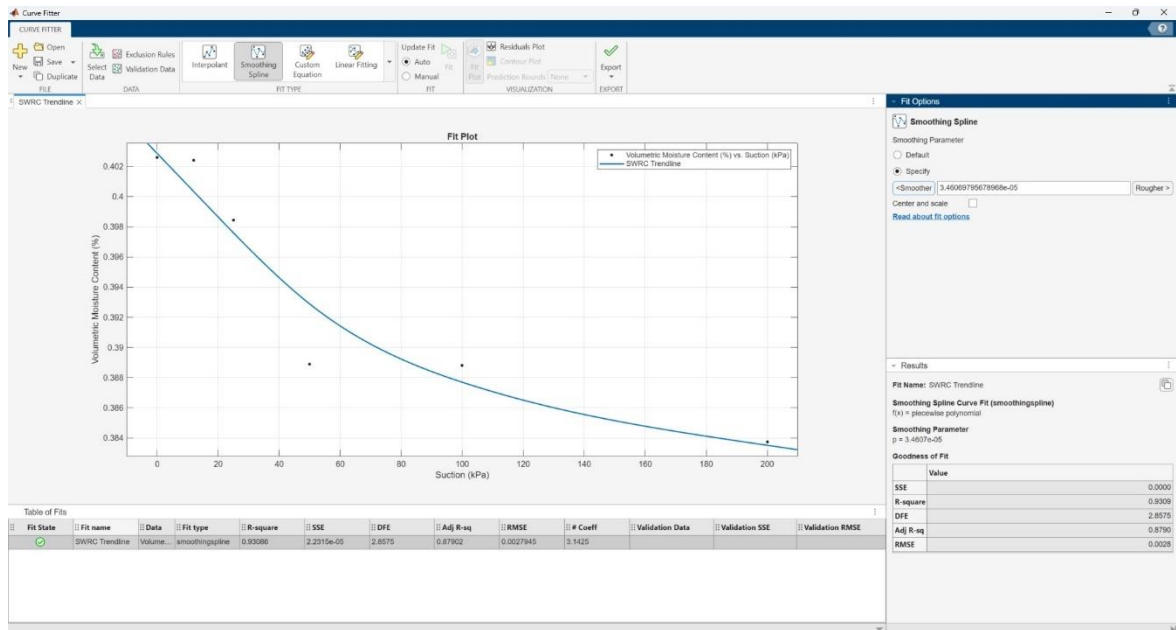


Figure 94: Curve fitting for initial SWRC Mid North 0-10 Greymare.

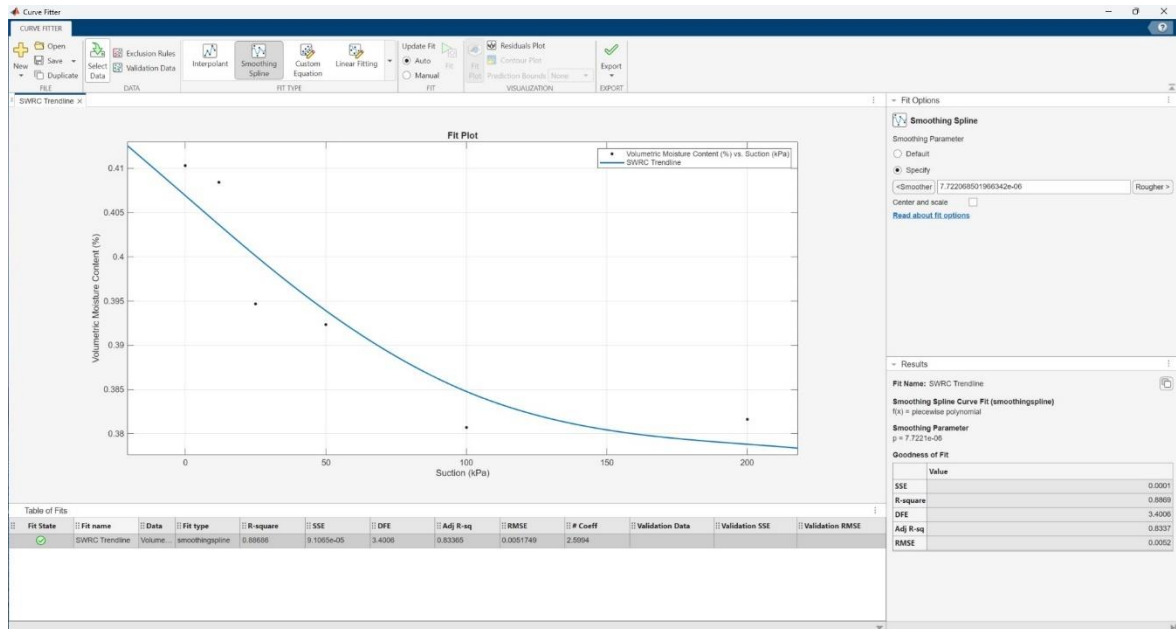
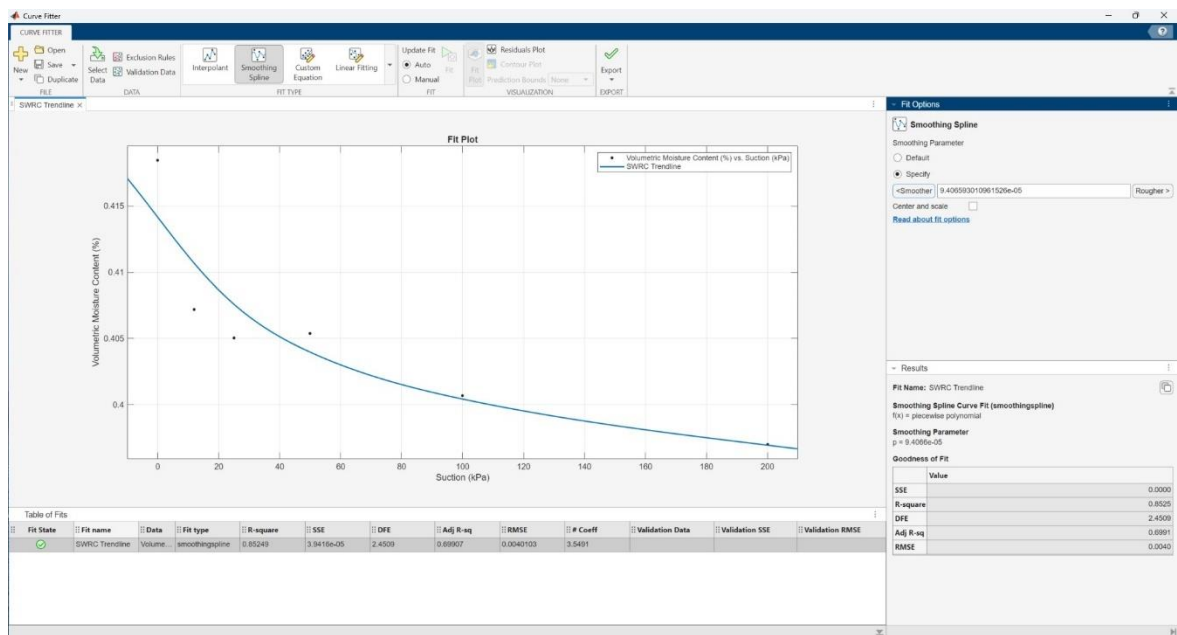
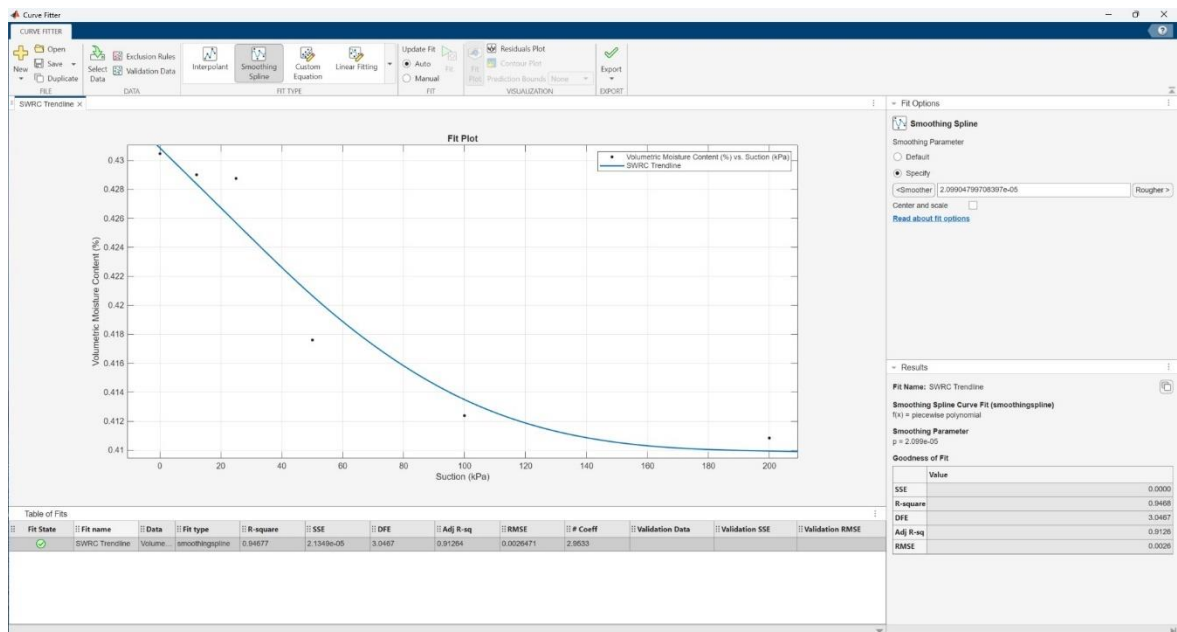


Figure 95: Curve fitting for initial SWRC Mid North 20-30 Greymare



**Figure 96: Curve fitting for initial SWRC Southwest corner 0-10 Greymare.**



**Figure 97: Curve fitting for initial SWRC Southwest corner 20-30 Greymare.**

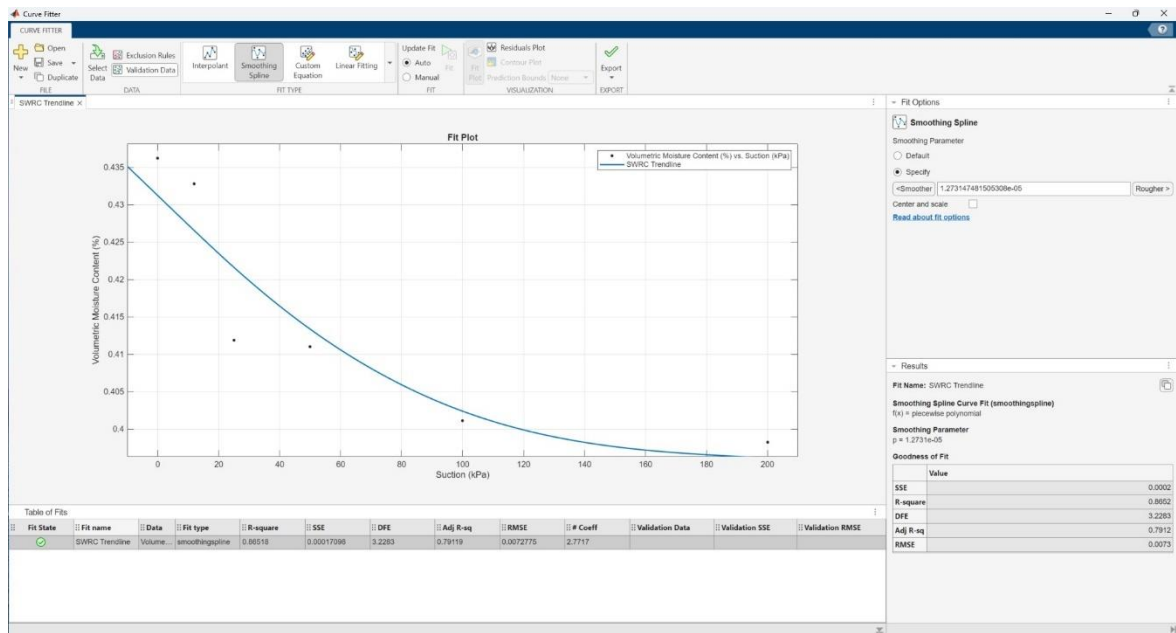


**Figure 98: Curve fitting for initial SWRC Mid-East 0-10 Armatree.**

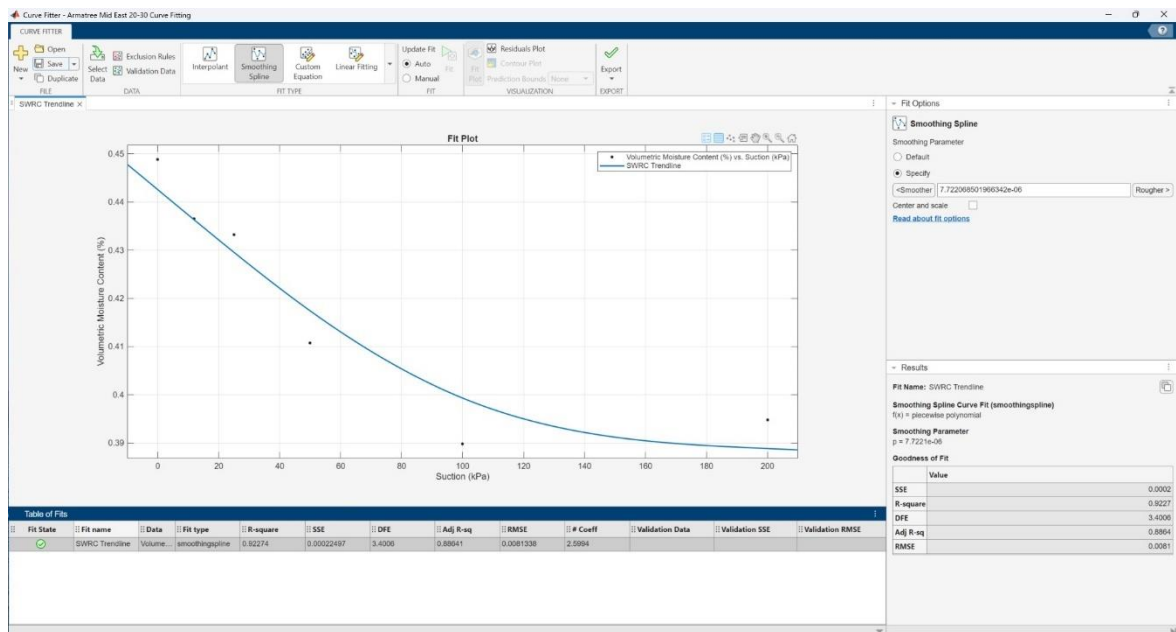


**Figure 99: Curve fitting for initial SWRC Mid-East 20-30 Armatree.**

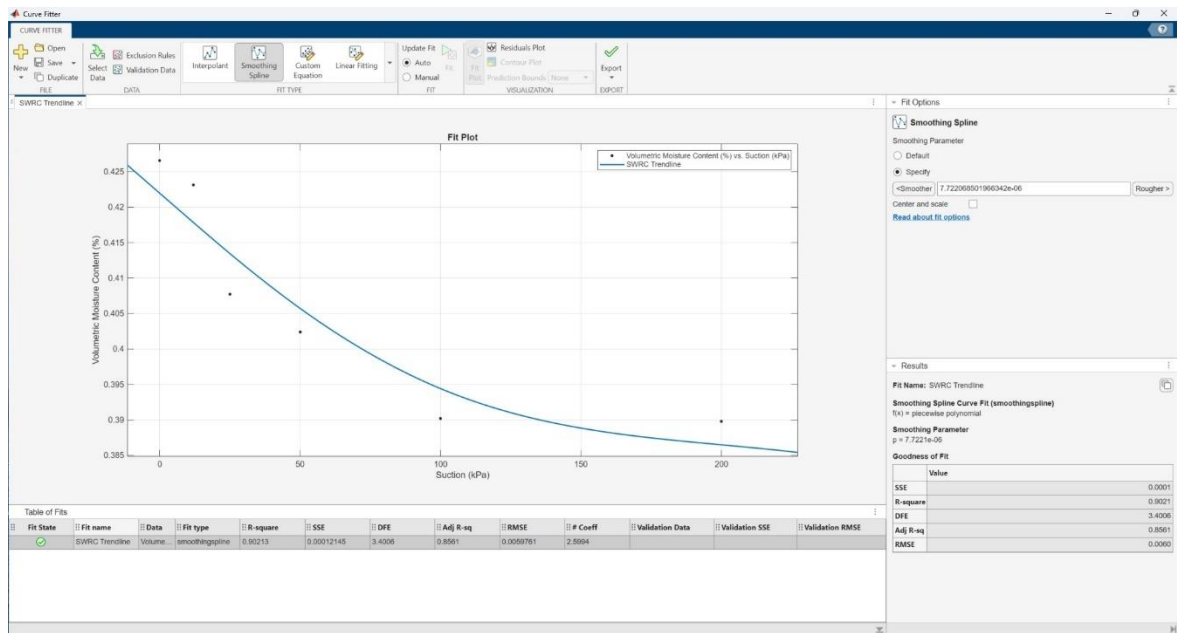


Figure 100: Curve fitting for initial SWRC Northwest corner 0-10 Armatree.

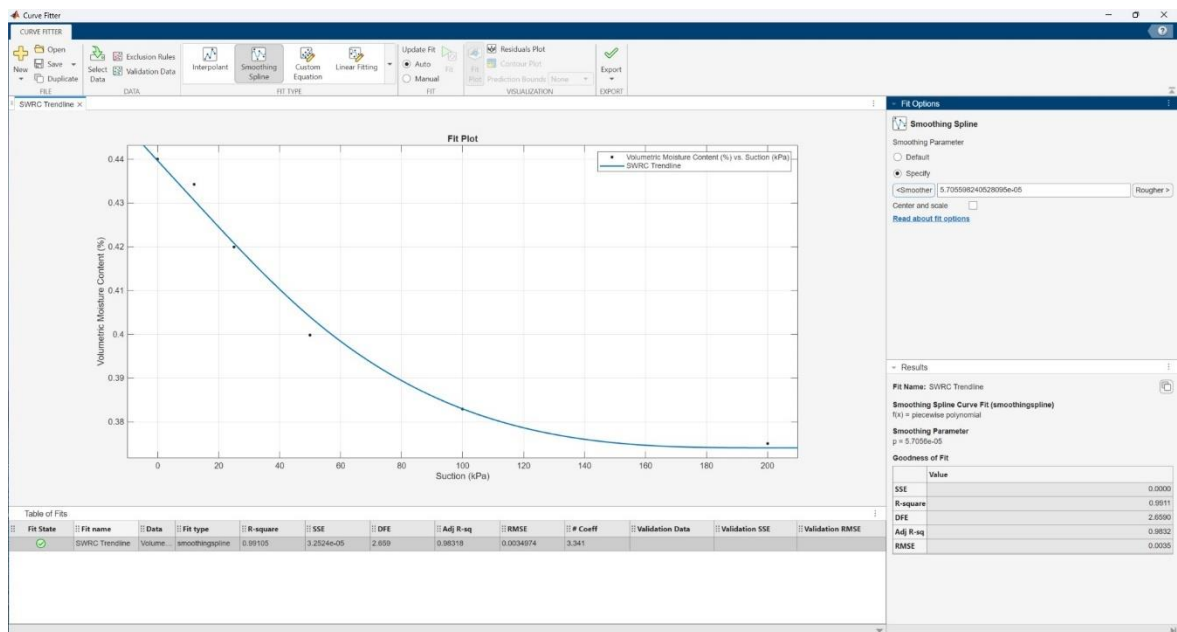
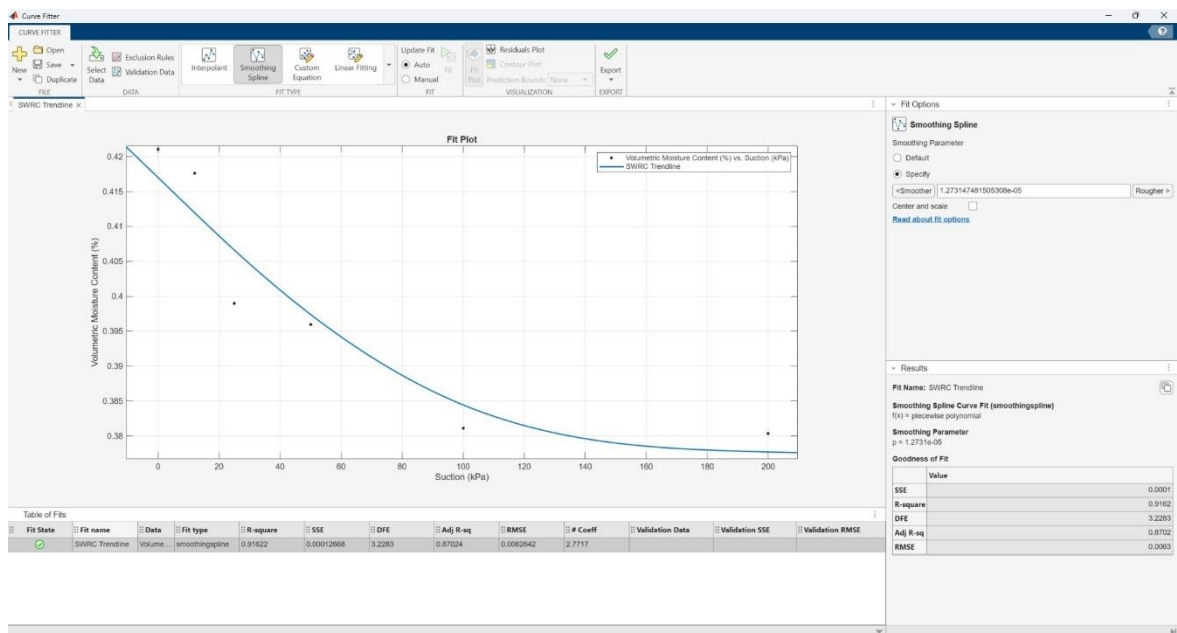
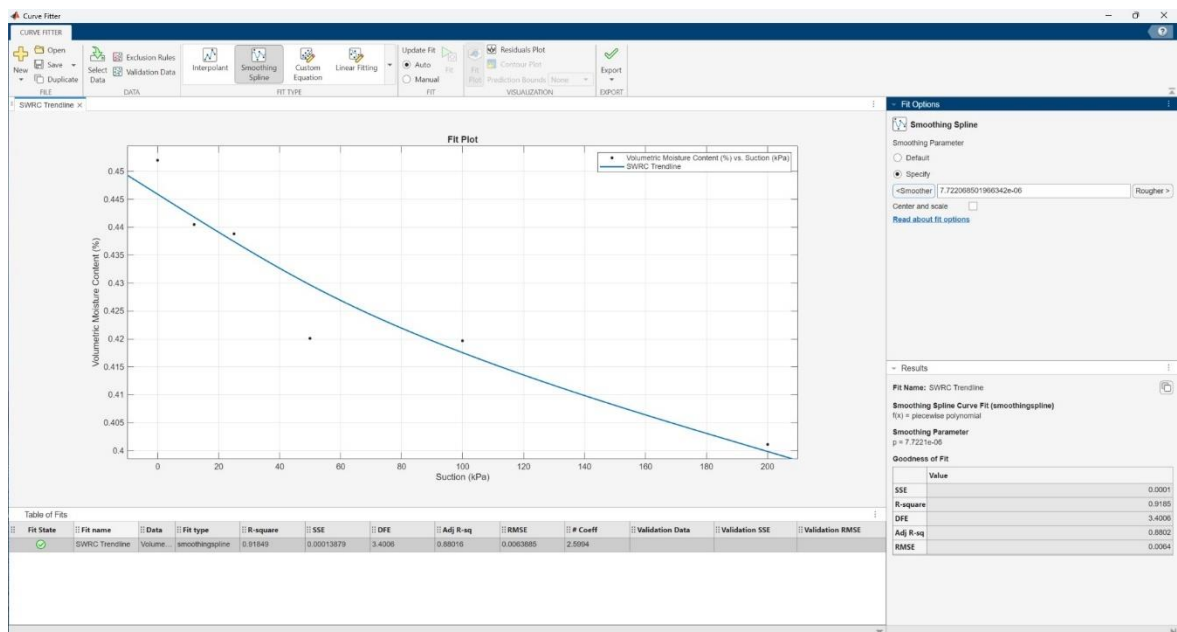


Figure 101: Curve fitting for initial SWRC Northwest corner 20-30 Armatree.





**Figure 102: Curve fitting for initial SWRC Southwest corner 0-10 Armatree.**



**Figure 103: Curve fitting for initial SWRC Southwest corner 20-30 Armatree.**

# APPENDIX H: CURVE FITTING FOR REVISED SOIL WATER RETENTION CURVES

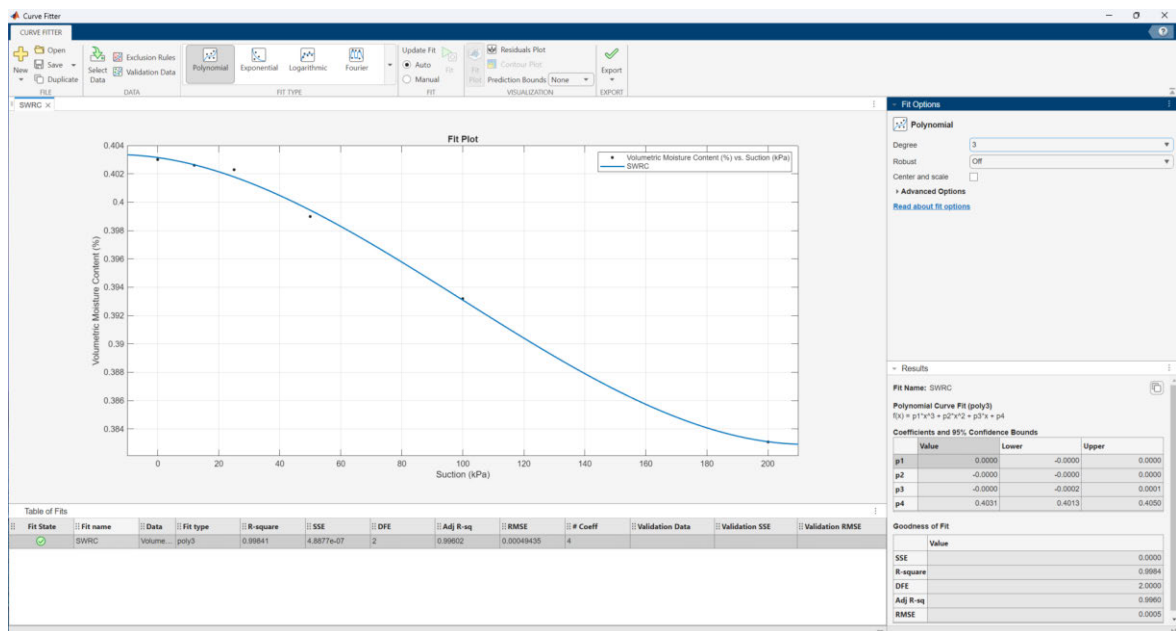


Figure 104: Curve fitting for revised SWRC Mid North 0-10 Greymare.

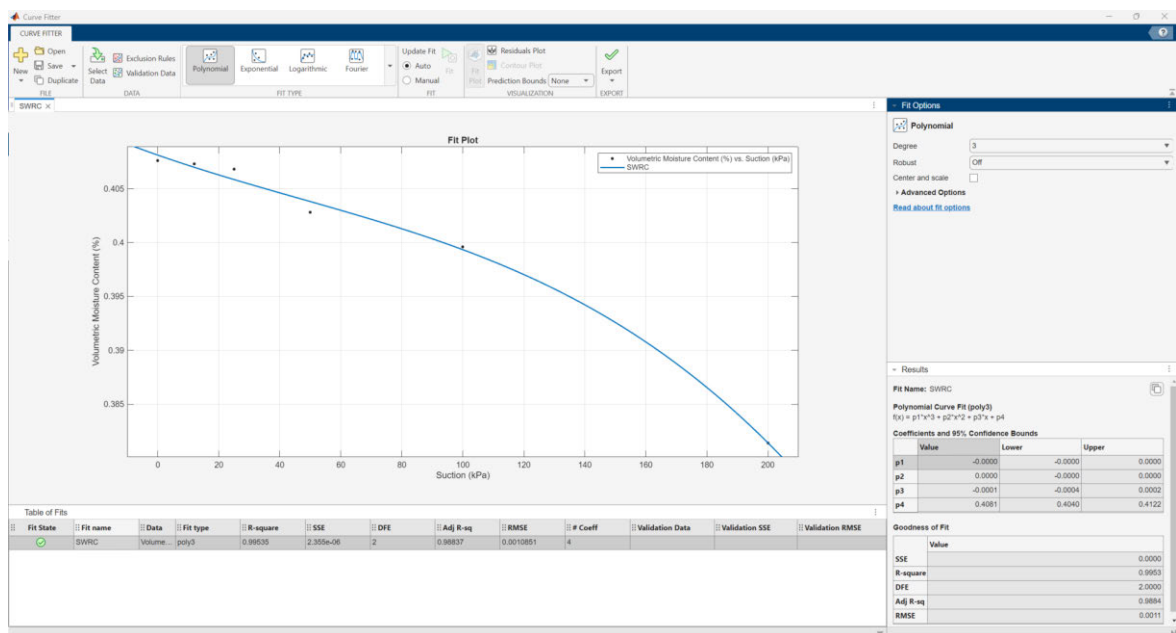
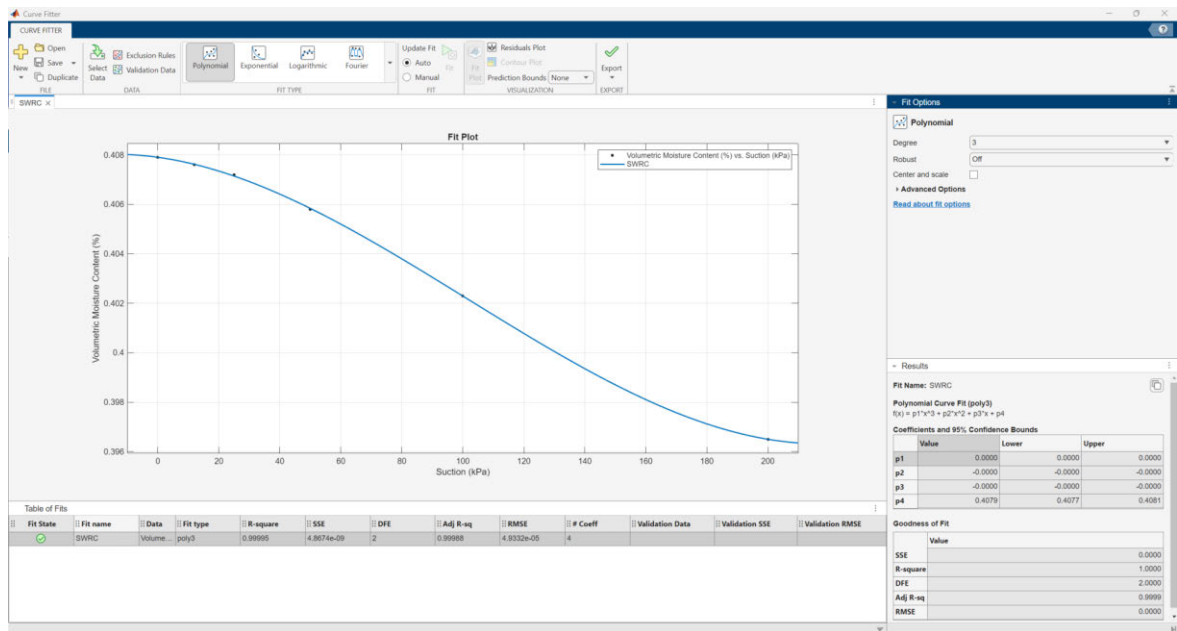
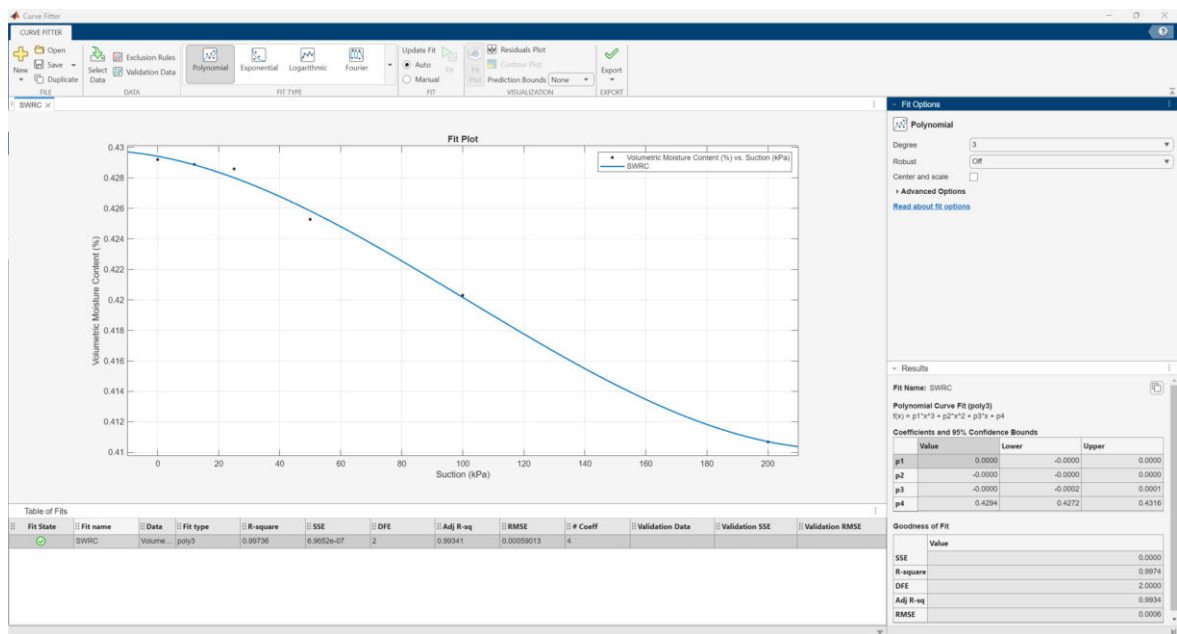


Figure 105: Curve fitting for revised SWRC Mid North 20-30 Greymare.



**Figure 106: Curve fitting for revised SWRC Southwest corner 0-10 Greymare.**



**Figure 107: Curve fitting for revised SWRC Southwest corner 20-30 Greymare.**

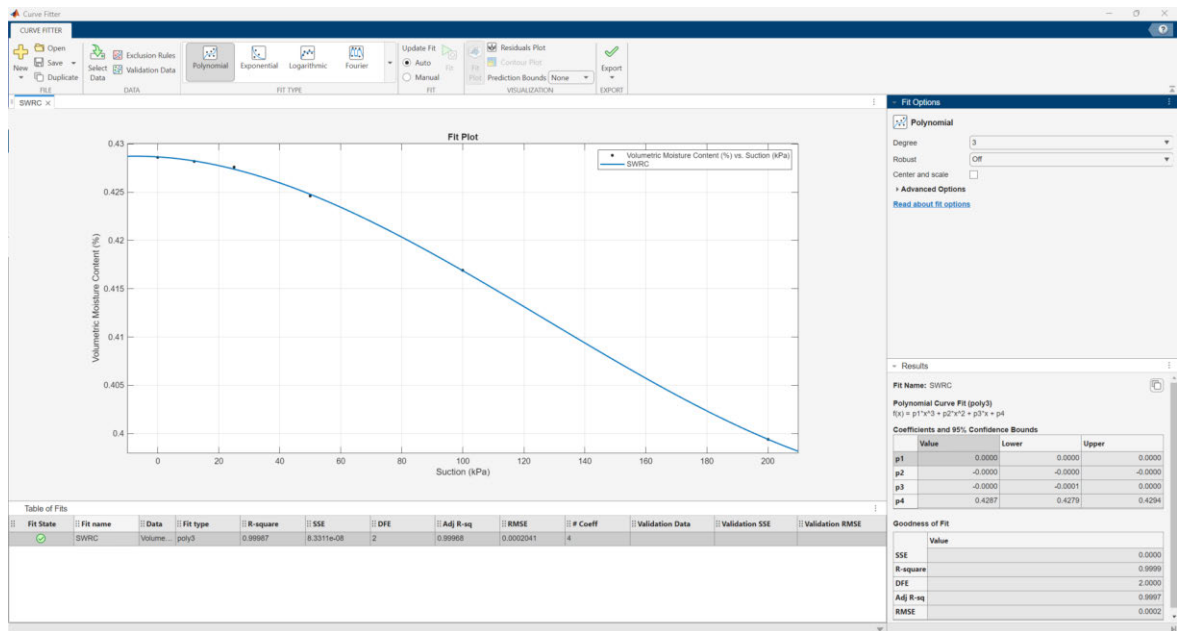


Figure 108: Curve fitting for revised SWRC Mid-East 0-10 Armatree.

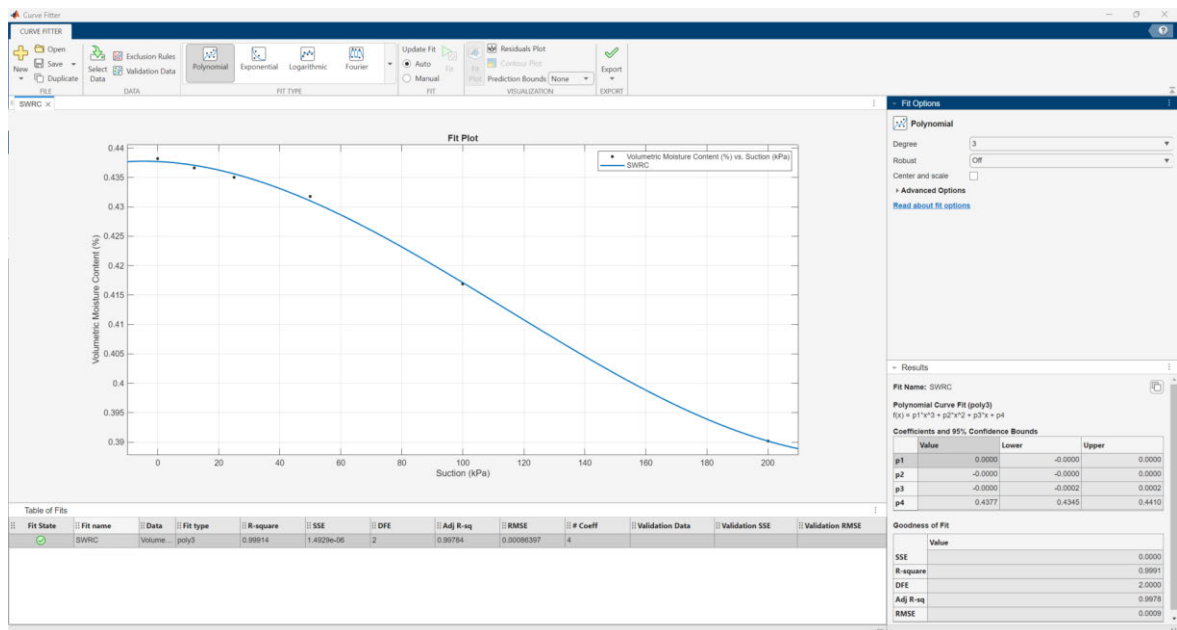
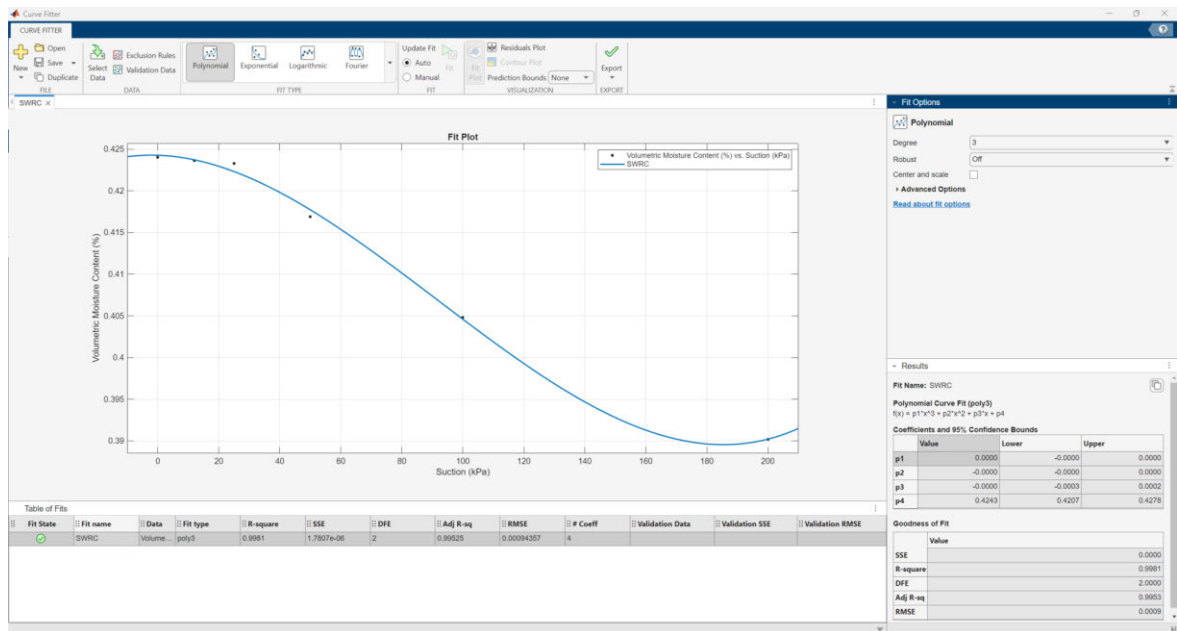
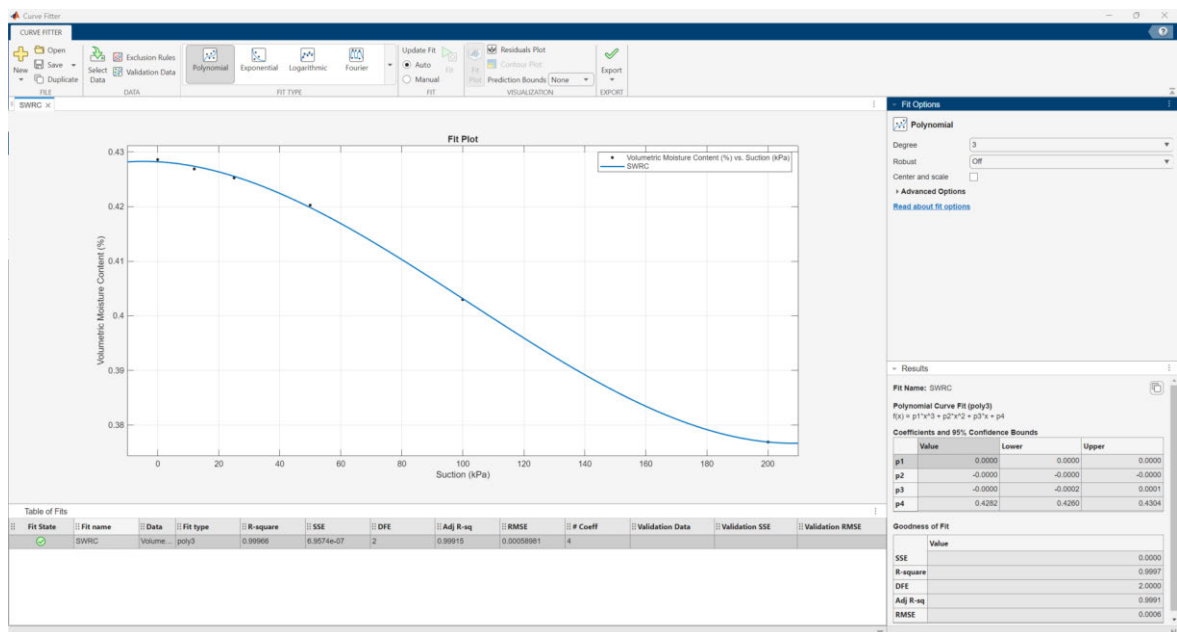


Figure 109: Curve fitting for revised SWRC Mid-East 20-30 Armatree.



**Figure 110: Curve fitting for revised SWRC Northwest corner 0-10 Armatree.**



**Figure 111: Curve fitting for revised SWRC Northwest corner 20-30 Armatree.**

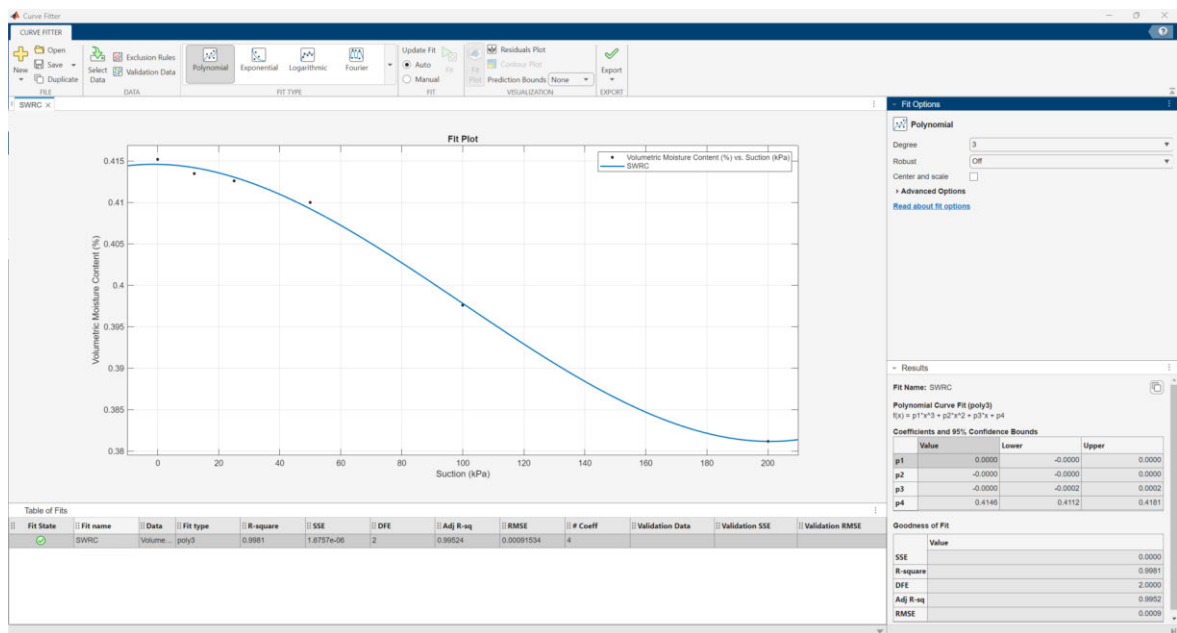


**Figure 112: Curve fitting for revised SWRC Southwest corner 0-10 Armatree.**

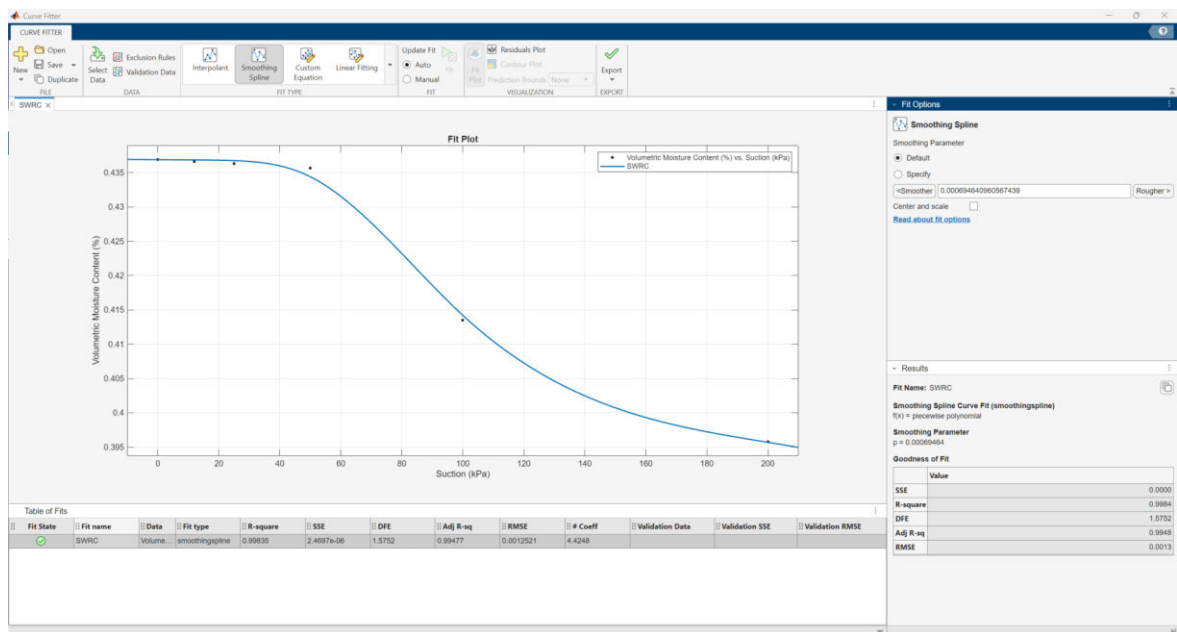


**Figure 113: Curve fitting for revised SWRC Southwest corner 20-30 Armatree.**